Journal of Pharmaceutical Analysis 13 (2023) 563–589

Contents lists available at ScienceDirect

Journal of Pharmaceutical Analysis

journal homepage: www.elsevier.com/locate/jpa

Review paper

Novel wine in an old bottle: Preventive and therapeutic potentials of andrographolide in atherosclerotic cardiovascular diseases

Tingting Gou [a, b, 1], Minghao Hu [a, b, 1], Min Xu [a, b], Yuchen Chen [a, b], Rong Chen [a, b], Tao Zhou [a, b], Junjing Liu [a, b], Li Guo [a, b], Hui Ao [a, c, **], Qiang Ye [a, b, *]

[a] State Key Laboratory of Southwestern Chinese Medicine Resources, Chengdu University of Traditional Chinese Medicine, Chengdu, 611137, China
[b] School of Pharmacy, Chengdu University of Traditional Chinese Medicine, Chengdu, 611137, China
[c] Innovative Institute of Chinese Medicine and Pharmacy, Chengdu University of Traditional Chinese Medicine, Chengdu, 611137, China

ARTICLE INFO

Article history:
Received 30 November 2022
Received in revised form
13 May 2023
Accepted 16 May 2023
Available online 20 May 2023

Keywords:
Andrographolide
Atherosclerosis
Atherosclerotic cardiovascular disease
Pharmacological effects
Pharmacokinetics properties
Toxicity

ABSTRACT

Atherosclerotic cardiovascular disease (ASCVD) frequently results in sudden death and poses a serious threat to public health worldwide. The drugs approved for the prevention and treatment of ASCVD are usually used in combination but are inefficient owing to their side effects and single therapeutic targets. Therefore, the use of natural products in developing drugs for the prevention and treatment of ASCVD has received great scholarly attention. Andrographolide (AG) is a diterpenoid lactone compound extracted from *Andrographis paniculata*. In addition to its use in conditions such as sore throat, AG can be used to prevent and treat ASCVD. It is different from drugs that are commonly used in the prevention and treatment of ASCVD and can not only treat obesity, diabetes, hyperlipidaemia and ASCVD but also inhibit the pathological process of atherosclerosis (AS) including lipid accumulation, inflammation, oxidative stress and cellular abnormalities by regulating various targets and pathways. However, the pharmacological mechanisms of AG underlying the prevention and treatment of ASCVD have not been corroborated, which may hinder its clinical development and application. Therefore, this review summarizes the physiological and pathological mechanisms underlying the development of ASCVD and the in vivo and in vitro pharmacological effects of AG on the relative risk factors of AS and ASCVD. The findings support the use of the old pharmacological compound ('old bottle') as a novel drug ('novel wine') for the prevention and treatment of ASCVD. Additionally, this review summarizes studies on the availability as well as pharmaceutical and pharmacokinetic properties of AG, aiming to provide more information regarding the clinical application and further research and development of AG.

1. Introduction

Atherosclerotic cardiovascular disease (ASCVD) can manifest as coronary heart disease (CHD), cerebrovascular disease or peripheral arterial disease (PAD) of atherosclerotic origin [1]. In 2019, ASCVD was reported to cause 17.9 million deaths [2–4]. Studies have shown that there are many risk factors of ASCVD, including gender, age, smoking, hypertension, hyperglycaemia, hyperlipidaemia and obesity [5,6]. Therefore, developing drugs for the prevention and treatment of ASCVD is necessary. Moreover, synthetic drugs that manage the risk factors of ASCVD, including obesity, diabetes, hyperlipidaemia and hypertension, can prevent ASCVD to some extents [7–11]. However, the development of ASCVD involves multiple targets and pathways. Drugs applied to treat ASCVD and its risk factors are single-targeted, and consequently elicit unsatisfactory efficacy and unavoidable side effects. Therefore, novel complementary and alternative medical approaches should be used to prevent and treat ASCVD.

Regular intake of spices, vegetables and fruits can minimize reactive oxygen species (ROS) production, oxidative stress and inflammation, which contribute to the occurrency and development of non-communicable diseases including ASCVD. Given that natural agents such as emodin, curcumin, nuciferine, puerarin, and

Peer review under responsibility of Xi'an Jiaotong University.
* Corresponding author. State Key Laboratory of Southwestern Chinese Medicine Resources, Chengdu University of Traditional Chinese Medicine, Chengdu, 611137, China.
** Corresponding author. State Key Laboratory of Southwestern Chinese Medicine Resources, Chengdu University of Traditional Chinese Medicine, Chengdu, 611137, China.
E-mail addresses: aohui2005@126.com (H. Ao), yeqiang@cdutcm.edu.cn (Q. Ye).
[1] Both authors contributed equally to this work.

https://doi.org/10.1016/j.jpha.2023.05.010

ginsenosides have multiple-targets, little toxicity, and great therapeutic potentials against non-communicable diseases [12–19], attention should be paid to discover natural compounds which can be applied in the prevention and treatment of ASCVD and in turn prolong the life expectancy of ASCVD patient.

In 1911, a crystalline agent, named andrographolide (AG), was first isolated from *Andrographis paniculata* and was considered a major active diterpenoid [20,21]. As a monomer component with multiple targets, AG has been proved to be effect in treating common cold, sinusitis, acute upper respiratory tract infection, pneumonia and bronchitis in clinical dosage forms such as tablets, capsules, soft gels, dispersible tablets and drops in China [22–25]. In addition to anti-inflammatory and antibacterial effects, AG exerts remarkable therapeutic effects against obesity, diabetes, hyperlipidaemia, CHD, cerebral ischemia and cerebral haemorrhage. Therefore, it may be used to prevent and treat ASCVD [26–31]. However, to the best of our knowledge, no review has summarized the preventive and therapeutic effects of AG on ASCVD.

Although previous studies have demonstrated the efficacy of AG in treating various diseases, its use in the prevention and treatment of ASCVD has been reported only in recent studies (signifying 'novel wine' in an 'old bottle'). However, its mechanisms of action and complications remain unclear (Fig. 1). In this review, we summarized the physiological and pathological mechanisms underlying the development of ASCVD and the therapeutic role of AG in ASCVD. Additionally, we discussed the safety, availability and pharmacokinetic properties of AG to provide a reference for the development and use of AG-based drugs for treating ASCVD.

2. Pathophysiological mechanism and complication of ASCVD

ASCVD is common in the general population and includes four main subtypes: (1) CHD, which manifests as myocardial ischemia and myocardial infarction (MI); (2) cerebrovascular diseases, which manifest as transient ischaemic attacks and strokes; (3) PAD, which manifests as claudication and severe limb ischemia; and (4) aortic atherosclerosis and aortic aneurysms [32,33]. Despite recent advances in preventive medicine, the risk of recurrence of ASCVD, a consequence of the enormous burden of atherosclerotic plaques, remains high. Therefore, early intervention is necessary to prevent progression to large plaques and substantially reduce the risk of ASCVD [34,35]. Additionally, atherosclerosis (AS), the primary risk factor of ASCVD, is usually caused by physiological, environmental and genetic factors [36,37]. Because it is difficult to control genetic and environmental factors, an effective approach to treat AS involves the management of its physiological factors, especially hyperlipidaemia, hypertension, diabetes and obesity [10,38]. The following sections describe the physiological characteristics of ASCVD, especially its

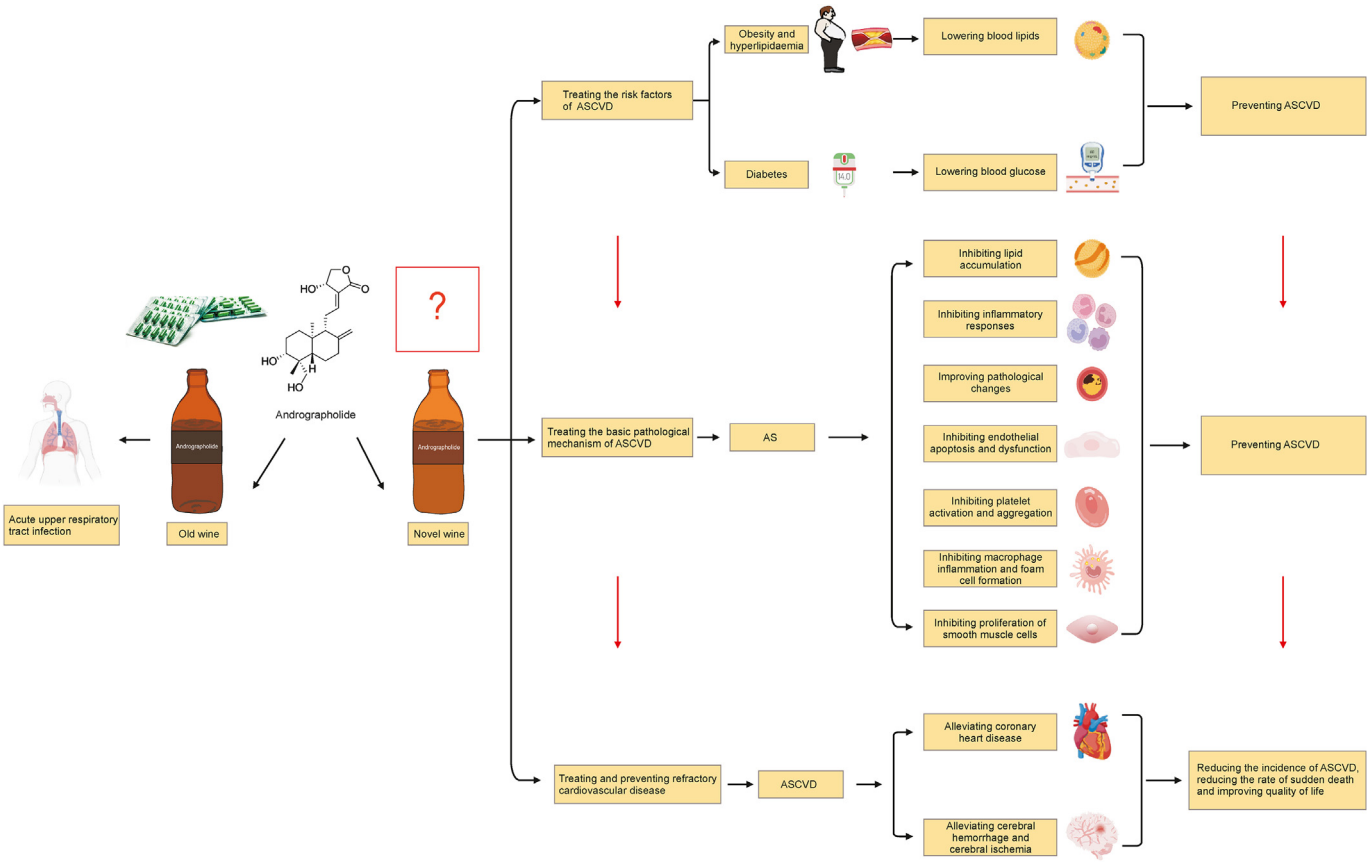

Fig. 1. Novel and old applications of andrographolide (AG) in different diseases. ASCVD: atherosclerotic cardiovascular disease; AS: atherosclerosis.

relationship with AS, hyperlipidaemia, hypertension, diabetes and obesity, and the drugs approved for ASCVD.

2.1. Pathophysiology of ASCVD

Because of the complex pathogenesis of ASCVD, we have described the underlying process by summarizing the risk factors, pathogenesis, complications and relevant signaling pathways and targets as separate topics.

2.1.1. Risk factors of ASCVD

Hypertension, hyperglycaemia, hyperlipidaemia and obesity, which are the main risk factors of ASCVD, usually contribute to the development of AS. These factors are related to oxidative stress, inflammation and endothelial dysfunction in AS. Dyslipidaemia is a major risk factor for AS [39]. Hyperlipidaemia causes lipid abnormalities and promotes thrombosis. Hyperlipidaemia and obesity can induce glucose and lipid disorders, which in turn induce oxidative stress and endothelial dysfunction associated with AS [40,41]. Additionally, hypertension activates oxidative stress and inflammatory processes, resulting in endothelial dysfunction [42]. Numerous studies have shown that the above mentioned risk factors are frequently concomitant in clinical settings and substantially increase the risk of cardiovascular diseases. For example, a study reported that the clinical complications of type 2 diabetes mellitus included hypertension in 82.1% of patients, obesity in 78.2% of patients and hyperlipidaemia in 77.2% of patients [43]. Therefore, controlling these risk factors may help to prevent ASCVD.

2.1.2. Pathogenesis of AS

AS, the pathological basis of ASCVD, is a chronic inflammatory disease of blood vessels, with the involvement of large and middle arteries. It is characterized as lipid accumulation, inflammation, oxidative stress, activation of endothelial cells (ECs), proliferation of arterial smooth muscle cells (SMCs), activation of macrophages and formation of foam cells [44]. Over the past few decades, researchers have investigated the pathogenesis of AS and proposed different hypotheses, such as the immune–metabolic, lipid, thrombogenic and response to injury hypotheses [45–49]. Notably, damage in vascular endothelial cells (VECs) is considered as the primary trigger for the occurrence and development of AS [50]. Endothelial dysfunction is associated with hyperglycaemia and hypertension. To be specific, hyperglycaemia triggers the apoptosis and endothelial dysfunction of ECs by disrupting the balance between the bioavailability of nitric oxide (NO) and the accumulation of ROS [51,52]. Moreover, hyperglycaemia leads to the activation, adhesion and aggregation of platelets [53]. Studies have shown that hypertension destroys the endothelial lining of vascular SMCs through altering forces of shear stress and enhancing oxidative stress. Correspondingly, these pathophysiological forces trigger cell proliferation, vascular remodeling and cell apoptosis [54].

In addition to hyperglycaemia and hypertension, endothelial damages are associated with lipid metabolism disorders [55]. In the early stage of AS, a large amount of low-density lipoprotein cholesterol (LDL-C) enters the intima and is converted to oxidized low-density lipoprotein (ox-LDL) owing to oxidative stress (Fig. 2). The deposition of ox-LDL in the intima of arteries activates the endothelium, which secretes adhesion molecules such as intercellular adhesion molecule-1 (ICAM-1), vascular cell adhesion molecule-1 (VCAM-1) and E-selectin, attracting monocytes into the endothelium and stimulating the activation and aggregation of platelets in damaged sites [56,57]. Subsequently, monocyte-derived macrophages internalise ox-LDL and become foam cells [58,59]. Dysfunctional VECs, macrophages and platelets secrete various growth factors and vasoactive substances, thereby promoting abnormal proliferation and migration of vascular smooth muscle cells (VSMCs) and formation of a stable fibrous cap. The fibrous cap covers complex plaques containing oxidized lipoproteins, cholesterol crystals, inflammatory cells (activated macrophages and T cells) and apoptotic VSMCs, which collectively promote inflammation [60,61]. In the late stage of AS, macrophages secrete matrix metalloproteinases (MMPs) and degrade collagen fibres in the extracellular matrix of the plaque, leading to plaque rupture and thrombosis [62,63]. Additionally, thrombosis decreases the blood flow, resulting in inadequate blood supply to the heart and brain, which eventually leads to life-threatening clinical events such as ischaemic myocardial infarction, stroke and peripheral vascular disease. Therefore, alleviating inflammation and oxidative stress, regulating lipid metabolism, improving endothelial function and decreasing blood pressure and glucose levels are essential approaches to alleviate AS.

2.1.3. Occurrence of ASCVD

AS-induced narrowing of the vessel lumen results in slow blood flow and tissue necrosis, contributing to the occurrence of ASCVD, including CHD, cerebrovascular diseases, chronic kidney disease, PAD and mesenteric AS [64]. CHD, referring to MI or ischemic heart disease, is caused by myocardial ischemia and hypoxia due to coronary atherosclerosis [65]. When a plaque ruptures, there is a loss of integrity of the fibrous cap that separates the necrotic core from blood in the lumen of the artery, which constitutes the major cause of coronary thrombosis [66]. Plaque rupture may physically cause irregular heartbeat, breath shortness and pains in the chest, arms, shoulders or back [67]. Internal carotid artery plaque rupture and subsequent embolisation of atherosclerotic material travel into the brain and lead to cerebrovascular diseases, such as ischaemic stroke [68]. A transient ischaemic attack often occurs before a stroke. The common features of ischemia and stroke include speaking difficulty, sudden weakness and visual impairment [69]. Additionally, the walls of cerebral arterioles are thin, and cerebral atherosclerotic lesions can form small aneurysms. If blood pressure increases suddenly, the small aneurysm may rupture and cause fatal brain haemorrhage [70]. Furthermore, PAD is a common circulatory condition in which narrowing arteries reduce blood flow to the extremities (usually the legs), leading to symptoms such as leg pain while walking [71]. Plaque build-up in renal arteries deprives the kidneys of oxygen-rich blood, resulting in kidney dysfunction [72]. Additionally, atheromatous plaques in the mesenteric arteries can lead to intestinal infarction. Consequently, patients may experience severe abdominal pain, stool bleeding and shock [73] (Fig. 3). Therefore, it is necessary to prevent or treat ASCVD.

2.1.4. Signaling pathways and targets of AS and ASCVD

Development of AS is a complex process and involves multiple signaling pathways related to inflammation, oxidative stress and lipid metabolism. Inflammation, which mainly involves the regulation of mitogen-activated protein kinase (MAPK), c-Jun amino-terminal kinases (JNK)/signal transducer and activator of transcription (STAT), phosphatidylinositol-3 kinase (PI3K)/protein kinase B (AKT) and noncanonical nuclear factor-kappa B (NF-κB) signalings, plays an important role in all stages of AS [74]. Activation or inhibition of these signaling pathways promotes not only the production of various factors (inflammatory factors, adhesion molecules, chemokines and growth factors) but also apoptosis and inflammation. In addition, the reduced bioavailability of endothelial NO synthase (NOS) can impair endothelial function and increase the proliferation of SMCs, thus playing a key role in the progression of AS. Studies have shown that inducible nitric oxide synthase (iNOS) and endothelial nitric oxide synthase (eNOS)

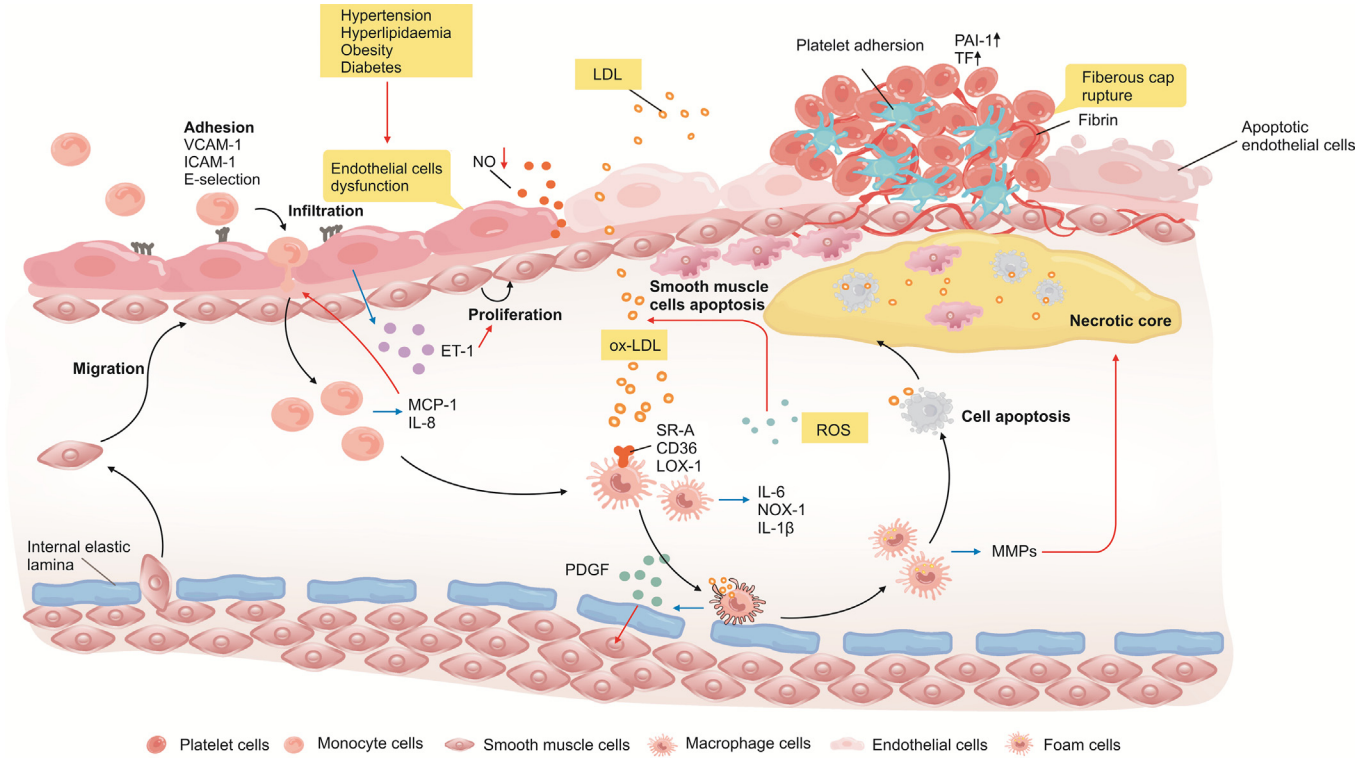

Fig. 2. Mechanism of atherosclerosis development. ROS: reactive oxygen species; ox-LDL: oxidized low-density lipoprotein; ET-1: endothelin 1; ICAM-1: intercellular adhesion molecule-1; TF: tissue factor; LDL: low-density lipoprotein; SR-A: class A scavenger receptor; PAI-1: plasminogen activator inhibitor-1; NO: nitric oxide; PDGF: platelet-derived growth factor; MCP-1: monocyte chemoattractant protein-1; NOX-1: NADPH oxidase-1; IL-8: interleukin-8; IL-6: interleukin-6; MMPs: matrix metalloproteinases; VCAM-1: vascular cellular adhesion molecule-1; IL-1β: interleukin-1β.

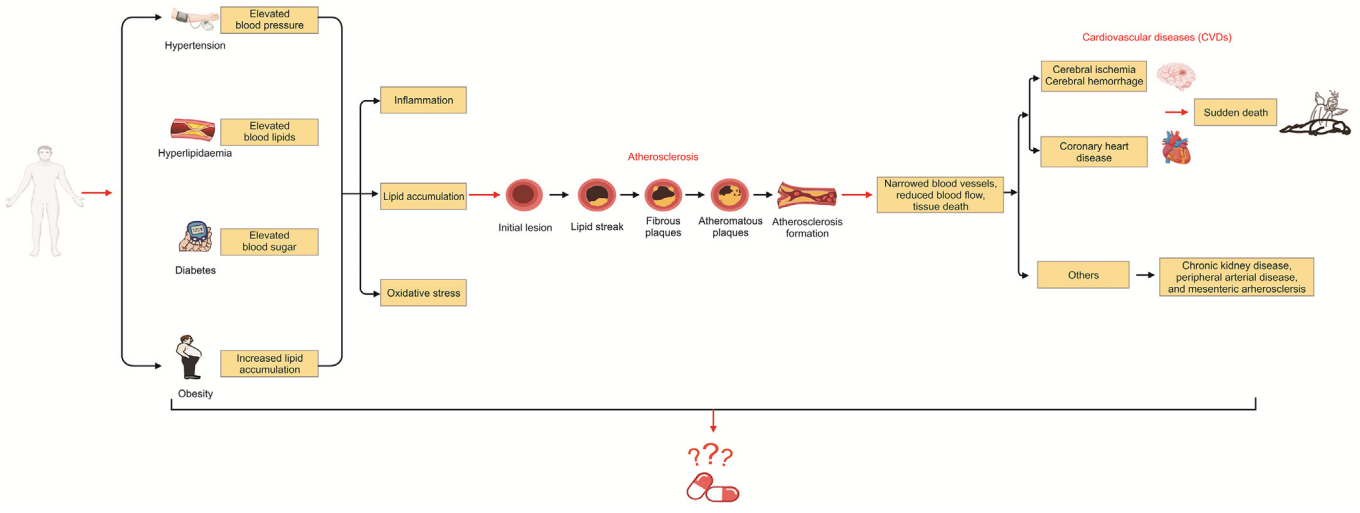

Fig. 3. Triggers and complications of atherosclerosis.

regulate NO production through the PI3K/AKT, nuclear factor erythroid 2-related factor 2 (Nrf2)/heme oxygenase-1 (HO-1) and NF-κB/iNOS/NO pathways [75,76]. Lipid metabolism disorders, such as abnormal cholesterol levels, can promote AS. Reverse cholesterol transport (RCT) is mainly regulated via the NF-κB signaling pathway. Excessive cholesterol is transported from peripheral tissues, such as cholesterol-loaded macrophages, in the vessel wall to the liver. ATP-binding cassette (ABC) transporter A1 (ABCA1), a transmembrane protein that mediates the intracellular transfer of cholesterol to apolipoprotein A-1 (apoA-1), plays a key role in RCT [77]. Additionally, other molecular mechanisms associated with AS further contribute to the development of cardiovascular diseases. For example, the abnormal expressions of inflammatory factors (e.g. tumor necrosis factor-alpha (TNF-α), interleukin-6 (IL-6) and monocyte chemoattractant protein-1 (MCP-1)) and dysfunction of the NF-κB pathway are observed in aortic AS. In CHD, excessive levels of ROS cause endothelial dysfunction, resulting in reduced antioxidant capacity.

Additionally, over-production of ROS activates inflammatory signaling (such as the Nrf2/HO-1 pathway) and the expressions of inflammatory factors (TNF-α, MCP-1, high-sensitivity C-reactive protein (hs-CRP) and interleukin-1β (IL-1β)), which can promote the development and progression of CHD [78]. Therefore, inhibiting the development of AS can help to reduce the incidence of cardiovascular disease.

Also, the pathophysiology of ischaemic stroke-induced brain damage is complex. Cerebral ischemia triggers the production of ROS and the activation of caspases in neuronal cells and inhibits oxidative stress and inflammation through the p38 MAPK/Nrf2 and PI3K/AKT pathways [79]. Inflammation plays a key role in secondary brain injury (SBI) induced by cerebral haemorrhage through activation of the NF-κB signaling pathway and the NOD-like receptor family pyrin domain containing 3 (NLRP3) inflammasome [80]. Therefore, inhibiting the expressions of signal pathways related to inflammation and oxidative stress is the key to reduce ischemic stroke and cerebral haemorrhage.

2.2. Approved drugs for the prevention and treatment of ASCVD

ASCVD is a general term for several cardiovascular diseases based on AS. Patients with ASCVD usually suffer from hypertension, hyperlipidaemia and hyperglycaemia. Therefore, it is necessary to decrease blood pressure and the levels of lipids and glucose in patients with ASCVD. Approaches including suppressing inflammatory responses, oxidative stress, as well as disturbances in lipid metabolism and cellular abnormalities can help to alleviate AS [81,82]. Cerebrovascular diseases and CHD are relieved by inhibition of thrombosis and platelet aggregation, regulation of lipids, and alleviation of vascular damages. Therefore, drugs used in the treatment of ASCVD mainly include lipid-lowering drugs (pravastatin and clofibrate), anti-platelet agents (aspirin and clopidogrel), vasodilatory agents (sodium nitrate and nitroglycerin), thrombolytic agents (urokinase and streptokinase) and anticoagulants (heparin and warfarin) [83–86]. These drugs exert anti-atherogenic effects by reducing blood lipid and triglyceride levels, improving endothelial function and inhibiting platelet aggregation and inflammation. However, these drugs have certain side effects in clinical settings, such as muscle toxicity, liver toxicity, rhabdomyolysis, cutaneous flushing, skin rashes and gastrointestinal symptoms [87–89]. Moreover, most of these drugs are one-targeted and exert minimal effects against the risk factors of ASCVD (obesity, hyperlipidaemia and diabetes mellitus), and inevitable toxicity. Given the serious disadvantages of the currently available anti-ASCVD agents, it is essential to identify and develop multi-targeted and multi-functional anti-ASCVD drugs that do not cause any significant side effects. Indeed, compounds derived from natural resources, especially those approved for other diseases, can be used to develop drugs for treating ASCVD at any stage.

3. Preventive and therapeutic effects of AG against ASCVD

As mentioned earlier, AS induces various refractory diseases, including CHD, cerebral haemorrhage, cerebral ischemia and PAD. Numerous studies have reported that AG has several pharmacological activities. Notably, it not only alleviates conditions contributing to the development of ASCVD (e.g. diabetes, hyperlipidaemia and obesity) but also has therapeutic implications for AS and ASCVD, including MI, ischaemic heart diseases, cerebral haemorrhage and cerebral ischemia. Therefore, we summarize the pharmacological effects of AG in the treatment of the risk factors of AS and ASCVD.

3.1. Therapeutic potentials of AG on the risk factors of ASCVD

3.1.1. Anti-obesity and hypolipidemic effect of AG

AG appears to be an efficient drug in the treatment of obesity and hyperlipidaemia. It inhibited the increase of visceral adipose tissues in obese mice and hyperlipidemic rats [90–92]. These effects of AG are achieved through inhibiting lipid production, adipocyte proliferation and adipocyte differentiation.

Researchers evaluated the anti-obesity effects of AG in the high fat diet (HFD)-treated mice. The results showed that AG presented anti-adipogenic effects by regulating the expressions of transcription factors and genes related to lipid metabolism in vivo. In the HFD-induced obese mice, AG (50 and 100 mg/kg) decreased the body weight (BW), which was due to increase of oxygen consumption (VO_2), energy expenditure (EE) and respiratory quotient (RQ). Furthermore, AG reduced total cholesterol (TC), triglyceride (TG) and LDL-C in blood, liver and adipose tissue of the HFD-induced obese mice [92]. This also appeared in the hyperlipidemic rats induced by 75% yolk emulsion or *Porphyromonas gingivalis* (PG) [90,91]. Sterol regulatory element-binding proteins (SREBPs) are major transcriptional regulators of TG, TC and fatty acid synthesis [93]. AG could regulate the SREBPs target genes and metabolism-associated genes in liver and BAT, which could help to alleviate obesity. Notably, in the mice with HFD-induced obesity, AG (50 and 100 mg/kg) decreased the mRNA expressions of SREBP-1, SREBP-2 and their target genes such as fatty acid synthase (FAS), stearoyl-coenzyme A desaturase 1 (SCD-1), and 3-hydroxy-3-methylglutaryl-coenzyme A reductase (HMGCR). However, AG did not affect the mRNA levels of ABCA1, ABC transporter G5 (ABCG5), or ABC transporter G8 (ABCG8), suggesting that AG might only suppress actions of SREBPs. Briefly, AG regulated the expressions of metabolic genes and proteins, which directly contributed to the lowered lipid level [92].

Inhibition of glutathione peroxidase1 (GPX1) and glutathione (GSH) depletion plays a key role in suppression of proliferation of 3T3-L1 preadipocytes [94]. In 3T3-L1 preadipocytes, AG (10 and 20 μg/mL) inhibited growth of 3T3-L1 preadipocytes in a dose- and time-dependent manner. This phenomenon could not be affected by the pancaspase inhibitor zVAD-fmk, suggesting that pro-apoptotic activity of AG in 3T3-L1 preadipocytes was not associated with caspase. Besides, AG stimulated accumulation of ROS, increased production of H_2O_2, reduced cardiolipin oxidation and induced mitochondrial membrane damage. Chen et al. [95] found N-acetylcysteine (NAC) (a free radical scavenger and GSH precursor) significantly hindered cardiolipin oxidation, loss of mitochondrial membrane, ROS generation and cell growth inhibition in 3T3-L1 preadipocytes, which were induced by AG. This suggested that the inhibitory effect of AG on preadipocytes was related to inhibition of GSH level. Besides, AG depleted GSH level, which resulted in excessive accumulation of ROS and enhanced activity of GPx (a key enzyme converting H_2O_2 into H_2O). In brief, the depletion of cell GSH pool and the inhibition of GPX activity by AG were responsible for its induction of ROS accumulation and growth inhibition of 3T3-L1 preadipocytes.

In obesity, lipid droplet accumulation is partly caused by hyperplasia which occurs during adipocyte differentiation [96,97]. AG could reduce lipid droplet accumulation in adipocytes by suppressing adipogenic differentiation. Chen et al. [98] found AG (0.87–5.26 μg/mL) inhibited adipocytes differentiation through decreasing the number of adipocyte in the S phase and increasing that in G0/G1 phase of 3T3-L1 cells. Furthermore, AG not only attenuated the levels of cyclins (cyclin A, cyclin E, and cyclin-dependent kinase 2 (CDK2)) in differentiation medium (DM)-induced adipocytes, but also inhibited aggregations of lipid droplets. Also, the inhibitory effect of AG (0.35–3.50 μg/mL) on lipid

droplet aggregation in human bone marrow mesenchymal stem cells (hBM-MSCs)-derived adipocytes was associated with the inhibition of positive regulators of adipogenic differentiation. Notably, during early adipogenic differentiation of hBM-MSCs, the mRNA expressions of CCAAT enhancer-binding protein-alpha (C/EBPα), CCAAT enhancer-binding protein-beta (C/EBPβ), sterol regulatory element-binding protein-1c (SREBP-1c) and peroxisome proliferator-activated receptor γ (PPARγ), and the protein levels of C/EBPα and PPARγ were significantly increased, which were suppressed by AG. This suggested that AG negatively regulated on key transcription factors (C/EBPα, C/EBPβ, SREBP-1c and PPARγ). Additionally, the role of AG in suppressing adipogenesis by inhibiting the expressions of C/EBPα, C/EBPβ and PPARγ in hBM-MSCs was consistent with the results found in 3T3-L1 cells [99,100]. Meanwhile, the expressions of adipocyte-specific marker genes (FABP4, LPL, adiponectin, and glucose transporters subtypes 4 (GLUT4) and the levels of adipokine (adiponectin, RPB4, and adipsin) were decreased by treatment of AG (0.87−5.26 μg/mL) in hBM-MSCs. Also, AG significantly down-regulated the expressions of adipocyte transcription factors (cAMP-response element-binding protein 3-like 1 (CREB3L1), cAMP response element-binding protein 5 (CREB5), Ets Variant Gene 1 (ETV1) and Kruppel-like factor 4 (KLF4)), growth factors (epidermal growth factor receptor (EGFR), human epidermal growth factor receptor-2 (ERBB2), fibroblast growth factor 1 (FGF1) and FGF2), and gene adipogenesis maintaining factors as well as fat metabolism regulatory molecules (filamin A (FLNA), fibronectin 1 (FN1), MMP7 and retinoblastoma susceptibility gene (RB1)). This suggested that AG inhibited adipogenic differentiation via negative regulation of key transcription factors, adipogenic marker proteins, and growth factors [98].

3.1.2. Anti-diabetic effect of AG

As known to all, in the presence of insulin, regulation of glucose homeostasis is achieved primarily by regulating the sensitivity of target tissues to insulin. However, in the absence of insulin, regulation of glucose homeostasis is generally achieved through non-insulin-dependent pathways, such as opioid μ-receptors [101−103]. AG can regulate blood glucose through both of insulin-dependent and insulin-independent pathways, eliciting its anti-diabetic effect.

Studies have shown that AG lowers blood glucose through insulin-dependent pathways, mainly in terms of restoring insulin levels and improving insulin resistance. First, AG could decrease blood sugar by restoring insulin level. Rats with streptozotocin (STZ)-induced diabetes were widely applied as type 1-like diabetes animal model, in which pancreatic beta cells are insufficiently functional [104]. In the STZ-induced diabetic rats, AG (1.5 and 4.5 mg/kg) inhibited STZ-induced atrophy of Langerhans islets and reduction of islet cells. Also, AG inhibited extensive degeneration of β cells, enhanced cellular density, and restored the pancreatic insulin contents [105]. Second, AG could improve insulin resistance. Insulin resistance is defined as an inadequate response of insulin target tissues to physiological levels of circulating insulin. Inflammation is an important feature of insulin resistance [106]. Therefore, suppression of inflammation is considered a potential therapeutic strategy to improve insulin resistance. In 3T3-L1 adipocytes, impairment of insulin sensitivity and AKT activation caused by TNF-α could be rescued by AG (1, 2, 5 and 10 μg/mL). Further, AG suppressed the phophorylation of IκB kinase beta (IKKβ)/inhibitor of kappaB-alpha (IκBα) and degradation of IκB-α instead of MAPK activation. Meanwhile, AG inhibited the expressions of TNF-α-induced cytokines, such as IL-6, iNOS, suppressor of cytokine signaling 3 (SOCS-3) and MCP-1. This suggested that AG reduced TNF-α-induced insulin resistance through inhibition on NF-κB signaling cascades and its downstream inflammation factors [107]. Moreover, serine phosphorylation of insulin receptor substrates (IRS-1) is tightly involved in insulin resistance [108]. In 3T3-L1 adipocytes, AG (1, 2, 5 and 10 μg/mL) increased the basal glucose uptake dose- and time-dependently. Furthermore, the phosphotyrosine of IRS-1 and recruitment of p85 (PI3K subunit) to IRS-1 are enhanced by AG, which could be abrogated by wortmannin (a PI3K inhibitor). Meanwhile, AG activated the PI3K signaling by increasing phosphorylation of atypical protein kinase C(lambda/zeta) (PKCλ/ζ), glycogen synthase kinase-3beta (GSK3β) and AKT. Therefore, AG ameliorated insulin resistance by mediating the PI3K/AKT pathway [107].

Also, AG could lower blood glucose through non-insulin dependent pathways. Studies have shown that actions of endogenous β-endorphin are recognized to be mediated by the opioid μ-receptors, including the regulation of plasma glucose [109]. Besides, the mediation of opioid delta-receptor located in skeletal muscles with regard to the hypoglycemic effect of β-endorphin-like immunoreactivity (BER) has been demonstrated [110,111]. In the STZ-induced diabetic rats, AG (1, 1.5 and 5 mg/kg) stimulated the release of BER from isolated adrenal medulla, which was reversed by $\alpha 1_A$-adrenoceptor antagonists (prazosin or RS17053). Meanwhile, AG decreased the plasma glucose concentrations in a dose-dependent manner, which was reversed by opioid μ-receptor antagonists (naloxone or naloxonazine) or opioid μ-receptor knockout. These results suggested that AG increased circulating β-endorphin concentrations in the diabetic rats to activate the opioid μ-receptors, resulting in a hypoglycaemic effect [112]. Additionally, insulin deficiency is associated with changes in hepatic metabolism, including increasing the expression of phosphoenolpyruvate carboxylase (PEPCK). Furthermore, reducing the expression of skeletal muscle GLUT4 is responsible for the insulin-mediated reduction in skeletal muscle glucose uptake [113,114]. In the liver of the STZ-diabetic rats, AG (1.5 mg/kg) inhibited the expression of PEPCK, and increased the mRNA and protein levels of GLUT4, which could be abolished by antagonists of opioid μ-receptor. This suggested that AG normalized concentrations of both hepatic PEPCK and muscle GLUT4 in the STZ diabetic rats through activation of opioid μ-receptors [115].

3.2. Anti-AS effect

AS is the leading cause of cardiovascular diseases and is characterized by endothelial dysfunction, activation and aggregation of platelet, formation of foam cells and apoptosis of SMCs [116−118]. Therefore, drugs that can alleviate inflammation, oxidative stress, endothelial dysfunction and cellular abnormalities (e.g. endothelial cell activation, macrophage formation and SMCs migration) may serve as potential candidates for the treatment of AS. AG has been demonstrated as a potential anti-AS agent both in vivo and in vitro (Fig. 4).

3.2.1. Improving pathological changes

Atherosclerosis develops from lipid deposition, a series of inflammatory responses and intimal thickening of the vessel wall, and its pathogenesis is characterized by plaque formation and intimal thickening [119]. AG (10 and 20 mg/kg) ameliorates the pathology of atherosclerosis in vivo, including lipid deposition, intimal thickenings, as well as plaque and foam cell accumulation. Histopathological examination found that AG effectively inhibited lipid deposition and intimal thickenings in rabbits induced by PG. Morphometric analysis found that few red-stained lipid-rich lesions were seen in the aortic tree after oral treatment with AG [120,121]. Meanwhile, there was almost no plaque accumulation in the aortic root of apolipoprote E-deficient ($ApoE^{-/-}$) mice after AG treatment (1 and 2.5 mg/kg) [122]. In addition, AG (40 mg/kg)

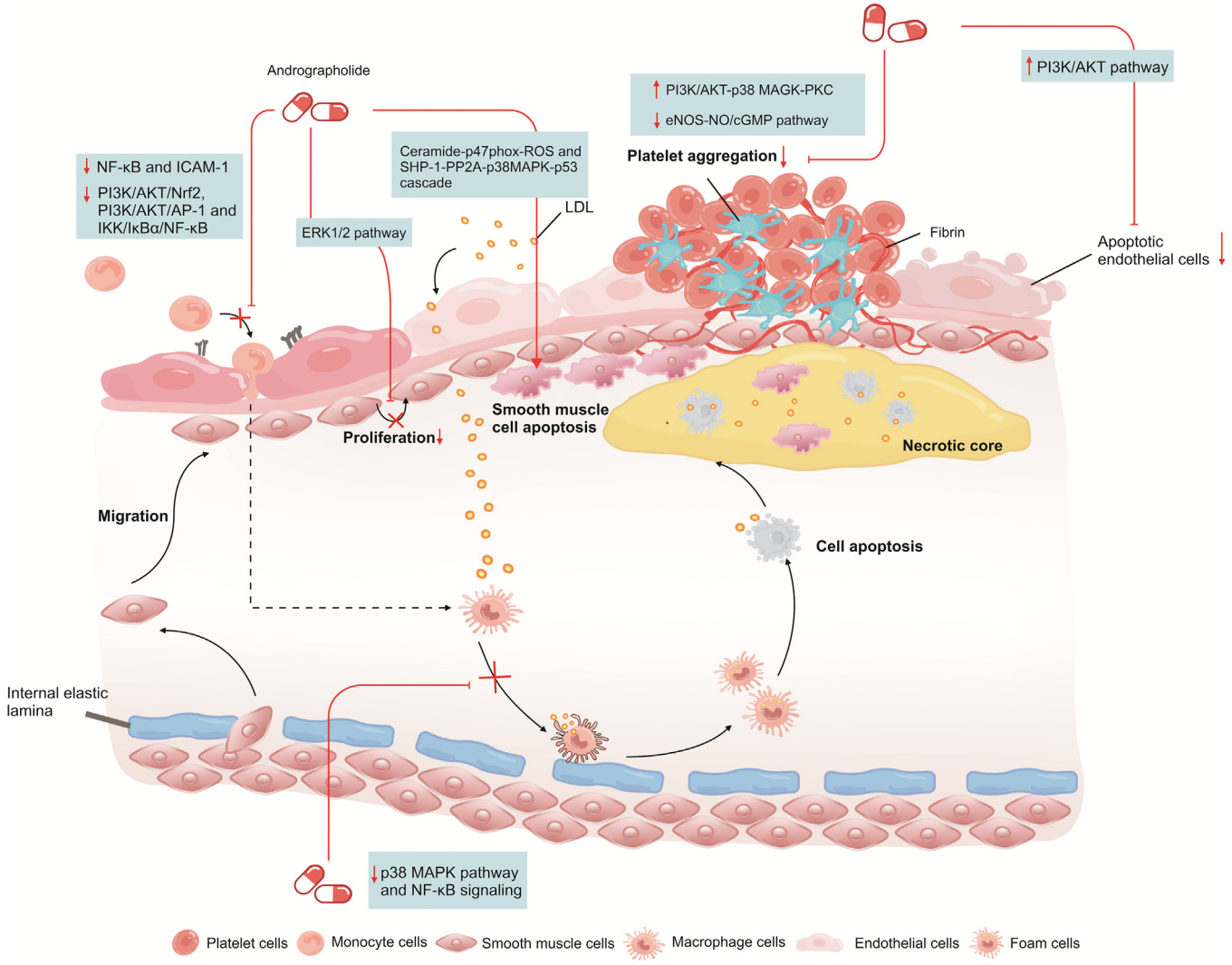

Fig. 4. Inhibition of atherosclerotic lesions by andrographolide (AG). ICAM-1: intercellular adhesion molecule-1; LDL: low-density lipoprotein; NF-κB: noncanonical nuclear factor-kappaB; PI3K: phosphatidylinositol-3 kinase; AKT: protein kinase B; Nrf2: nuclear factor erythroid 2-related factor 2; IKK: ikappaB kinase; IκBα: inhibitor of kappaB-alpha; AP-1: activator protein-1; PP2A: protein phosphatase 2A; P38MAPK: P38 mitogen-activated protein kinase; PKC: protein kinase C; NO: nitric oxide; eNOS: endothelial nitric oxide synthase; PKC: protein kinase C; ERK1/2: extracellular regulated protein kinase 1/2; cGMP: cyclic guanosine monophosphate.

reduced the accumulation of foam cells in atherogenic diet induced rat aortic lesions [123,124].

3.2.2. Inhibiting lipid accumulation

Cholesterol, lipids and metabolic waste products accumulate on vascular wall, resulting in cholesterol deposition and oxidative stress, which contributes to forming atherosclerosis [125]. Studies have shown that AG is effective in inhibiting lipid levels, improving liver and kidney function and suppressing oxidative stress. In aortic atherosclerotic rabbits induced by PG, AG (10 and 20 mg/kg) decreased the levels of TC, TG, LDL-C, and increased high-density lipoprotein cholesterol (HDL-C) level. Moreover, AG improved liver and kidney function by significantly reducing serum levels of alkaline phosphatase (ALP), alanine aminotransferase (ALT), aspartate aminotransferase (AST), creatinine (Cr), and urea (UE). Additionally, AG inhibited oxidative stress in PG induced rabbits. It reduced the levels of C-reactive protein (CRP), malondialdehyde (MDA) and nitrotyrosine and increased the levels of total GSH and antioxidant enzymes such as superoxide dismutase (SOD), catalase (CAT), and GPx [120,121].

3.2.3. Inhibiting systemic inflammatory responses

AG inhibits atherosclerotic lesions by suppressing systemic inflammatory responses. For example, in PG induced rabbits, AG (10 and 20 mg/kg) decreased the serum levels of TNF-α, ICAM-1 and VCAM-1 and increased the expression of α-smooth muscle actin (α-SMA). Moreover, AG decreased the serum levels of MCP-1 and IL-6 in PG rabbits [120,121].

3.2.4. Inhibiting endothelial apoptosis and dysfunction

Apoptosis of ECs occurs in the early stage of AS. It impairs vasodilation and increases endothelial permeability, resulting in the loss of the ability of ECs to regulate lipid homeostasis [126,127]. Therefore, inhibiting endothelial apoptosis is considered an efficient approach to alleviating AS. AG could reduce endothelial apoptosis by suppressing the expressions of apoptosis-related proteins and the PI3K/AKT pathway (Fig. 5). For example, treatment of AG (4.38, 8.76 and 17.52 μg/mL) could decrease the expressions of Bax and caspase-3 and increase the expression of Bcl-2 in human umbilical vein endothelial cells (HUVECs) cultured in a high-glucose medium [128]. Additionally, AG (0.35–35.00 μg/mL) could inhibit apoptosis by

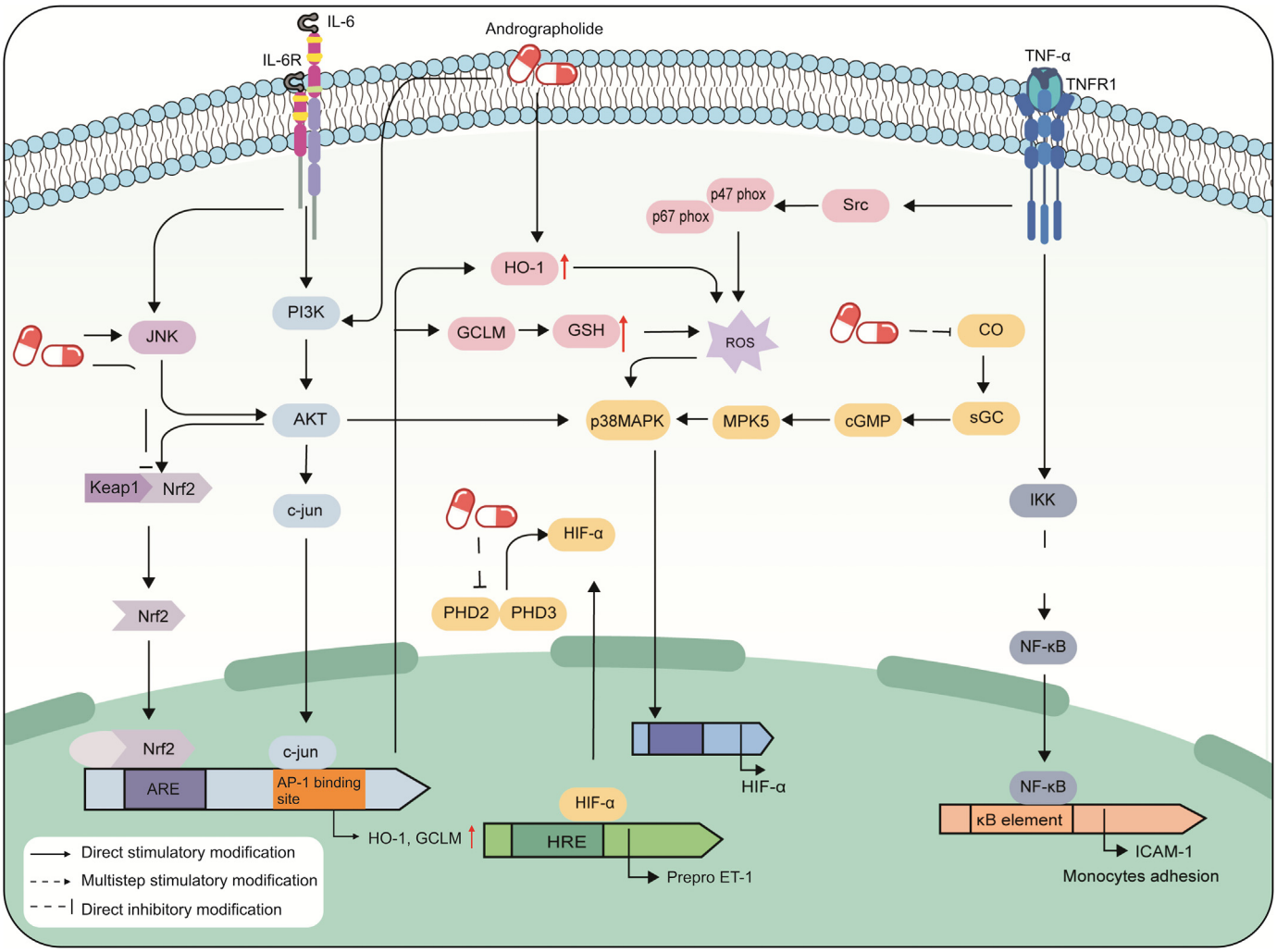

Fig. 5. Schematic representation of the main targets and signaling pathways of ECs regulation by andrographolide (AG). Schematic summarizes that AG inhibited TNF-α-induced inflammation by up-regulating HO-1 and GCLM expression via the PI3K/AKT/Nrf2 and PI3K/AKT/AP-1 pathways. The inhibition of HIF-1α and ET-1 expression by AG was controlled by activation of the Nrf2/HO-1 pathway, production of HO-1 byproducts, inhibition of p38 MAPK activation and enhancement of PHD2/3 expression. IL-6: interleukin 6; ECs: endothelial cells; TNF-α: tumor necrosis factor-alpha; ROS: reactive oxygen species; TNFR1: tumor necrosis factor receptor-1; HIF-1α: hypoxia-inducible factor 1-alpha; HO-1: heme oxygenase-1; GCLM: glutathione cysteine ligase modulatory subunit; PI3K: phosphatidylinositol-3 kinase; AKT: protein kinase B; Nrf2: nuclear factor erythroid 2-related factor 2; AP-1: activator protein-1; ICAM-1: intercellular adhesion molecule-1); P38 MAPK: P38 mitogen-activated protein kinase; JNK: c-Jun amino-terminal kinases; ET-1: endothelin 1; ARE: antioxidant response element; MKP-5: phosphatase-5; GSH: glutathione; PHD 2/3: hydroxylases 2/3 protein; sGC: soluble guanylate cyclase; Keap1: kelch-like ECH-associated protein 1; Src: src-family kinases.

suppressing the expressions of apoptosis-associated cysteine proteases, namely, caspase-3 and caspase-9, in HUVECs. This inhibitory effect was associated with a complex consisting of apoptotic protease activating factor-1 (Apaf-1) and cytochrome C released from the mitochondria. Besides, AG could activate AKT and Bcl-associate death protein (Bad), a downstream target of AKT, in growth factor (GF)-deprived HUVECs. PI3K inhibitors and dominant negative mutants of AKT could reverse the anti-apoptotic effects of AG. However, AG did not affect the expressions of extracellular regulated protein kinase 1/2 (ERK1/2), NOS and NF-κB, suggesting that it reduced apoptosis of HUVECs via the PI3K/AKT pathway, independent of ERK1/2, NOS and NF-κB signaling [129].

Endothelial dysfunction occurs in the early stage of AS and is associated with inflammation, oxidative stress and increases the expression of adhesion molecules [130–134]. In vitro and in vivo studies have shown that AG can improve endothelial dysfunction by inhibiting oxidative stress and inflammation. First, AG (0, 4.38, 8.76 and 17.52 μg/mL) suppresses oxidative stress and inflammation. Exactly, AG exerted anti-oxidative effects by reducing the levels of lactate dehydrogenase (LDH), MDA, IL-1β, IL-6 and TNF-α in HUVECs under high-glucose conditions [128]. Over-expression of hypoxia-inducible factor 1-alpha (HIF-1α) and endothelin 1 (ET-1) can result in the generation of inflammatory responses, which further contribute to the development of AS [135,136]. Therefore, HIF-1α and ET-1 are considered as therapeutic targets for the anti-AS effects of natural compounds. Similar to ROS inhibitors, AG (2.63 μg/mL) could inhibit ROS generation and HIF-1α expression in EA.hy926 cells treated by $CoCl_2$. In addition, AG inhibited $CoCl_2$-induced over-expression of HIF-1α in EA.hy926 cells by increasing hydroxylases 2/3 protein (PHD 2/3) expression, activating Nrf2/HO-1 signaling and suppressing p38 MAPK signaling. Besides, AG increased the protein expression of PHD 2/3 in a time-dependent manner, resulting in hydroxylation and degradation of the HIF-1α protein. However, downregulation of Nrf2 and HO-1 could reverse AG-induced inhibition of the mRNA expression of HIF-1α. Additionally, the mRNA expression and secretion of ET-1 was suppressed by AG and the by-products of HO-1, suggesting that the inhibitory effects of AG on HIF-1α expression were associated with

the Nrf2/HO-1 pathway. Furthermore, AG could inhibit the phosphorylation of p38 MAPK and the expressions of HIF-1α and ET-1 in $CoCl_2$-stimulated EA.hy926 cells. Overall, AG inhibited hypoxia-induced over-expressions of HIF-1α and ET-1 by increasing PHD 2/3 expression, activating the Nrf2/HO-1 signaling and suppressing the p38 MAPK pathway, thereby alleviating endothelial inflammatory responses [137]. Meanwhile, in $CoCl_2$-treated EA.hy926 cells, Lin et al. [138] found that AG (2.63 μg/mL) inhibited the expression of HIF-1α and ET-1 by suppressing the HO-1/CO/cyclic guanosine monophosphate (cGMP)/MAPK phosphatase-5 (MKP-5) pathway. Specifically, AG induced the expressions of HO-1 and MKP-5. Similar to the HO-1 by-product CO and cGMP analogues (8-Br-cGMP), AG increased the expression of MKP-5 and the content of cGMP and inhibited the expressions of HIF-1α and ET-1. However, these changes could be reversed by vanadate (an efficient inhibitor of tyrosine phosphatases and MKPs) and MKP-5 siRNA. Therefore, AG could inhibit the expressions of HIF-1α and ET-1 by inducing MKP-5 expression. However, it did not affect the phosphorylation of AKT or ERK1/2. In conclusion, AG ameliorated inflammation and oxidative stress by activating the Nrf2/HO-1 pathway and inhibiting the p38 MAPK signaling and the HO-1/CO/cGMP/MKP-5 pathway. Second, AG prevented monocyte-endothelial cell adhesion [139]. In particular, AG (0.87–2.63 μg/mL) could inhibit TNF-α-induced over-expression of ICAM-1 in EA.hy926 cells in a dose-dependent manner, resulting in decreased adhesion of HL-60 cells to EA.hy926 cells. Additionally, AG significantly increased the expression of HO-1 and the nuclear translocation rate of Nrf2 and induced antioxidant response element (ARE)-luciferase reporter activity. The inhibitory effects of AG on ICAM-1 expression were significantly reversed by HO-1 siRNA. Therefore, AG could inhibit monocyte adhesion by stimulating Nrf2-dependent expression of HO-1 [140]. In the same model, Chao et al. [141] reported AG (0.18–7.01 μg/mL) suppressed the activation of IKK, phosphorylation of IκBα, nuclear translocation of p65 and DNA binding activity of NF-κB. Moreover, AG reduced the adhesion of EA.hy926 cells to HL-60 cells induced by TNF-α and inhibited ICAM-1 expression. However, cyclic adenosine monophosphate (AMP) response element binding protein (CREB) knockdown did not reverse AG-induced inhibition of ICAM-1, suggesting that AG downregulated ICAM-1 expression by attenuating NF-κB activation instead of CREB activation. Also, in EA.hy926 cells stimulated by TNF-α, AG could inhibit ROS generation, ICAM-1 expression and adhesion to HL-60 cells. Notably, AG reduced TNF-α-induced ROS generation, which was essential for Src phosphorylation. In addition, AG inhibited Src phosphorylation, thereby suppressing the expression of ICAM-1 and the adhesion of EA.hy926 cells to HL-60 cells. Also, it repressed the activation of nicotinamide adenine dinucleotide phosphate (NADPH) p47phox and p67phox oxidases and nuclear translocation of p65, which could be reversed by NADPH inhibitors (apocynin and diphenyleneiodonium). Moreover, AG (2.63 μg/mL) increased the expressions of HO-1 and GSH-associated, glutathione cysteine ligase modulatory subunit (GCLM) instead of glutamate-cysteine ligase regulatory subunit (GCLC). Meanwhile, AG increased the expressions of HO-1 and GCLM by inducing the nuclear translocation of Nrf2 and phosphorylation of the activator protein-1 (AP-1) transcriptional factor c-Jun. However, these effects could be reversed by the PI3K/AKT inhibitor LY29400, suggesting that AG suppressed ICAM-1 expression and cell adhesion by increasing the expressions of HO-1 and GCLM via the PI3K/AKT/Nrf2 and PI3K/AKT/AP-1 pathways [142]. Similarly, Lin et al. [143] reported that AG (2.63 and 5.26 μg/mL) inhibited TNF-α-induced ICAM-1 expression and the adhesion of EA.hy926 cells to HL-60 cells via the IKK/IκBα/NF-κB pathway. Additionally, AG could inhibit the phosphorylation of IKKβ and IκBα, degradation of IκBα and nuclear translocation of p65 in EA.hy926 cells and mitigate the binding of NF-κB to the IκB site on the ICAM-1 promoter. In conclusion, AG inhibited the adhesion of monocytes to ECs through the PI3K/AKT/Nrf2, PI3K/AKT/AP-1 and IKK/IκBα/NF-κB pathways and by suppressing NF-κB activation.

3.2.5. Inhibiting platelet activation and aggregation

Several studies have shown that promoting platelet apoptosis hinders progress of AS [144–146]. Lien et al. [147] found that AG (8.76–35.00 μg/mL) limited platelet lifespan by causing an exogenous apoptotic pathway dependent on caspase-8 (Fig. 6). In washed human platelets stimulated by collagen, AG could eliminate platelet mitochondrial membrane potential ($\Delta\psi m$) by an around two-fold increase compared to the solvent control and activate extrinsic apoptosis pathway protein caspase-3, caspase-8 and Bid in a concentration-dependent manner. Besides, AG-induced over-expression of caspase-8 could be inhibited by the caspase-8 inhibitor z-IETD-fmk, but not by the anti-Fas receptor (ZB4) and anti-tumor necrosis factor-R1 (H398) monoclonal antibodies. Therefore, AG-induced platelet apoptosis was associated with the exogenous apoptotic pathway.

Platelet activation and aggregation are associated with all stages of inflammation-related AS, from endothelial dysfunction, plaque rupture to atherothrombotic events [148,149]. First, AG can effectively inhibit platelet aggregation. In vivo, AG (0.022 and 0.055 mg/kg) could reduce adenosine diphosphate-induced thrombotic mortality, inhibit p38MAPK and p47 phosphorylation, and prolong platelet thrombosis in the sodium fluorescein-induced mice, indicating that AG was effective in preventing thromboembolism [150]. In vitro, AG (0.35–35.00 μg/mL) inhibited human platelet aggregation induced by thrombin, collagen, platelet-activating factor (PAF), arachidonic acid (AA), and U46619 in a concentration- and time-dependent manner [149–152]. However, Thisoda et al. [151] found that AG (8.76–35.00 μg/mL) had no remarkable effects on thrombin induced platelet aggravation. Moreover, Arnroyan et al. [152] found AG (0.35, 3.50 and 35.00 μg/mL) inhibited PAF-induced human platelet aggregation, with equal efficiency to PAF-antagonists Ginkgo extract (Ginkgo hi/aha) containing Ginkgolides. However, the underlying mechanism of AG was different from that of non-steroidal anti-inflammatory drugs (NSAID), which was mainly evidenced by the fact that AG made no differences to the calcium ionophore and AA-induced biosynthesis of any 5-, 12- and 15-lipoxygenase pathway products, such as LTB4, 6E-LTB4, 5(S) 6E-LTB4, 5-HETE, 12-HETE and 15-HET, and 12-HHT (the cyclooxygenase product). Second, AG inhibits platelet activation and aggregation. Notably, AG (0.35–35.00 μg/mL) inhibited thrombin-induced platelet aggregation and extracellular signal-regulated kinase 2 (ERK2) phosphorylation in human platelet, suggesting that AG inhibited platelet aggregation by inhibiting the ERK1/2 pathway [151]. Moreover, in human platelets, AG (8.76–26.28 μg/mL) inhibited collagen-induced [Ca^{2+}] mobilization, thromboxane B(2) (TxB-2) formation, phospholipase Cγ2 (PLCγ2) and p47 phosphorylation, but does not affect AA- or thrombin-stimulated TxB-2 formation and sorbitol-12,13-dibutyrate (PDBu)-induced p47 phosphorylation. Furthermore, AG could inhibit collagen-stimulated platelet activation, stimulate eNOS phosphorylation and nitrate formation, and increase cyclic GMP (cyclic nucleotides) level but not cyclic AMP, which could be reversed by 1H- [1,2,4] oxadiazolo[4,3-a]quinoxalin-1-one (ODQ) (an inhibitor of guanylate cyclase), protein kinase C (PKC) inhibitor (Ro318220) and N (omega)-nitro-L-arginine methyl ester (L-NAME) (a NOS inhibitor). Therefore, AG inhibited platelet activation through the eNOS/NO/cGMP pathway. In addition, ODQ reversed AG-induced phosphorylation of VASP Ser157. In parallel, AG stimulated the phosphorylation of ERK2, JNK1/2 and p38 MAPK which could be reversed by inhibitors of ODQ and PKC. Therefore, AG inhibited platelet

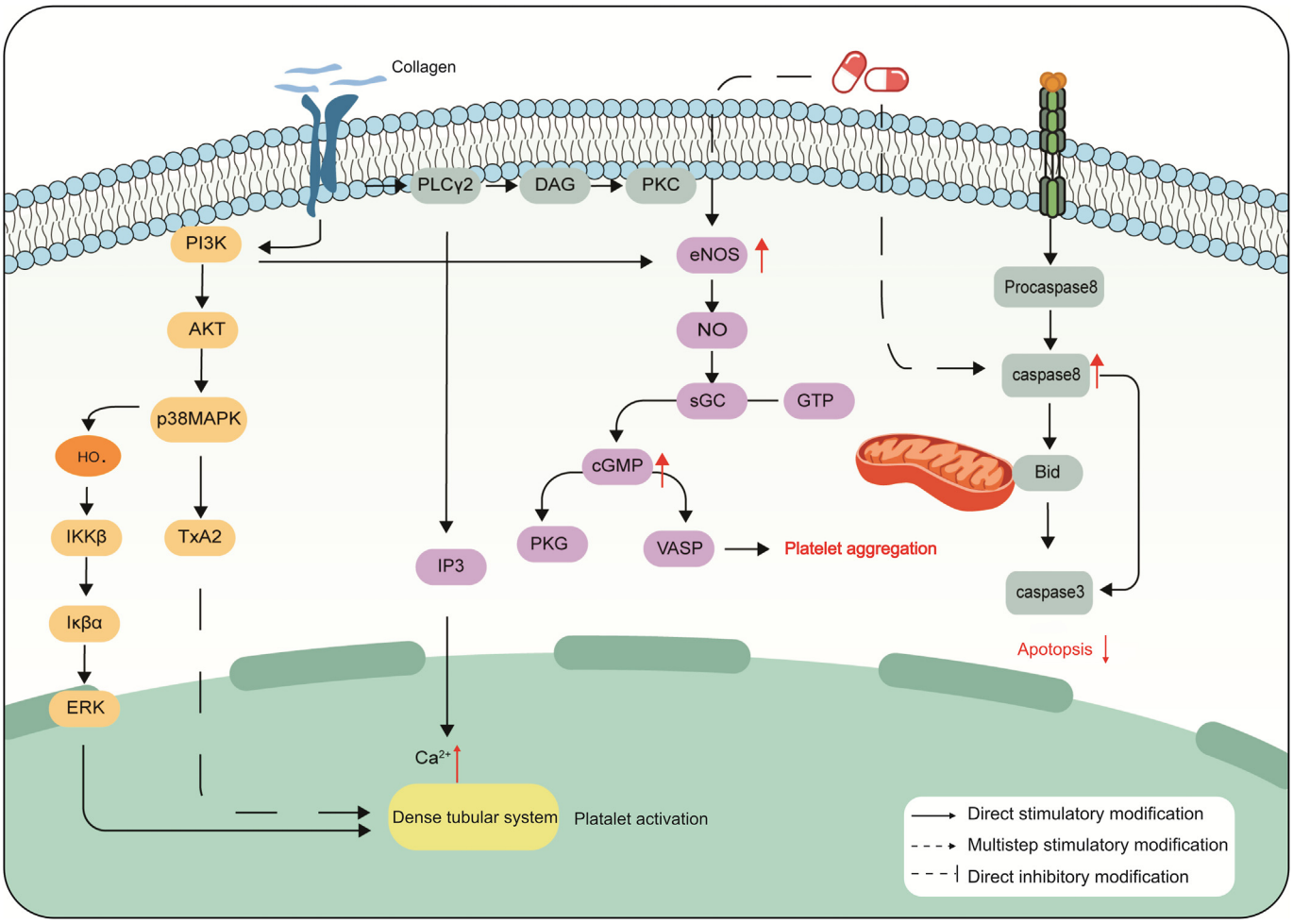

Fig. 6. Schematic representation of the main targets and signaling pathways of platelet regulation by andrographolide (AG). Schematic summarizes that AG could activate the eNOS–NO–cyclic GMP pathway, inhibit the PLCγ2-PKC and PI3 kinase/AKT cascades, and ultimately inhibit platelet aggregation. And AG activated caspase-8 and caspase-3, induced Bid cleavage, and caused platelet apoptosis. Sgc: soluble guanylate cyclase; VASP: vasodilator-stimulated phosphoprotein; PI3K: phosphatidylinositol-3 kinase; AKT: protein kinase B; P38 MAPK: P38 mitogen-activated protein kinase; DAG: diacylglycerol; IP3: inositol triphosphate; IKKβ: IκB kinase beta; NO: nitric oxide; eNOS: endothelial nitric oxide synthase; PKC: protein kinase C; PKG: protein kinase G; PLCγ2: phospholipase Cγ2; TxA2: thromboxane A2; ERK: extracellular regulated protein kinase; IκBα: inhibitor of kappaB-alpha; cGMP: cyclic guanosine monophosphate; GTP: guanosine triphosphate.

aggregation by activating the eNOS/NO/cGMP pathway, thereby inhibiting the PI3K/AKT/p38 MAPK and PLCγ2/PKC cascade responses [150]. Furthermore, Lu et al. [153] found that AG (12.3 and 26.3 μg/mL) also inhibited platelet activation and aggregation via a GMP/protein kinase G (PKG)-dependent cyclic pathway. To be specific, AG inhibited collagen-stimulated activation of NF-κB and phosphorylation of IKKβ and p65, which could be reversed by ODQ and PKG inhibitors. At the same time, AG inhibited collagen-stimulated phosphorylation of p38 MAPK and ERK2, and reduced the formation of hydroxyl radicals, which was alleviated by PKG inhibitors. In short, the inhibitory effects of AG on platelet activation and aggregation are mainly achieved through inhibition of the ERK1/2 and GMP/PKG pathways, and activation of the eNOS/NO/cGMP pathway.

3.2.6. *Inhibiting macrophage inflammation and foam cell formation*

Studies have shown that AG inhibits inflammatory responses and foam cells formation by increasing cholesterol efflux and preventing the production of NO (Fig. 7). AG exerts anti-inflammatory effects through the NF-κB signaling pathway. In RAW264.7 cells with ox-LDL-induced inflammation, AG could decrease the expressions of MCP-1 and IL-6. These effects were similar to those of PDTC (a selective NF-κB inhibitor). Additionally, AG (0.35 or 1.75 μg/mL) decreased p-p65 levels in a dose-dependent manner, indicating that it exerted anti-inflammatory effects by inhibiting NF-κB signaling pathway [122]. Similarly, in lipopolysaccharide (LPS)–treated RAW264.7 cells and found that the combination of Notch1 siRNA and AG-loaded nanoparticle (A-NP) (1.75 μg/mL) inhibited LPS-induced over-expressions of MCP-1 and IL-6 and the NF-κB signaling pathway and increased expressions of interleukin 10 (IL-10) and arginase-1 more significantly than A-NP. These results suggested that combination therapy based on Notch1 siRNA and A-NP was a viable strategy for the treatment of AS and enhanced the anti-inflammatory effects of AG [154].

AG inhibits the formation of foam cells by preventing the phagocytosis of cholesterol from macrophages. Notably, AG (0.18, 0.35 and 1.75 μg/mL) could reduce cholesterol uptake and the mRNA and protein expression of CD36 in J774A.1 (a murine macrophage cell line) and RAW264.7 cells stimulated by ox-LDL. However, AG did not affect the protein expressions of SREBP-1c or class A scavenger receptor (SR-A) [122,155]. Furthermore, AG (0.18 and 0.35 μg/mL) could enhance the binding of liver X receptor alpha (LXRα) to DNA and upregulate the mRNA and protein expressions of ABC transporters such as ABCA1 and adenosine

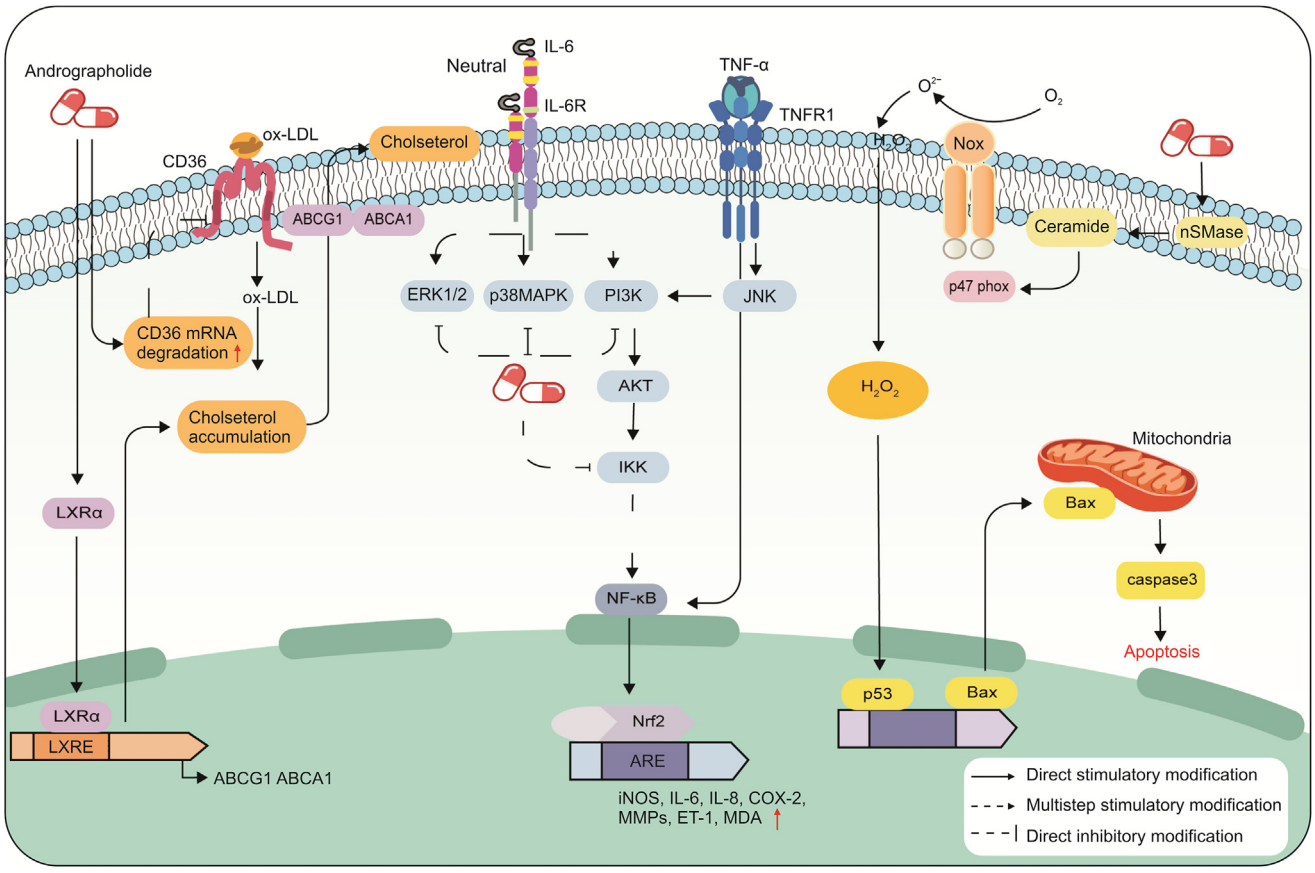

Fig. 7. Schematic representation of the main targets and signaling pathways of foam cells and VSMCs regulation by andrographolide (AG). Schematic summarizes that AG inhibited foam cell formation by activating LXRα, increasing ABCA1 and ABCG1 expression, stimulating degradation of CD36 mRNA, blocking the p38 MAPK and NF-κB pathways, and reducing the levels of NF-κB p65, p-p38 MAPK and p-ERK1/2. In addition, AG stimulated the ceramide-mediated signal events, resulting in the activation of the p47phox-ROS cascade, ultimately stimulating active caspase-3 expression and VSMC apoptosis. IL-6: interleukin 6; IL-6R: interleukin 6 receptor; TNF-α: tumor necrosis factor-alpha; ROS: reactive oxygen species; TNFR1: tumor necrosis factor receptor-1; COX-2: cyclooxygenase-2; MDA: microdermabrasion; MMPs: matrix metalloproteinases; iNOS: inducible nitric oxide synthase; IL-8: interleukin 8; NOX: NADPH oxidase; ET-1: endothelin 1; ox-LDL: oxidized low-density lipoprotein; LXRα: liver X receptor alpha; PI3K: phosphatidylinositol-3 kinase; AKT: protein kinase B; P38 MAPK: P38 mitogen-activated protein kinase; IP3: inositol triphosphate; IKK: ikappaB kinase; ABCG1: adenosine triphophate (ATP)-binding cassette (ABC) transporter G1; CD36: cluster of differentiation 36; ABCA1: ATP-binding cassette (ABC) transporter A1; JNK: c-Jun amino-terminal kinases; NF-κB: noncanonical nuclear factor-kappaB; ARE: antioxidant response element; LXRE: LXR response element; nSMase: neutral sphingomyelinase; ERK1/2: extracellular regulated protein kinase 1/2.

triphophate ABC transporter G1 (ABCG1) in J774A.1 cells stimulated by ox-LDL. However, these effects could be reversed by LXRα siRNA and geranylgeranyl pyrophosphate (GGPP) (an antagonist of LXRα). Therefore, AG inhibited the formation of foam cells by activating LXRα, increasing the expressions of ABCA1 and ABCG1, promoting cholesterol efflux and stimulating the degradation of cluster of differentiation 36 (CD36) mRNA [155]. Studies have shown that NO promotes the uptake of LDL-C by macrophages, thereby promoting the formation of foam cells [156]. Inhibition of NO synthesis reduces the formation of foam cells. Indeed, AG (3.50 or 10.51 μg/mL) could inhibit NO synthesis by directly or indirectly interfering with the synthesis and activity of iNOS in LPS-induced RAW 264.7 cells [157]. In LPS/interferon-γ (IFN-γ) induced cells, AG (0.35– 35.00 μg/mL)could inhibit the accumulation of nitrite accumulation and protein expression of iNOS and reduce the stability of iNOS protein. Similar to cycloheximide (an inhibitor of protein synthesis), AG suppressed *de novo* protein synthesis, which could be demonstrated via [35S]-methionine incorporation [158]. Therefore, AG (50 μg/mL) suppressed NO generation by promoting iNOS degradation and reducing *de novo* protein synthesis in LPS-induced RAW 264.7 cells. Furthermore, AG could decrease the levels of NF-κB p65, p-p38 MAPK and p-ERK1/2 without affecting the activation of p-JNK in mouse peritoneal macrophages stimulated by ox-LDL. This phenomenon suggested that AG could reduce the formation of foam cells by blocking the p38MAPK and NF-κB pathways [159].

3.2.7. *Inducing apoptosis, inflammation and proliferation of VSMCs*

Apoptosis of VSMCs plays a key role in the pathogenesis and progression of AS. Studies have shown that AG induces apoptosis of VSMCs via the ceramide/p47phox/ROS and Src homology 2 domain-containing protein tyrosine phosphatase 1 (SHP-1)/protein phosphatase 2A (PP2A)/p38MAPK/p53 cascades. In rat VSMCs, AG (17.52 μg/mL) could enhance the activation of p53, Bax and caspase-3 and phosphorylation of the NADPH oxidase (NOX) subunit p47phox. However, pre-treatment with ROS scavengers could suppress these changes. AG increased ceramide activity and promotes p47phox phosphorylation, both of which could be significantly attenuated by the neutral sphingomyelinase (nSMase) inhibitor 3-O-methyl-sphingomyeline (3-OMS). In brief, AG increased ROS levels by activating ceramide and p47phox, resulting in apoptosis of VSMCs [160]. It could increase the expressions of Bax, caspase-3 and caspase-9 and decrease $\Delta\psi m$, thereby inducing apoptosis in rat VSMCs. Furthermore, AG (7.01 or 17.52 μg/mL) increased the phosphorylation of p53 Ser-15 and p38 MAPK, which could be suppressed by p38MAPK inhibitors, indicating that AG-induced phosphorylation and activation of p53 were mediated by the p38 MAPK pathway. Besides, AG could increase the activity of

PP2A, the expression of p38 MAPK and phosphorylation of p53 and caspase-3 in rat VSMCs, which could be inhibited by PP2A siRNA. Therefore, the effects of AG on the p38 MAPK/p53 cascade were associated with the modulation of PP2A. Furthermore, AG significantly inhibited the phosphorylation of PP2A at the tyrosine 307 (Tyr307) residues, which could be reversed by SHP-1 inhibitors or SHP-1 siRNA, but had no effects on the demethylation of PP2A-C. Therefore, AG might activate PP2A by regulating the phosphorylation of PP2A-C at Tyr-307, and increase the activity of SHP-1 and its phosphorylation at Tyr564. Overall, AG induced apoptosis of VSMCs through the SHP-1/PP2A/p38MAPK/p53 cascade [161].

Studies have shown that neointimal hyperplasia in arterial restenosis is closely related to inflammatory responses. In a study on mouse models of arterial restenosis, AG (5 mg/kg) could decrease the expressions of NF-κB target genes, including tissue factor (TF), E-selectin and VCAM-1, and the deposition of leukocytes ($CD68^+$ macrophages). However, these changes were not observed in $p50^{-/-}$ mice, suggesting that AG had abrogative effects on the *p50* gene and was a special inhibitor of *p50* [162]. Additionally, in rat models with autogenous vein grafts, AG could significantly decrease the mRNA and protein expressions of E-selectin, p65 and MMP-9 [163]. In another study, the primary mechanism underlying AG-induced inhibition of vascular inflammation was the inhibition of NF-κB activation induced by AG via the JNK/AKT/p65 and nSMase/ceramide/PP2A cascades. Notably, AG (7.01 and 17.52 μg/mL) suppressed vascular inflammation by reducing the phosphorylation of JNK and AKT without altering the phosphorylation of p38 MAPK or ERK1/2 in TNF-α-induced VSMCs. However, AG and inhibitors of PI3K/AKT and JNK could inhibit TNF-α-induced phosphorylation of p65 and AKT, suggesting that AG suppressed p65 phosphorylation by inhibiting the JNK/AKT signaling. Besides, AG could inhibit TNF-α-induced NF-κB activation by phosphorylating p65 instead of degrading IκBα. Therefore, AG mediated NF-κB activation through the JNK/AKT/p65 cascade in TNF-α-stimulated VSMCs [164]. Further, Hsieh et al. [165] found that AG (7.01 and 17.52 μg/mL) could attenuate vascular inflammation and MMP-9 activity without affecting MMP-2 in LPS/IFN-γ-induced VSMCs. Additionally, it could inhibit the expression of NF-κB, a transcription factor that promotes the expressions of inflammation-related proteins (MMP-9 and iNOS). Although AG inhibited LPS/IFN-γ-induced binding of p65 to NF-κB and slightly reduced the levels of IκBα phosphorylation induced by LPS/IFN-γ, it failed to restore the levels to normal. This phenomenon suggested that AG-induced phosphorylation of IκBα did not involve in the inhibition of NF-κB activation. Moreover, AG could inhibit NF-κB expression by suppressing p65 Ser536 and increasing PP2A activity instead of IKK phosphorylation. AG-induced Ser536 dephosphorylation and iNOS downregulation could be inhibited by the PP2A inhibitor okadaic acid and PP2A siRNA. Meanwhile, AG-induced ceramide formation, PP2A activation, p65 Ser536 dephosphorylation and iNOS expression could be suppressed by the nSMase inhibitor 3-OMS. In conclusion, AG inhibited inflammatory responses by suppressing NF-κB activation through the nSMase/ceramide/PP2A and JNK/AKT/p65 cascades.

Overproduction of pro-inflammatory cytokines and cytokine signaling in AS promote the proliferation of SMCs, which can be inhibited by AG [166]. In platelet-derived growth factor-BB (PDGF-BB)-induced VSMCs, AG (3.50– 7.01 μg/mL) could down-regulate the expression of proliferating cells nuclear antigen (PCNA) in a concentration-dependent manner and inhibit PDGF-BB-induced phosphorylation of ERK1/2. Therefore, AG inhibited the proliferation of VSMCs via the ERK1/2 signaling pathway [167].

3.3. Anti-ASCVD effect of AG

3.3.1. Anti-CHD effect of AG

CHD is a dynamic process of interaction between endothelial dysfunction and inflammatory responses [168]. NF-κB activation regulates inflammatory factors (IL-1β, IL-6 and TNF-α) and cytokines/chemokines [169,170]. PPARα, a major transcriptional regulator of energy metabolism, is essential for the regulation of inflammation and angiogenesis [171]. Shu et al. [172] reported that AG (10 and 50 mg/kg) alleviated endothelial cell disorder by increasing the levels of NO and prostaglandin I2 (PGI2) and decreasing the levels of thromboxane A2 (TxA2) and ET-1 in the HFD-induced CHD mice. To improve fibrinolytic activity and decrease coagulation function, AG upregulated t-PA level and decreased plasminogen activator inhibitor-1 (PAI-1) level. Moreover, AG ameliorated the macrophage phenotype and myocardial inflammation by decreasing the CD86+/CD206+ ratio in macrophages, and the levels of TNF-α, MCP-1, hs-CRP and IL-1β in myocardial tissue and serum. However, these phenomena were attenuated by GW6471 (a PPARα antagonist), suggesting that inhibition of AG on endothelial dysfunction and inflammation was associated with PPARα. Furthermore, AG inhibited cardiac apoptosis by increasing the expression of caspase-3 and activity of PPARα, and decreasing the protein of NF-κB (p65 and IκBα). Therefore, AG regulated the PPAR and NF-κB signaling pathways and thus alleviated myocardial injury, endothelial dysfunction and inflammatory response during coronary heart disease.

Studies have shown that reperfusion therapy is considered to be the most effective measure when an ischaemic attack has occurred [173]. However, myocardial ischemia-reperfusion therapy may induce damage and dysfunction in cardiomyocytes, thereby exacerbating ischaemic myocardial injury [174]. AG (1.75 or 3.50 μg/mL) protected cardiomyocytes from hypoxia/reoxygenation (H/R) damage through increasing activities of antioxidant enzymes and increasing the level of GSH. In particular, AG could increase the levels of SOD, CAT, GR, and Gpx and decrease MDA level in neonatal rat cardiomyocytes (NRCs) subjected to H/R damage. However, AG did not have a significant protective effect on NRCs during hypoxia. In addition, the cardio protective effect of AG was mediated through up-regulation of intracellular GSH level, independent of peroxidase activity. This protective effect disappeared completely after treatment of L-Buthionine-sulfoximine (BSO) (a specific γ-glutamate cysteine ligase (GCL) inhibitor) instead of 3-amino-1,2,4-triazole (ATA) (a specific peroxidase inhibitor), further confirming that the cardio-protective effect of AG on cardiomyocytes was associated with GSH. Moreover, regulation of 12-*O*-tetradecanoylphosphate 13-acetate response element (AG-1) and ARE were involved in the mRNA and protein expressions of GCLM and GCLC increased by AG. Furthermore, the higher induction of GCLM mRNA by AG was attributed to its higher induction of GCLM-ARE1 than GCLC-ARE4 [175].

MI is usually resulted from prolonged myocardial cell death caused by ischemia [176]. Histopathological findings revealed that AG (20 mg/kg) improved histological lesions in the hearts of rats with ISO-induced MI, including reduction of myocardial infarction area, maintenance of normal heart morphology and color, reduction in inter tissue edema, and repairing of myocardial cell damage [177,178].

Studies have shown that AG is effective in suppressing MI through maintaining cardiac function index, biological characteristic index, and myocardial injury biomarkers, and inhibiting prolongation of cardiac myocytes action potential duration (APD). In

the MI mice induced by ISO, AG (20 mg/kg) remarkably ameliorated electrocardiography profile and cardiac dysfunction by maintaining heart rate (HR) and ST-segment, and decreasing (±) dp/dt. One study have shown that AG suppressed ISO-induced (±) dp/dt in rat cardiomyocytes by alleviating overload of intracellular Ca^{2+} and enhancing intracellular Ca^{2+} cycling [178]. Besides, pre-treatment of AG (20 mg/kg) could decrease heart weight/body weight (HW/BW) ratio, heart weight/tibia length (HW/TL) ratio, lung weight (LW)/BW, and heart weigh in the ISO-induced rats. However, there was no difference of tibia length (TL) and BW among groups. Besides, AG inhibited increase of creatine kinase (CK) and creatine kinase-MB fraction (CK-MB), LDH, AST, and troponin I (cTnI). In vivo and in vitro, AG prevented APD prolongation by decreasing the peak L-type Ca^{2+}(ICaL) density and increasing the transient outward potassium current (Ito) in the ISO mice and isolated cardiomyocytes. Therefore, the protective mechanism of AG against MI was related to the inhibition of L-type Ca^{2+} and the increase of transient outward K^{+} current [177,178].

Studies have shown that AG prevents MI by inhibiting inflammatory responses and mediating the Nrf2/HO-1 pathway in vivo and in vitro. In the left coronary artery ligation (LAD) ligation mice model, AG (25 mg/kg) protected cardiac remodeling against MI by improving cardiac dysfunction indexes and suppressing myocardial hypertrophy markers and myocardial fibrosis-associated proteins. Furthermore, to inhibit inflammatory responses caused by MI, AG suppressed the expressions of CD45 and CD68 and the levels of TNF-α, IL-1β, IL-6 and MCP-1. Additionally, AG inhibited oxidative stress via the Nrf2/HO-1 pathway in the LAD mice. Notably, it promoted the expressions of Nrf2 nuclear translocation and HO-1, a downstream signal molecule of Nrf2 without altering HIF-1α. Meanwhile, AG inhibited ROS generation, increased the mRNA expressions of Gpx, superoxide dismutase 2 (SOD2) and NADPH dehydrogenase quinine 1 (NQO1), and downregulated the transcription of p67 phox, Gp91 and NADPH oxidase (NOX4). In vitro, both of the Nrf2 inhibitor (ML385) and Nrf2 siRNA inhibited Nrf2 expression and promoted ROS generation in H9C2 cells. However, AG did not reverse this phenomenon, suggesting the antioxidant effect of AG was attributed to Nrf2 activation. Therefore, AG inhibited oxidative stress by activating the Nrf2/HO-1 pathway both in vivo and in vitro, and in turn alleviated MI [179].

3.3.2. Anti-cerebral haemorrhage and cerebral ischemia of AG

Cerebral ischemia induces the loss of blood supply followed by a cascade of events including glutamate excitotoxicity, calcium overload, oxidative stress and inflammation, leading eventually to cell death. In fact, AG ameliorated ischemic brain damage by inhibiting oxidative stress, inflammation as well as apoptosis. In vivo models of cerebral ischemia, AG (30, 60 and 120 mg/kg) attenuated pathological abnormalities, including atrophy of neuronal nuclei (NeuN), microglia infiltration, neuronal disorders and tissue edema in the hippocampal region [180]. In addition, AG (0.01, 0.1 and 1 mg/kg) inhibited microglia activation, and reduced infarct volume and neurological deficits in a rat model of permanent middle cerebral artery occlusion (pMCAO) [181].

First, AG exerts protective effects against cerebral ischemia by inhibiting oxidative stress. In the middle cerebral artery occlusion (MCAO) rats, AG (0.1 mg/kg) markedly reduced MCAO-induced free radical production, which was reversed in the presence of the inhibitor of HO-1(ZnPP). It was shown that AG inhibited free radical formation induced by MCAO by mediating HO-1 expression. Meanwhile, AG elevated the expressions of HO-1 mRNA and protein, and the phosphorylation of ERK1/2, p38 MAPK, and JNK1/2, which could be abolished by p38 MAPK inhibitor. These results suggested that AG mediated HO-1 expression through p38MAPK. Besides, Nrf2 siRNA or p38 MAPK inhibitor could abolish HO-1 down-regulation and Nrf2 expressions induced by AG. Therefore, AG enhanced HO-1 expression through the p38 MAPK-Nrf2 pathway in the MCAO rats [182]. Second, AG exerts a protective effect against cerebral ischemia by reducing inflammation. Notably, AG (0.01, 0.1 and 1 mg/kg) attenuated pMCAO-induced increase in cytokines (IL-1β and TNF-α) and prostaglandin E2 (PGE2) levels in ischemic brain areas. In addition, AG suppressed NF-κB activation through hindering the translocation of p65. These results showed that AG exerted anti-inflammatory effects in the cerebral ischemia model through suppressing NF-κB activation, resulting in reduction in the production of IL-1β, TNF-α, and PGE2 [181]. Moreover, AG attenuated the inflammatory responses by regulating the expression of important proteins in the PI3K/AKT pathway, thereby providing protection against ischemia-reperfusion injury in rats. In cerebral ischemia-reperfusion injury (CICR) model, AG (30, 60 and 120 mg/kg) increased Nissl-positive cells and NeuN expression, and decreased glial fibrillary acidic protein (GFAP) expression. Compared with the CICR group, the serum BDNF level and BDNF mRNA level in the brain tissues were significantly increased in mice pre-treated by AG. Besides, AG increased the levels of TRκB and downstream proteins p-PI3K and p-AKT, and decreased the levels of IL-1β, IL-6 and TNF-α. Overall, AG played a protective role against cerebral ischemia-reperfusion injury in mice by reducing the inflammatory responses and cell apoptosis, and regulating the PI3K/AKT pathway [180]. Further, the protective effect of AG (0.01–0.1 mg/kg) on CICR mice was through inhibition of PI3K/AKT dependent NF-κB and HIF-1α activation. Notably, AG inhibited ROS level and nitrotyrosine formation, decreased the expressions of pro-oxidative enzymes (NOX2 and iNOS) and inhibited the infiltration of inflammatory cells (CD11b). Furthermore, AG decreased the expressions and activation/nuclear translocation of p65 NF-κB and HIF-1α. In oxygen-glucose deprivation (OGD)-induced BV-2 cells, generations of NO and ROS were suppressed by AG (1.75–3.50 μg/mL) and PI3K inhibitor. Further, like AG, PDTC (a NF-κB inhibitor), echinomycin (an inhibitor of HIF-1α), and L-NAME (a nonspecific NOS inhibitor) inhibited OGD-induced NO production. Overall, the inhibition of OGD-induced NO production by AG was related to activation of NF-κB and HIF-1α. Similarly, an inhibitor of NOX suppressed the ROS production. Therefore, AG significantly ameliorated cerebral ischemic/reperfusion (CI/R)-induced production of ROS and NO as well as protein nitrosylation by inhibiting the PI3K/AKT-dependent NF-κB and the HIF-1α pathways [183].

Finally, AG ameliorated cerebral ischemic injury by inhibiting apoptosis of brain microvascular endothelial cells (BMECs). It had shown that AG (3.50 μg/mL) promoted tube formation and alleviated MMP injury in bEnd.3 cells subjected to OGD. Further, AG suppressed endothelial barrier leakage, mitochondrial oxidative stress and inflammatory responses by increasing the levels of transendothelial electrical resistance (TEER) and MDA, and decreasing the levels of EB-albumin, ROS, SOD and CAT and the expressions of IL-1β and TNF-α. Moreover, AG up-regulated the expressions of TJ membrane proteins (ZO-1, Occludin and Claudin 5), Nrf2 and HO-1. Meanwhile, AG suppressed OGD-induced apoptosis by decreasing the number of terminal deoxynucleotidyl transferase-mediated dUTP nick end labeling (TUNEL)-positive apoptotic cells. This indicated that AG alleviated OGD-induced endothelial permeability impairment and apoptosis by reducing Nrf2-associated mitochondrial oxidative stress and inflammation [184].

Studies have shown that AG can ameliorate intracerebral haemorrhage (ICH) induced SBI by inhibiting neuroinflammation. Li et al. [185] found AG (0.5, 1 and 2 mg/kg) could improve ICH -induced SBI in rats by decreasing brain water content and reducing the TUNEL-positive and FJB-positive cell numbers. Additionally, AG significantly improved microglia infiltration, decreased the levels of

IL-6, p65and TNF-α, and inhibited the phosphorylation of IκBα. Besides, caspase-1 activation and Gasdermin-D (GSDMD) cleavage that was related to NLRP3 inflammasome activation and pyroptosis were reduced after treatment of AG. Meanwhile, AG inhibited the interaction of adapter protein apoptosis associated speck-like protein containing a CARD (ASC) with caspase-1 (Casp-1) or NLRP3. In vitro, AG also decreased the levels of IL-6, TNF-α, IL-1β, and LDH, and increased neuronal cell viability in oxyHb-induced microglia. Meanwhile, AG inhibited p65 nucleus translocation and NLRP3/ASC/CASP-1 complex formation. Overall, AG could attenuate neuroinflammation and improve SBI through hindering the NF-κB signaling pathway and NLRP3 inflammasome activation.

In addition, we collated the literature on AG in the treatment and prevention of ASCVD (Table 1). In Table 1 we list detail information, model, dosage and time, and application.

4. Toxicity and adverse reactions

AG can cause certain side effects in clinical settings. For example, intravenous infusion of AG (100–750 mg, intravenous drip once a day, 1–6 doses; cumulative dose 690 ± 670 mg) could cause acute renal tubular necrosis, accompanied by abdominal pain, decreased urine volume, nausea or vomiting [186]. In a phase-I clinical study on the use of AG (5 mg/kg for 3 weeks, escalating to 10 mg/kg for 3 weeks, and to 20 mg/kg for a final 3 weeks, oral) for treating HIV, AG caused mild-to-moderate adverse events, such as headache, fatigue, rash, bitter/metallic/decreased taste, loose stool/diarrhoea or pruritus [187]. Additionally, AG (140 mg oral twice daily for 24 months) could induce adverse reactions such as mild rashes and dysgeusia in patients with multiple sclerosis [188].

In an acute toxicity study, a single oral dose of AG was given at 100 mg/kg or 500 mg/kg in rats, which did not show any toxicological symptoms, and a safe dose of AG was established at 500 mg/kg [91]. Furthermore, animal and cell studies showed that AG can cause reproductive toxicity, nephrotoxicity and cerebral toxicity. Akbarsha et al. [189] found that AG (25 mg/kg and 50 mg/kg, 48 days, oral gavage) could cause male reproductive toxicity, mainly manifested as decreased sperm count or changes in sperm morphology, but this reproductive toxicity is reversible and did not affect the quality of sexual life. Thus, AG can be used as a male contraceptive. Additionally, AG could exert adverse effects on fertility in female rodents. Specifically, AG (3.50 μg/mL, 14 h) disrupted first polar body extrusion and decreased the proportion of oocytes reaching the MII stage in a time- and concentration-dependent manner. It led to the formation of abnormal spindles in oocytes, with multiple, absent or disrupted poles, and promoted scattering and misalignment of chromosomes. Additionally, AG could disrupt the formation of actin cap, promote oocyte apoptosis and decrease the fertility of mature oocytes in vitro. Overall, AG adversely affected the fertility of female mice by interfering with the meiosis of oocytes [190]. Huang et al. [191] reported that AG (10 μg/mL, 24 h) could induce apoptosis in human embryonic stem cells (ESCs). AG could induce ROS accumulation, damage the $\Delta\psi m$, and increase caspase-3 levels. However, these effects could be reversed by NAC, an inhibitor of ROS. Furthermore, AG could upregulate the protein and gene expression of Nrf2 and its target genes (SOD1, GCLC and glutathione reductase (GSR). These effects could also be reversed by NAC. Therefore, AG could induce apoptosis of human ECs via ROS-mediated oxidative stress responses and the Nrf2 pathway. Besides, in vivo toxicity studies revealed that the pregnant mice were intraperitoneal injection of 5 mg/kg/day AG significantly decreased the mouse fetal size and weight.

In vitro studies have shown that AG could cause renal toxicity. AG (0, 3.50, 10.51, 21.03, 35.05, 52.57 and 87.62 μg/mL for 24 h) suppressed cell proliferation in a dose- and time-dependent manner, induced apoptosis, decreased SOD content and increased MDA levels in human renal tubular epithelial (HK-2) cells. It could increase the expressions of C/EBP homologous protein (CHOP) and caspase-4 and decreased the protein expression of glucose-regulated protein 78 (GRP78/Bip), resulting in the activation of endoplasmic reticulum (ER) stress signaling. Additionally, AG could alter the protein expressions of kidney injury molecule-1 (KIM-1), TNF-α and IL-6. Therefore, AG could cause nephrotoxicity through ER stress signaling and inflammatory responses [192].

High doses of AG are toxic to animal models of certain diseases. For example, Yen et al. [193] found that AG at a high dose (a single dose of 5 mg/kg, intraperitoneal injection) aggravated middle cerebral artery occlusion (MCAO)/reperfusion-induced brain injury in rats. Specifically, infarct volume was significantly higher in AG-treated rats than in control rats. Additionally, AG (17.52 μg/mL) induced apoptosis, activated caspase-3, increased LDH levels in cerebral endothelial cells (CECs), arrested cell growth in the G0/G1 phase and prevented the entry of cells in the S or G2/M phase.

5. Other aspects of AG

AG has a wide range of pharmacological effects, which may facilitate the management of ASCVD and the associated risk factors. In this section, we have discussed the availability, pharmacokinetic properties, pharmaceutical activities and safety of AG.

5.1. Availability of AG

The methods available for the synthesis and extraction of AG are summarized below.

5.1.1. Extraction of AG

The extraction method plays an important role in the preservation of bioactive components and physiological activity of medicinal herbs. To date, different methods, such as reflux, microwave-assisted extraction (MAE), soxhlet extraction, supercritical CO_2 extraction, ultrasonic extraction, cold impregnation and three-phase distribution, have been used to increase the extraction rate of AG from *Andrographis paniculata* (Fig. 8).

Although traditional extraction methods have numerous drawbacks, they are widely accepted, mainly owing to their applicability, versatility and simplicity of operation. In a study, 9.6% AG was obtained from *Andrographis paniculata* powder via cold maceration in a mixture (dichloromethane and methanol) and recrystallisation [194]. Wongkittipong et al. [195] used the Soxhlet extraction method and found that extraction time, ethanol content and extraction temperature influenced the diffusion coefficient of AG, whereas particle size had minimal effects on the extraction rate and final concentration. At an extraction rate of <1 mg/g, the optimal extraction conditions were as follows: temperature, 22 °C; ethanol concentration, 60%; extraction time, 3 h. In a similar study, Sharma et al. [196] reported that the extraction rate of AG obtained via Soxhlet extraction with methanol for 1.5 h (1.790%) was lower than that obtained by reflux extraction with methanol for 1 h (2.040%), suggesting that the highest extraction yield of AG was obtained via reflux extraction. Kumoro et al. [197,198] investigated the effects of different solvent properties on the Soxhlet extraction of AG from the leaves of *Andrographis paniculata*. 16 solvents, such as hexane, petroleum ether, dichloromethane, ethyl acetate, chloroform, acetone and water, were applied to extract AG.75% methanol was the optimal solvent for AG extraction (38.08%). A mathematic model was established to describe the extraction phenomenon based on rapid mass transfer at the solid-liquid interface after a volumetric mass transfer coefficient was applied.

Table 1
Preventive and therapeutic effects of AG on ASCVD.

Pharmacological properties		Detail information	Models	Daily dosages (or concentration), methods of administration and treatment courses	Application	Refs.
Preventive effects of AG	Anti-obesity and hypolipidemic effect	Decreasing the levels of triglyceride, TC and LDL-C	Hyperlipidemia mice	2, 20, and 50 mg/kg/day, oral administration for five days	In vivo	[90]
		Attenuating HFD-induced body weight gain and fat accumulation in liver or adipose tissues, and improving serum lipid levels	HFD-induced mice	50 and 100 mg/kg/day, oral gavage for 4 weeks	In vivo	[92]
		Suppressing GPX1activity and depleting GSH level	3T3-L1 preadipocytes	10.00 and 20.00 μg/mL, for 24 h–48 h	In vitro	[95]
		Suppressing the adipogenic differentiation	Human bone marrow mesenchymal stem cells	0.87, 1.75, and 3.50 μg/mL, for 16 h–24 h	In vitro	[98]
	Anti- diabetic effect	Decreasing the levels of blood glucose and improving diabetic rat islet and beta cells	STZ-induced diabetic rats	1.5 and 4.5 mg/kg/2 days, oral administration for 8 days	In vivo	[105]
		Suppressing the activation of NF-κB signaling pathway and its downstream inflammatory factors expressions	3T3-L1 preadipocytes	1.00, 2.00, 5.00, and 10.00 μg/mL, for 1, 3, 6, 12, 24 h	In vitro	[107]
		Reducing the expression of phosphoenolpyruvate carboxykinase and increasing expression of the glucose transporter subtype 4	STZ-induced diabetic rats	1.5 mg/kg/day, oral administration for 90 min	In vivo	[112]
		Enhancing the uptake of radioactive glucose and increasing the GLUT4	STZ-induced diabetic rats	1.5 mg/kg/day, oral administration for 90 min	In vivo	[115]
Therapeutic effects of AG	Anti-atherosclerosis effect	Decreasing TC, TG, and LDL levels, inhibiting IL-1β, IL-6 and CRP expressions, and inhibiting thickening of atherosclerotic plaques	PG-induced New Zealand rabbits	10 and 20 mg/kg/day, oral administration for 12 weeks	In vivo	[120]
		Increasing the levels of SOD,CAT,GPX, GSH, decreasing MDA,VCAM-1, ICAM-1 and MCP-1 levels, and reducing intima thickening plaque	PG-induced New Zealand rabbits	10 and 20 mg/kg/day, oral administration for 12 weeks	In vivo	[121]
		Down-regulating MCP-1 and IL-6 levels, blocking the NF-κB signaling, decreasing oxidative stress and hindering foam cell formation	Ox-LDL-induced RAW264.7 cells, E-deficient mice	0.44–14.01 μg/mL for 48 h, 1 and 2.5 mg/kg/3 days, intraperitoneal injection for 8 weeks	In vitro In vivo	[122]
		Inhibiting the formation of foam cells	Atherogenic diet-induced Wistar rats	40 mg/kg/day, oral gavage for 3 days	In vivo	[123]
		Reducing the accumulation of foam cells and inhibiting MCP-1 expression	Atherogenic diet-induced Wistar rats	40 mg/kg/day, oral gavage for 3 days	In vivo	[124]
		Inhibiting the inflammatory responses (IL-1β, IL-6, and TNF-α), ameliorating the levels of p-PI3K, p-AKT, and p-eNOS	High glucose-induced HUVECs	17.52 μg/mL, for 6–36 h	In vitro	[128]
		Suppressing the mitochondrial pathway of apoptosis by inhibiting release of cytochrome *c* into the cytoplasm and dissipation of mitochondrial potential and preventing caspase-3 and-9 activation	HUVECs	0.35–35.00 μg/mL, for 18 h	In vitro	[129]
		Increasing the expression of PHD2/3	Hypoxia-induced EA.hy926	2.63 μg/mL, for 16 h	In vitro	[137]
		Enhancing HO-1 and MKP-5 expressions and cellular cGMP content in addition to inhibiting hypoxia-induced ROS generation	Hypoxia-induced EA.hy926	2.63 μg/mL, for 16 h	In vitro	[138]
		Inhibiting ICAM-1 mRNA and protein levels, suppressing IκB, IKK and IκBα activation, p65 nuclear translocation, NF-κB and DNA binding activity	TNF-α-induced EA.hy926	0.18–7.01 μg/mL, for 16 h	In vitro	[141]
		Attenuating ROS generation, Src phosphorylation, membrane translocation of the NADPH oxidase subunits p47phox and p67phox, and ICAM-1 expression	TNF-α-induced EA.hy926	2.63 μg/mL, for 16 h	In vitro	[142]
		Inhibiting ICAM-1 protein and mRNA expressions, ICAM-1 promoter activity, and monocyte adhesion	TNF-α-induced EA.hy926	2.63 and 5.26 μg/mL, for 16 h	In vitro	[143]
		Disrupting mitochondrial membrane potential and inhibiting the p38 MAPK/●HO–NF-κB-ERK2 cascade	Human platelets	8.76–35.00 μg/mL, for 10–60 min	In vitro	[147]
		Inhibiting collagen-stimulated platelet activation accompanied by relative Ca^{2+} mobilization, thromboxane A2 formation and PLCγ2, PKC, mitogen-activated protein, kinase MAPK and AKT phosphorylation	Healthy human volunteers platelets	8.76–26.28 μg/mL, for 6 min	In vitro	[150]
		Inhibiting ERK1/2 pathway	Male Wistar rats platelets	0.35–35.00 μg/mL, for 15, 30, and 60 min	In vitro	[151]
		Attenuating IKKβ phosphorylation, IκBα degradation, and P65 phosphorylation	Human platelets	12.27 and 26.28 μg/mL, for 6 min	In vitro	[153]
		Inhibiting IL-6 and MCP-1 expression as well as blocking NF-κB signal activation, interfering the Notch1 gene expression and increasing anti-inflammatory cytokines	LPS-induced macrophage cell line RAW264.7	0.22, 0.44, 0.88, 1.75, 3.5, 7.01 and 14.02 μg/mL, for 24 h	In vitro	[154]

(*continued on next page*)

Table 1 (*continued*)

Pharmacological properties		Detail information	Models	Daily dosages (or concentration), methods of administration and treatment courses	Application	Refs.
		Reducing ox-LDL-induced lipid accumulation, decreasing the mRNA and protein expression of CD36	Ox-LDL-induced macrophage cell line J774A.1	0.18 and 0.35 μg/mL, for 24 h	In vitro	[155]
		Inhibiting NO synthesis by directly or indirectly interfering with the synthesis and activity of iNOS	LPS-induced macrophage cell line RAW264.7	0.35−17.52 μg/mL, for 5 h	In vitro	[157]
		Inhibiting NO synthesis, reducing the expression of iNOS protein level without a significant effect on iNOS mRNA	LPS/IFN-γ-induced macrophage cell line RAW264.7	3.50, 10.51 and 17.52 μg/mL, for 2, 6, and 12 h	In vitro	[158]
		Inhibiting the activation of ERK1/2, p38MAPK and NK-κB	Mouse peritoneal macrophages	50 μg/mL, for 72 h	In vitro	[159]
		Inducing ROS formation, p53 activation, Bax, and active caspase-3 expression	VSMCs	17.52 μg/ml, for 48 h	In vitro	[160]
		Activating the p38MAPK, activating the SHP-1, and induced PP2A dephosphorylation	VSMCs	7.01 and 17.52 μg/mL, for 20 and 8 h	In vitro	[161]
		Reducing E-selection, VCAM-1 and TF levels, inhibiting neointima hyperplasia	$p50^{-/-}$ mice	5 mg/kg/2 days, intraperitoneal injection for 7 days	In vivo	[162]
		Suppressing the expressions of inducible NO synthase, reducing JNK, AKT, and p65 phosphorylation	TNF-α-induced primary rat aortic smooth muscle cells	7.01 and 17.52 μg/mL, for 20 min	In vitro	[164]
		Suppressing NOS and MMP-9 expressions, inhibiting p65 nuclear translocation, DNA binding activity, p65 Ser536 phosphorylation, and NF-κB reporter activity, and increasing ceramide formation and PP2A activity	LPS/IFN-γ induced Wistar rats, LPS/IFN-γ induced VSMCs	5 mg/kg/day, intravenous injection for 2 weeks; 7.01 and 17.52 μg/mL, for 30 min	In vivo In vitro	[165]
		Inhibiting cell proliferation and reducing the expression of ERK1/2, diminishing iNOS and COX2 expressions	PDGF-BB-induced VSMCs	7.01−35.00 μg/mL, for 24 h or 48 h	In vitro	[167]
	Anti-CHD effect	Increasing NO and PGI2 levels and decreasing TXA2 and ET-1levels, up-regulating t-PA and decreasing PAI-1, decreasing levels of TNF-α, MCP-1, hs-CRP and IL-1β in myocardial tissue and serum	HFD induced coronary heart disease mice	50 mg/kg/day, oral administration for 42 days	In vivo	[172]
		Increasing the levels of SOD, CAT, GR, and Gpx and decreasing MDA level in NRCs. Subjecting to H/R damage, mediating through up-regulation of intracellular GSH level	Neonatal rat cardiomyocytes subjected to H/R damage	0.35, 1.05 and 3.50 μg/mL, for 3 days	In vitro	[175]
		Decreasing the peak ICaL density and increasing Ito	ISO-induced male Wistar rats	20 mg/kg/day, subcutaneous injection for 21 days	In vivo	[177]
		Maintaining heart rate and ST-segment	ISO-induced mice	20 mg/kg/day, subcutaneous injection for 21 days	In vivo	[178]
		Increasing mRNA expressions of Gpx, SOD2 and NQO1, down-regulating p67 phox, Gp91 and NOX4 transcription, improving activation of the Nrf2/HO-1 pathway	Left coronary artery ligation mice	25 mg/kg/day, oral administration for 14 days	In vivo	[179]
	Anti-cerebral haemorrhage and cerebral ischemia effect	Decreasing the expression of glial fibrillary acidic protein and increasing the expression of NeuN, and the levels of pro-inflammatory cytokines (IL-1β, IL-6 and TNF-α)	Mouse model of bilateral common carotid artery occlusion	30, 60 and 120 mg/kg/day, oral administration for 14 days	In vivo	[180]
		Exhibiting neuroprotective effects, with accompanying suppression of NF-κB and microglial activation, and reducing the production of cytokines including TNF-α and IL-1β, and PGE2	Rats with pMCAO	2 mg/kg, intraperitoneal injection for 1 h	In vivo	[181]
		Suppressing free radical formation, blood-brain barrier disruption, and brain infarction, increasing HO-1 protein and Nrf2 phosphorylation, and nuclear translocation	MCAO-induced ischemic stroke in rats	0.1 mg/kg, intraperitoneal injection for 6 h	In vivo	[182]
		Decreasing the expressions of NOX2, iNOS, and the infiltration of CD11b cells	CI/R mice OGD-induced BV-2 cells	0.01−0.1 mg/kg, intravenous injection for 1 h 1.75−3.50 μM, for 24 h	In vivo In vitro	[183]
		Inhibiting the endothelial barrier, cell viability, matrix metalloproteinases, and tube formation	OGD-induced brain microvascular endothelial cells	0.18, 0.35, 0.70, 1.75, and 3.50 μg/mL, for 6 h	In vitro	[184]

AG: andrographolide; ASCVD: atherosclerotic cardiovascular disease; AS: atherosclerosis; CHD: coronary heart disease; PAD: peripheral arterial disease; ECs: endothelial cells; VSMCs: vascular smooth muscle cells; VECs: vascular endothelial cells; NO: nitric oxide; ROS: reactive oxygen species; LDL-C: low-density lipoprotein cholesterol; ox-LDL: oxidized low-density lipoprotein; HFD: high-fat diet; GPX: glutathione peroxidase; GLUT4: glucose transporters subtypes 4; PG: porphyromonas gingivalis; TC: total cholesterol; TG: triglycerides; HDL-C: high-density lipoprotein cholesterol; MDA: malondialdehyde; SOD: superoxide dismutase; CAT: catalase; GSH: glutathione; GPx: glutathione peroxidase; ET-1: endothelin 1; Nrf2: nuclear factor erythroid 2-related factor 2; ERK1/2: extracellular regulated protein kinase 1/2; ICAM-1: intercellular adhesion molecule-1; NADPH: nicotinamide adenine dinucleotide phosphate; PP2A: protein phosphatase 2A; NRCs: neonatal rat cardiomyocytes; H/R: hypoxia/reoxygenation; MCAO: middle cerebral artery occlusion; OGD: oxygen-glucose deprivation; HUVECs: human umbilical vein endothelial cells; STZ: streptozotocin; ox-LDL: oxidized low-density lipoprotein.

Common methods consume a lot of energy, time, solvents and raw material. The use of modern extraction methods can overcome these problems. Supercritical CO_2 extraction offers the advantages of being non-toxic and non-flammable. Chen et al. [199] compared different pressures, extraction times and temperatures for supercritical CO_2 extraction of AG and found that the maximum crystallinity and purity of AG (72.29% (*m/m*) and 79.78% (*m/m*), respectively) was obtained under the following conditions: pressure, 24 MPa; temperature, 55 °C; time, 105 min. In addition, a mixture of carbon dioxide and ethanol has been used as a solvent to obtain 0.175 g/g of AG via supercritical fluid extraction at 323 K, 15 Mpa and 2 mL/min [200]. Similarly, 0.20% of AG was obtained via MAE using ethanol as a solvent, 0.15% of AG was obtained using water as a solvent and 0.589% of AG was obtained using a mixture of chloroform and water as solvents [201,202]. This suggested that binary solvents are more effective in extracting AG compared to pure solvents. Mohan et al. [203] found that MAE was more efficient when methanol was used as a solvent instead of water, resulting in higher extraction rates and increased contents of extracted AG. In addition, an MAE method based on ionic liquid was developed to extract AG, wherein 4.71% (*m/m*) of AG was obtained using 1-butyl-3-methylimidazole. Compared with the conventional MAE method, this modified MAE method with green solvent/ionic liquid reduced environmental pollution [204]. In a study, the content of AG obtained via ultrasound-assisted MAE (UMAE) (1066.49 mg/L) was higher than that obtained via MAE (781.65 mg/L) and ultrasonic extraction (UAE) (559.24 mg/L) alone [205]. A high extraction rate could be achieved in a short time with dynamic microwave-assisted high-performance liquid chromatography, and 98% of AG can be extracted within 6 min [206]. In a study, AG was rapidly extracted from *Andrographis paniculata* using the three-phase partitioning (TPP) method, and a yield of 26.55 mg/g of AG was obtained under the following optimal conditions: temperature, 40 °C; concentration of ammonium sulfate, 40%; solute-to-solvent ratio, 1:40; time, 120 min [207]. However, TPP has the disadvantage of mass transfer resistance, which can be overcome by combining it with MAE or UAE. In a study, the combination of TPP and MAE (MTPP) improved the yield of AG (38.53 mg/g). However, the yield of AG extracted via TPP and ultrasound-assisted partitioning (UTPP) was 35.28 mg/g and 26.55 mg/g, respectively, both of which were lower than the yield of MTPP [208].

5.1.2. Synthesis of AG

AG is a labdane diterpenoid with a complex structure. In 2014, AG was first synthesised using homoiodo allylsilanes for facile assembly of the respective diastereomeric allylsilanes, the biomimetic cation-olefin annulation precursors [209]. Subsequently, AG was synthesised using a simple method, which involved fewer steps and resulted in better diastereoselectivity and enantioselectivity compared with previous synthetic methods. The key steps of this method include iridium-catalysed carbonyl reductive coupling to form a quaternary carbon stereocentre at C4, diastereoselective alkene reduction to establish a *trans*-decalin ring and carbonylative lactonisation to incorporate α-alkylidene-γ-butyrolactone [210].

5.2. Pharmacokinetic properties of AG

For research and development of drugs, pharmacokinetic analysis has attracted the attention of many researchers owing to its

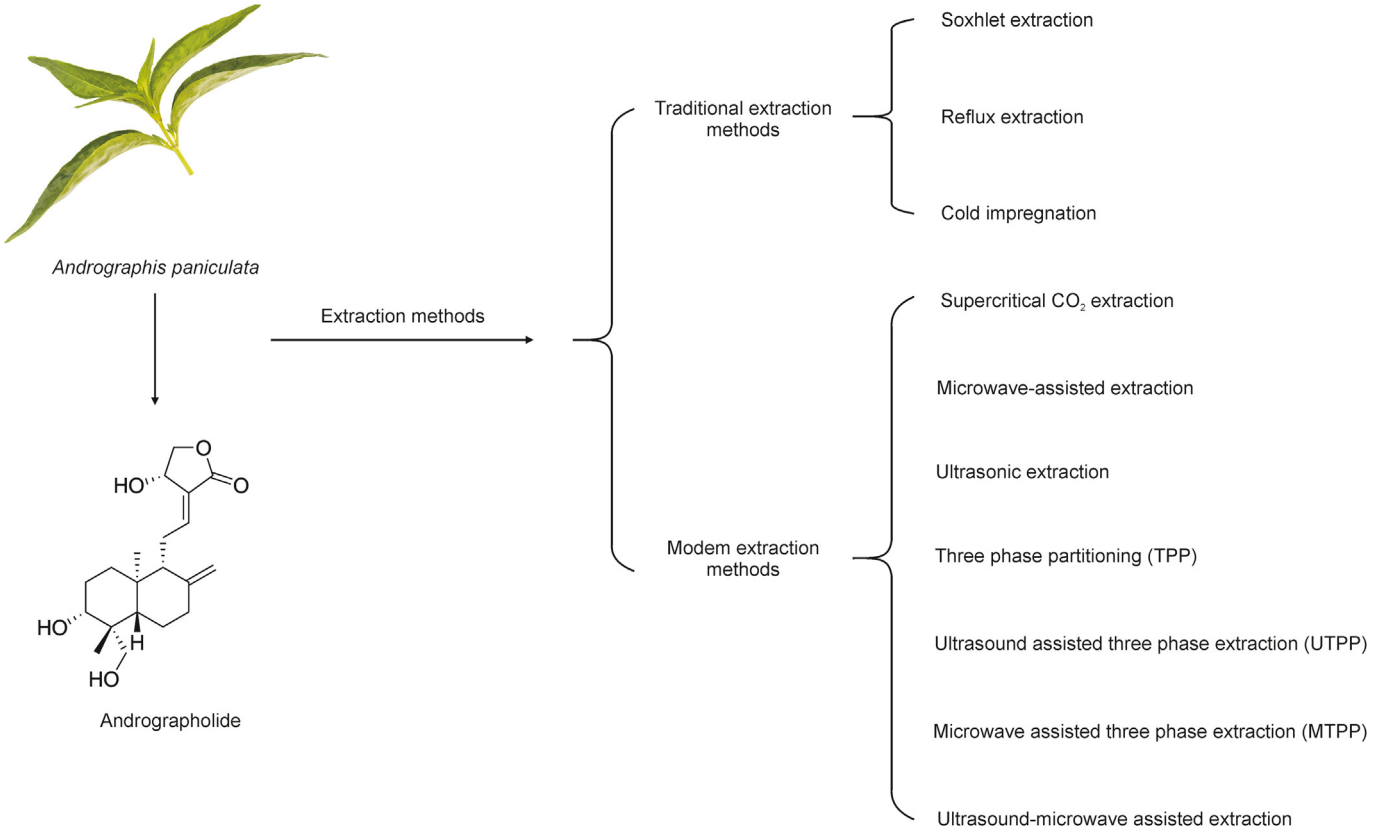

Fig. 8. Extraction methods of andrographolide (AG).

contribution to rational dose selection and dosing regimens. Studies have extensively reported the pharmacokinetic properties of AG. The absorption, distribution, metabolism and excretion of AG in living organisms are described below.

5.2.1. Absorption

The pharmacokinetic parameters of AG are different across species. For example, a study reported that after oral administration of AG (120 mg/kg), the maximum plasma concentration (C_{max} of AG was 0.23 ± 0.05 μg/mL, which was observed after 29.75 ± 0.5 min in SD rats, with an area under the curve ($AUC_{0-\infty}$) value of 29.45 ± 3.73 μg/min·mL [211]. Chen et al. [212] reported that the C_{max}, T_{max} and $AUC_{0-12\ h}$ values in rats were 0.35 ± 0.05 μg/mL, 0.05 ± 0.43 h and 0.50 μg/mL·h, respectively, after the administration of 50 mg/kg of AG. Another study on rats showed that the T_{max}, C_{max} and $AUC_{0-\infty}$ values were 2.41 ± 0.15 h, 1.27 ± 0.2 μg/mL and 8.34 μg·h/mL, respectively, after oral administration of 20 mg/kg of AG [213]. Bera et al. [214] found that after oral administration of 100 mg/kg/day of AG for 4 weeks to rats, the C_{max}, T_{max} and $AUC_{0-\alpha}$ values were 0.12 μg/mL, 0.75 h and 0.28 μg·h/mL, respectively. In a study on beagle dogs, Xu et al. [215] found that the T_{max} and AUC_{0-t} values were 1.30 ± 0.57 h and 0.49 ± 0.15 μg·h/mL, respectively. In a study on chickens, the $AUC_{0-\infty}$, T_{max} and C_{max} values were 320.6 ± 24.6 μg/mL·min, 53.5 ± 5.2 min and 1.63 ± 0.28 μg/mL, respectively, after oral administration of *Andrographis paniculata* powder (5 g/kg) [216]. Moreover, clinical studies have shown that differences in pharmacokinetic properties of AG among humans are attributed to differences in nationality and geographical locations. In a study on healthy Chinese volunteers, the mean plasma T_{max}, C_{max} and $AUC_{0-\infty}$ values of AG were 1.6 h, 0.16 μg/mL and 0.29 ± 0.06 μg·h/mL, respectively, after oral administration of 200 mg of AG [217]. However, in a study on healthy Thai volunteers, C_{max}, T_{max} and AUC values of AG were 0.34 μg/mL, 1 h and 0.05 μg·h/mL, respectively. In another study, after Thai volunteers were orally administered by *A. paniculata* capsules (97.92 mg/day for 3 days), the C_{max} of AG reached 0.03 mg/mL after 0.78 h [218,219]. The above mentioned studies suggested that doses and dosage regimens affect the absorption of AG.

The absolute bioavailability of AG is low. In a study, the bioavailability of 120 mg/kg AG was 2.67% in rats [211]. In another study, the bioavailability of AG was 1.19% in rats, which was 4-fold lower than that of AG derived from 940 mg/kg ethanolic extract of *A. paniculata*. This finding indicated that the absorption of AG was altered in the presence of other compounds in *A. paniculata* extracts [212]. This suggested that other components in the extract could change the pharmacokinetics of AG, thereby increasing its bioavailability. Besides, Ye et al. [211] found that the effective permeability (P*eff) of AG in the ileum and colon of rats was significantly increased by verapamil (a P-glycoprotein (P-gp) inhibitor), suggesting that penetration of AG into the ileum and colon was hindered by P-gp efflux. Additionally, the amount of AG in bile samples was affected by the P-gp inhibitor, which resulted in substantially elevated excretion of AG in the bile tract than AG was perfused alone. Therefore, the poor oral bioavailability of AG could be attributed to biliary excretion and P-gp efflux.

5.2.2. Distribution

AG may not targeted to organs and mainly existed in blood. Bera et al. [214] demonstrated the distribution of AG in rat tissues using liquid chromatography-tandem mass spectrometry (LC-MS/MS). After oral administration of 100 mg/kg/day AG for 4 weeks, the blood to plasma ratio of AG was 0.93, which indicated that AG did not accumulate sufficiently in the red blood cells. In addition, the highest concentration of AG was found in the kidney of rats 1 h after administration (156.12 ng/g), followed by the liver, spleen and brain, whereas the concentration of AG was similar in the heart and lung. However, AG could not be detected in the testis. A study on rats showed that the metabolites of AG were found in the small intestine instead of bile [220]. The distribution of AG in human and chicken plasma had been described using an open two-compartment model, whereas that in rats had been described using a single-compartment model [213,216]. The lipophilicity and protein-binding activity of drugs play an important role in their distribution in vivo because the proportion of free fraction determines the membrane transport rate and the amount of drug distribution. AG has a good affinity for human serum proteins. In a study, after oral administration of four Kan Jang tablets (equivalent to 20 mg AG), 55% of AG in the body was bound to human plasma proteins. In particular, 64% of AG was bound to bovine serum albumin, whereas only approximately 40% of AG was absorbed into the tissues. These findings indicated that AG was non-specifically bound to albumin in human blood [213]. Human serum albumin (HSA) and α-1-acid glycoprotein (AGP) (another important plasma protein) were major proteins driving the transport of AG in vivo. Yeggoni et al. [221] found that AG could be bound to HSA more easily than to AGP.

5.2.3. Metabolism

The metabolites of AG are different in human and animals. In a study, 13 metabolites were identified in liver microsomes after the administration of AG to humans and animals (Fig. 9). Specifically, 8 phase I metabolites and 5 phase II metabolites were identified via dehydration, deoxygenation, hydrogenation and glucuronidation [222]. It has been proved that sulfonate metabolite of AG was the main metabolite in rat serum, urine and small intestine, including 14-deoxy-12-hydroxyandrographolide (DEO-AND), 14-deoxy-12(*R*)-sulfo andrographolide 3-sulfate, 14-deoxy-12(*S*)-sulfo andrographolide 3-sulfate, 14-sulfo isoandrographolide 3-sulfate, 14-deoxy-11,12-dide-hydroandrographolide, isoandrographolide, 14-deoxy-12(*R*)-sulfo andrographolide 1, and 14-deoxy andrographolide (compounds 1–17) [220,223,224]. However, due to species differences in the catalytic properties of metabolizing enzymes, the metabolites of AG in humans were mainly derived from glucuronide conjugates and urea adducts, including andrographolide-19-*O*-β-D-glucuronide, isoandrographolide-19-*O*-β-D-glucuronide, 14-deoxy-12-carbamidoandrographolide-19-*O*-sulfate, 14-deoxy-12(*R*/*S*)-carbamido-andrographolide-19-*O*-β-D-glucuronide (compounds 18–28) [225,226].

5.2.4. Excretion

Urine is the main excretion mode of AG. In a study, after the administration of four dispersible tablets (200 mg AG), the elimination half-life of AG was 10.50 ± 2.07 h in human plasma [227]. In a study on rats, the total clearance rate was 3.6 ± 0.12 L/h/kg, mean residence time (MRT) was 4.6 ± 0.09 h and elimination half-life ($t_{½}$-) was 1.3 ± 0.10 h after intramuscular injection of 50 mg/kg AG. These results indicated that AG was cleared rapidly in vivo and had a high overall clearance rate and low elimination half-life, suggesting that AG was distributed in the blood after intramuscular administration [228]. These results were consistent with those of another study, in which the MRT, clearance rate (Cl) and elimination constants (K_{el}) of AG were 4.71 ± 0.7 h, 0.29 ± 0.07 mL/min and 0.34 ± 0.15 h^{-1}, respectively, in rats after oral administration of 20 mg/kg *A. paniculata* extract (AGE). However, renal excretion was not the primary method of AG elimination. A study reported that the rate of urinary AG excretion was 8.2% and 0.53% within 72 h of oral administration of 20 mg/kg and 20 mg/kg AG in rats, respectively. Approximately 90% of AG was eliminated in other ways, mainly through metabolic conversion. The authors suggested that this phenomenon was most likely attributed to the intensive

metabolism of AG. The metabolism of AG increased with an increase in its dose [213].

5.3. Pharmaceutical properties of AG

As mentioned earlier, AG has low water solubility and oral bioavailability and unstable metabolism, which greatly limit its clinical application [229]. To overcome these drawbacks and maximise clinical therapeutic effects, various formulations have been developed based on new technologies and encapsulation strategies, such as solid dispersions (SDs), inclusion bodies, nanoemulsions, nano-suspensions, microspheres, liposomes, micelles and nanoparticles [230]. At present, AG is primarily delivered via liposomes, microspheres, SDs and nano-formulations (Fig. 10). These delivery vehicles are described below.

Lipid-based microemulsion formulations, which mainly include macroemulsions (coarse emulsion), microemulsions, self-microemulsifying drug delivery systems (SMEDDSs), solid lipid nanoparticles (SLNs), liposomes and lipoplexes, offer promising delivery platforms for poorly soluble drugs and natural compounds [231]. Microemulsion, which is a mixture of oil, water and surfactant, is considered a potential drug delivery vehicle [232]. In a study, AG-loaded microemulsions were prepared, and the content of AG was detected to be 8.02 mg/mL. The microemulsion system consisted of isopropyl myristate as the oil phase (2.5% (*m*/*m*)), Tween 80 as the surfactant phase (25% (*m*/*m*)) and ethanol as the co-surfactant (50% (*m*/*m*)). Compared with AG tablets, AG-loaded microemulsions had better water solubility, longer shelf life, stronger anti-inflammatory effects, higher bioavailability and lower acute oral toxicity [233]. A special emphasis has been placed on SMEDDSs, which are more stable than traditional emulsions (EMLs) [234]. In a study, SMEDDSs were prepared and transformed via extrusion/spheronization and had higher dissolution rates compared with the crude extract AG powder in vitro. Additionally, the C_{max} and AUC_{0-12h} values of AG in SMEDDS were 6 and 13 times higher than those of AG extract in an aqueous suspension, respectively [235]. Nanoparticle drug delivery systems have been used to target cells or organs without causing damage to normal tissues [236]. SLNs have advantages such as long-term stability and improved bioavailability of active ingredients [237]. The bioacceptable and biodegradable nature of SLNs makes them less toxic and more suitable for targeting the brain [238]. Studies have shown that AG could be rapidly delivered to the brain by SLNs. Graverini et al. [239] demonstrated that SLNs successfully promoted the penetration of AG in an in vitro blood–brain barrier (BBB) model as evidenced by the results of parallel artificial membrane permeability assay (PAMPA). Additionally, a study demonstrated that gelatin hydrogels of AG were embedded in poly (lactic-co-glycolic acid) (PLGA) nanoparticles, which prolonged the delivery and retention time of AG in the joints of mice [240].

PLGA microspheres with sustained release can help to achieve long-term effects of drugs, shorten drug administration time and reduce the fluctuation of drug concentration in the blood [241]. In a study, PLGA microspheres encapsulated with AG were developed with significant sustained release property. A solid-in-oil-in-water (s/o/w) emulsification solvent volatilisation method was used to prepare AG-encapsulated microspheres. These microspheres had high entrapment (75.79% ± 3.02%) and drug loading (47.06% ± 2.18%) efficiency. After intramuscular injection of AG-encapsulated PLGA microspheres, the absolute bioavailability of

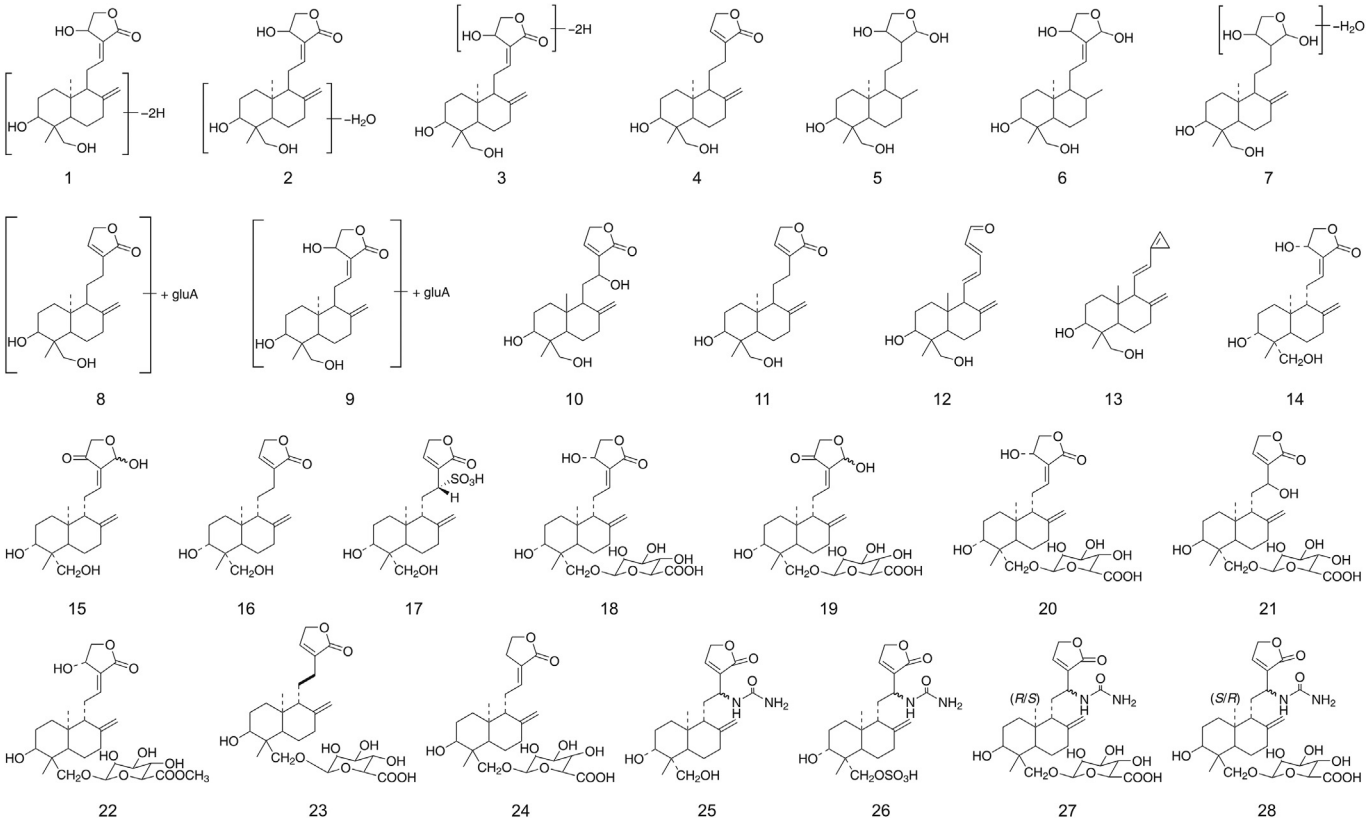

Fig. 9. Metabolites of andrographolide (AG).

the microspheres was 67.51%. Moreover, the microspheres maintained a relatively high plasma concentration of AG after 1 week [242]. In another study, AG pellets with a core-shell structure were prepared via wet milling, which had >90% solubility and adequate stability. In beagle dogs, T_{max} value of the pellets was 1.38 h, and the relative bioavailability was 1.57 times higher. These results suggested that the solubility and bioavailability of AG could be significantly improved by stabilising pellets with HPMC films [243].

Solid dispersion (SD) is an effective method for increasing the solubility, dissolution rate and bioavailability of poorly water-soluble drugs. Materials such as SiO_2, polyethylene glycol, polyethylene pyrrolidone, hydroxyapatite and poly (vinyl pyrrolidone-vinyl acetate) are often used as carriers to prepare AG-SD [244–246]. In a study, AG-encapsulated SDs were developed, and the optimal absorption organ was the jejunum. The concentration of AG in SDs was approximately 2.7 times higher than that in unconfigured suspensions. Pharmacokinetic analysis revealed that the C_{max} and AUC values of AG were 3.7-and 3.0-fold higher than those of oral AG suspension, respectively [247]. In another study, nanocrystalline solid dispersions (NC-SDs) with high drug loading efficiency were used to improve the dissolution of AG. The dissolution rate of AG-NC-SDs was barely altered compared with the precursor NC suspension, and the drug loading efficiency of AG-NC-SDs was 67.83% ± 1.26%. Compared with coarse AG, AG-NC-SDs had lower C_{max} values, higher mean peak concentration and 4.72-fold higher $AUC_{0-\infty}$ values in rats [248].

Over the past few decades, nanotechnology has been widely used for the development of drug delivery systems, which are easy to prepare, have good stability and can improve the solubility and bioavailability of drugs. Nano-emulsions can be incorporated into hydrogels to overcome their low viscosity. AG nano-emulsions have been prepared using octanol 90 as the oil phase, Kolliphor RH 40 as the surfactant and propylene glycol as the auxiliary solvent [249]. EMLs are lipid-based vesicle systems that combine the properties of EMLs and liposomes. Structurally, EMLs consist of an internal lipid core in a solid or liquid crystal phase surrounded by a phospholipid (PL) multilayer film [250]. Elsheikh et al. [251] developed AG-loaded emulsions (EML-AG) as a novel tool to overcome the disadvantages of oral delivery obstacles of AG. The size of EML-AG was 281.62 ± 1.73 nm, and the encapsulation rate was 96.55% ± 0.25%. Compared with free AG, EML-AG had higher absorption rate and C_{max} value (9.64 μg/mL) at a shorter T_{max} (0.5 h) and AUC $_{0-\infty}$ (23.88 μg·h/mL). EML-AG had a significantly longer elimination half-life ($t_{1/2}$), its MRT was thrice that of free AG, and its clearance rate was significantly reduced by 5 folds.

In addition to the above mentioned materials, other materials can be used to improve the solubility and bioavailability of AG, such as carboxymethyl chitosan, pH-sensitive nanoparticles and titania nanotubes. In a study, the content of AG in AG-carboxymethyl chitosan nanoparticles prepared using an ionic gelation method was 12.09% ± 0.26%. The release rate of AG from carboxymethyl chitosan nanoparticles was increased by 6.3 folds, and the in vivo antimalarial activity was significantly increased by 1.65 folds in mice infected with *Plasmodium* [252]. In another study, the ability of AG to inhibit bacterial adhesion and biofilm formation in ATCC 35984, *Staphylococcus epidermidis* 389 and *Streptococcus aureus* 376 was enhanced by encapsulating AG in titania nanotubes [253]. Previous studies have demonstrated that pH-sensitive nanoparticles can increase the oral bioavailability of drugs [254]. Chellampillai et al. [255] prepared pH-sensitive nanoparticles encapsulated with AG via a nanoprecipitation technique using Eudragit EPO (a cationic polymethacrylate copolymer) to enhance the bioavailability of AG. The pH-sensitive matrix-type dispersed particles could release the drug at a specific pH in the GI tract. Compared with the release of pure AG, AG encapsulated in the nanoparticle suspension was 6-fold higher in an acidic medium within 10 min. Compared with AG, the nanoparticle suspension had 2.2-and 3.2-fold higher $AUC_{0-\infty}$ and C_{max} values, whereas the relative bioavailability of AG in the suspension was increased by 121.53%. Therefore, the nanoparticle formulation improved the bioavailability, pharmaceutical activity and therapeutic efficacy of AG.

In conclusion, AG can be delivered to tissues (such as the lung, liver and brain) more accurately and efficiently in novel dosage forms, which may help to overcome problems associated with the use of AG in clinical practice.

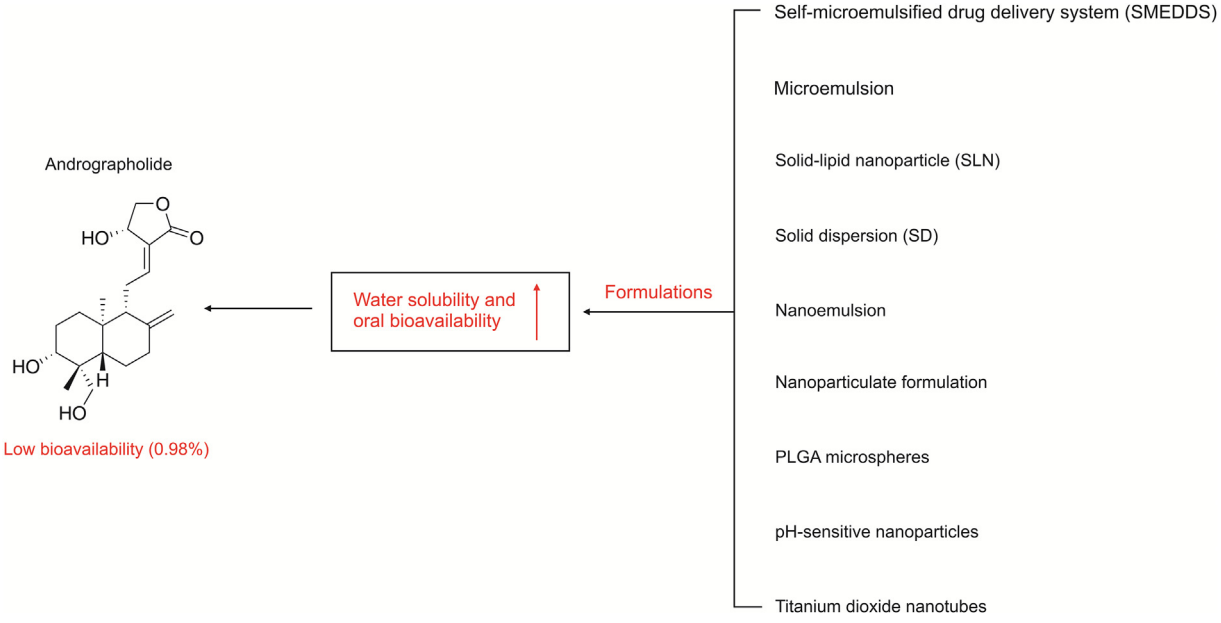

Fig. 10. Pharmaceutics of andrographolide (AG). PLGA: poly (lactic-co-glycolic acid).

6. Discussion

ASCVD is an inflammatory disease that manifests as CHD and cerebrovascular disease owing to plaque instability or thrombosis. It is characterized by lipid accumulation, cellular abnormalities and dysregulation of signaling pathways associated with oxidative stress and inflammation (e.g. MEK5/ERK5/MEF2, PI3K/AKT/p38 MAPK/PKC and Nrf2/HO-1) [256,257]. Therefore, ASCVD can be effectively prevented and treated by targeting ECs, monocytes, foam cells, SMCs, platelets and their associated signaling pathways. ASCVD is often associated with hypertension, diabetes, hyperlipidaemia and obesity. Therefore, controlling these risk factors can help to prevent ASCVD [258]. NSAID, anti-platelet drugs, and hypotensive drugs are applied to manage ASCVD [259,260]. However, the use of multiple drugs in the treatment of ASCVD is inefficient and causes unavoidable side effects, Therefore, it is indispensable to develop natural products with multi-targeted nature, little toxicity and preventive and therapeutic potentials in ASCVD which can be applied in combination with synthetic drugs.

A line of pharmacological studies on the preventive and therapeutic effects of AG produced fruitful results. Unlike most of the currently available drugs for the prevention and treatment of ASCVD, AG has applicable potentials in the entire processes of ASCVD, including the risk factors, AS and ASCVD. There are two differences existed when AG was applied to prevent or treat ASCVD. First, the general doses of AG for the treatment and prevention of ASCVD in vivo were 1.5–4.5 mg/kg, 20–50 mg/kg, whereas its treatment course was 1 week-1 month, 1 week-3 months, respectively. The general dose of AG for the treatment of ASCVD (10.51 μg/mL) was higher than that to prevent ASCVD (5.26 μg/mL) in vitro. Moreover, the maximum dose of AG for prevention of ASCVD was 100 mg/kg for 4 weeks in vivo (mice) or 20.00 μg/mL for 24, 48, 72 h in vitro [92,95]. Meanwhile, the maximum dose of AG for treatment of ASCVD was 500 mg/kg for 4 weeks in vivo (rats) or 35.00 μg/mL for 24 or 48 h in vitro [91,167]. In conclusion, the dose and treatment course of AG for the prevention of ASCVD were smaller than those for its treatment. Similarly, the efficient concentration of AG in different cell models were different. In the cellular model of the risk factor of AS (3T3-L1 cells and hBM-MSCs), the concentration range of AG was 0.35–20.00 μg/mL [99,100,107]. In the cellular model of AS (ECs, platelets, monocyte/macrophage-like cells, and VSMCs), the concentration range of AG was 0.35–35.00 μg/mL [129,140,147,152,158,164]. In the cellular models of ASCVD, the concentration of AG was 1.75–3.50 μg/mL [175,183]. Therefore, different dosing concentrations need to be considered for different models and pharmacological effects. Notably, the effective concentration ranges of AG were 0.35–35.00 μg/mL and 0.18–35.00 μg/mL in rat cells and human cells in vitro, respectively, higher than the C_{max} values of 0.12 μg/mL and 0.03 μg/mL in rats and humans [141,151,153,214,218]. However, as known to all, in vivo and in vitro experiments are quite different. It could not be absolutely concluded that AG could did not reach the effective concentration. Also, it is suggested that the poor bioavailability of AG may lead to its unsatisfactory efficacy. Second, the mechanisms responsible for the preventive and therapeutic potentials were different. AG exerted preventive effects by inhibiting lipogenesis, inducing the proliferation and differentiation of adipocytes and negatively regulating adipogenic marker proteins and growth factors. However, AG exerted therapeutic effects by blocking the adhesion of monocytes to ECs, inhibiting aggregation and activation of platelets and foam cell formation, and inducing proliferation and apoptosis of smooth muscle cells. In addition, the mechanisms underlying the anti-diabetic effects mainly involved regulation of NF-κB and PI3K/AKT pathways [107], whereas those underlying the therapeutic effects of AG against AS mainly involved regulation of PI3K/AKT-p38 MAPK/PKC, HO-1/CO/cGMP/MKP-5, PI3K/AKT, IKK/IκBα/NF-κB, p38MAPK/NF-κB, JNK/AKT/p65, ceramide/p47phox/ROS and SHP-1/PP2A/p38MAPK/p53 pathways. Also, modulation of AG on the PPAR and NF-κB signaling pathways contributed to its anti-CHD effects whereas regulation of PI3K/AKT, Nrf2, and NF-κB signaling pathways played a vital role of the protective effects of AG against cerebrovascular diseases [129,138,139,150,159–161,164]. Notably, although the mechanisms underlying the preventive and therapeutic effects of AG were different, regulation of PI3K/AKT and NF-κB signalings were involved in both of the preventive and therapeutic effects of AG. Moreover, there were a multitude of biomolecular targets for AG in the prevention and treatment of ASCVD. In vitro, AG regulated targets such as GPX1, GSH and NF-κB (in 3T3-L1 cells), PI3K, AKT and eNOS (in HUVECs), PHD2/3, HO-1, MPK-5, ICAM-1, ROS, Nrf2 and NF-κB (in EA.hy926 cells), ERK1/2, P38 MAPK, PKC and PLCγ2 (in platelets), NO, iNOS and NF-κB (in macrophage cell lines RAW264.7 and J774A.1), SHP-1, P38 MAPK, PP2A, JNK, AKT, COX2 and Bax (in VSMCs), HO-1, NOX and Nrf2 (in BV-2 cells and brain microvascular endothelial cells) [95, 107, 122, 129, 137, 138, 141–143, 147, 150–155, 157, 158, 160, 161, 164, 167, 183, 184]. In vivo, the anti-obesity and hypolipidemic effects of AG were attributed to its regulation of SREBPs, FAS, SCD-1, HMGCR, GSH, C/EBPα, C/EBPβ, SREBP-1c and PPARγ, anti-diabetic activity were resulted from its adjustment on the PKCλ/ζ, GSK3β, TRS-1, PEPCK, opioid μ-receptor and AKT. Also, AG could regulate ERK1/2, NOS, NF-κB, HIF-1α, ROS, HO-1, PKC, PKG, ODQ, LXRα, p50, p38MAPK, PP2A and SHP-1 pathways, eliciting anti-AS action. The anti-CHD effect of AG was associated with its regulation of the PPAR, NF-κB, PAI-1, PGI2 and TxA2 pathways. Moreover, AG possessed anti-cerebral haemorrhage and cerebral ischemia activities by regulating the ERK1/2, p38 MAPK, ZO-1, Occludin, Claudin 5 and JNK1/2 pathways [90,92,98,105,112,115,120,121,124,159,162,165,172, 177–183]. Based on the aforementioned studies in vivo and in vitro, targets that can be directly regulated by AG for the prevention and treatment of ASCVD include SREBPs, ERK1/2, NOS, NF-κB, HIF-1α, ROS, PI3K, AKT, etc. Among them, SREBPs, PHD2/3, HO-1, PP2A, PKC and PLCγ2 which could interact directly with AG are new targets. Therefore, AG is a promising candidate drug for the treatment of ASCVD and its risk factors, such as obesity, hyperlipidaemia, hypertension, diabetes, CHD, MI, ischaemic heart disease, cerebral ischemia and cerebral haemorrhage.

Nevertheless, pharmacological studies of AG regarding the prevention and treatment of ASCVD had several drawbacks. First, animal models of AS were inaccurate. For example, lipid metabolism in rodents is primarily based on HDL levels instead of LDL levels as in humans [261,262]. Therefore, in the future, it is necessary to establish novel animal models minimizing differences between the models and the human body. Second, the role of AG in the prevention and treatment of other risk factors (e.g. hypertension and hyperuricemia) and other ASCVD (e.g. unstable angina and peripheral vascular disease) remains unreported. In the future, more in-depth studies should be conducted to elucidate the implications of AG in clinical treatment. Third, due to lackage of specific studies focusing on the dosage and course of AG in the prevention and treatment, this issue needed further investigation. Fourth, most published studies are limited to in vitro and in vivo experimental studies and the effects of AG in the prevention and treatment of ASCVD has not been validated in human trials. Finally, there was no relevant literature on the structure-activity relationship of AG in the treatment of ASCVD, which provided an idea for the follow-up researches.

Attention should be paid to the safety profile of AG. The difference between toxicity and pharmacological profile of AG lied in the dose administered. In clinical practice, the minimum toxic dose of AG (1,400 mg, for 3 weeks, oral administration to humans equivalent to

125 mg/kg, oral administration in rats), much higher than the maximum dose for pharmacological profile (100 mg/kg, for 4 weeks, oral gavage in mice equivalent to 70 mg/kg, oral gavage in rats), caused only minor side effects, which were relieved after discontinuation [92]. Furthermore, the acute toxicity studies showed that AG was found to be safe up to a maximum dose of 500 mg/kg, single oral administration in rats [91]. This indicated that AG was safe enough and could be used to prevent and treat ASCVD. However, AG elicited three toxicities to some extends. AG with doses used to treat ASCVD (25 and 50 mg/kg in rats) could cause male reproductive toxicity [189]. Notably, the patients suffering from ASCVD and its risk factors are mainly middle-aged and elderly, most of whom have no desire to have children. Therefore, in most cases, AG, with a little male-reproductive toxicity, can be applied in the prevention and treatment of ASCVD. Moreover, the reproductive toxicity of AG was temporary. If some patients have reproductive requirement, they can stop taking AG and prepare to give births after the reproductive indexes were reversed. Furthermore, AG had been demonstrated to destroy the maturation and fertilization potential of female oocytes [190]. However, further in vivo studies in animals and clinical trials in humans are needed to determine whether AG caused reproductive toxicity in females. Also, the dose of AG that caused brain toxicity in rats (5 mg/kg, intraperitoneal) was much greater than that for ischaemic stroke (0.1 mg/kg, intraperitoneal), suggesting that the brain toxicity of AG could be avoided [182,193]. Additionally, AG induced certain renal toxicity to a certain extent in vitro and renal toxicity of AG injection, rather than oral preparations of AG were reported. Therefore, it is suspected that AG might cause renal toxicities, mainly due to long courses (e.g. 48 days of administration) and specific modes of administration (e.g. intraperitoneal injection). Conclusively, in addition to reducing the dosage of AG, approaches including controlling extremely long treatment courses and modes of administration and monitoring the renal, reproductive and cerebral toxicities, and developing targeted drug delivery systems are required to alleviate the toxicities of AG, if necessary, in clinical settings.

In-depth studies on the availability and pharmacokinetics of AG will help to improve its clinical application. With a complex structure that is difficult to synthesise, AG was often isolated and purified from plants using different methods (e.g. reflux, MAE, Soxhlet extraction and supercritical CO_2 extraction). The content of AG was higher in plant leaves than in roots and stems but varied depending on the origin, harvest time and processing method [263,264]. According to the aforementioned literature, the best method for extracting AG from the leaves of *A. paniculata* is the microwave-assisted MAE methanol solvent technique [205]. Pharmacokinetic studies have reported that, the *AUC* values of AG in rats, chickens, dogs and humans are low due to biliary excretion and P-gp efflux. Furthermore, AG does not exhibit organ-targeting ability and is mainly found in blood. Due to differences of metabolic pathways, the metabolites of AG among animals and human were different. Additionally, AG had a long half-life and slow in vivo elimination. Besides, some issues are worthy further studying. For example, the elimination half-life of AG in humans was 10.50 ± 2.07 h, suggesting a long half-life and slow in vivo elimination of AG [188,265]. Therefore, in order to maintain the blood concentration of AG in a high level, the dosing frequency should be twice or three times one day, instead of one time per day.

The low bioavailability and non-targeting to organs of AG greatly limited its pharmacological activity in vivo. Therefore, the efficacy of AG could be improved using effective derivative substitutes and drug delivery systems (e.g. nano-emulsions, nanosuspensions, microspheres, liposomes, micelles and nanoparticles). For example, bioavailability of AG was improved when it was administered in the forms of nanoemulsion vesicles and pH-sensitive nanoparticles [251,255]. Additionally, administration of AG niosomes and nanosuspensions can help target the liver [266,267]. However, some delivery systems have shortcomings. For example, liposomes have drawbacks such as poor stability, insufficient circulation, drug leakage, large particle size and low capacity to encapsulate lipophilic drugs [268,269]. Liposomal and polymeric nanoparticles do not meet the requirements for high drug delivery efficiency, which affects efficacy [270]. Polymers and micelles may cause toxic effects at the site of administration [271]. Liposomes occasionally induce oxidative and hydrolysis-like reactions that cause side effects after drug administration [272]. Notably, intraperitoneal injection of AG (5 mg/kg) induced neurotoxicity in rats, which might be attributed to the dosage form rather than AG itself [193]. Besides, to date, no literature has reported that the new dosage forms enhance the therapeutic effect of AG on ASCVD [273–276]. Therefore, dosage forms of AG that can promote efficiency but bring little adverse effects need further research.

Altogether, AG, which is a widely used drug (old bottle), can be used for the prevention and treatment of ASCVD (novel wine). This review systematically summarized the pathogenesis of ASCVD, the potential role of AG in the treatment of ASCVD, AS and AS-related risk factors in vitro and in vivo and the mechanism of action of AG. To the best of our knowledge, no systematic review has summarized the role and mechanism of action of AG in ASCVD to date. Therefore, this paper provides a comprehensive review focusing on the pathogenesis of ASCVD and preventive and therapeutic potentials of AG in ASCVD and offers new directions for future research.

CRediT author statement

Tingting Gou: Writing - Original draft preparation, Conceptualization, Visualization; **Minghao Hu:** Writing - Original draft preparation, Visualization; **Min Xu:** Writing - Original draft preparation, Term, Data curation; **Yuchen Chen:** Data curation, Investigation; **Rong Chen:** Data curation, Investigation; **Tao Zhou:** Writing - Reviewing and Editing, Visualization; **Junjing Liu:** Writing - Reviewing and Editing, Visualization; **Li Guo:** Writing - Reviewing and Editing, Supervision; **Hui Ao:** Conceptualization, Writing - Reviewing and Editing, Funding acquisition; **Qiang Ye:** Conceptualization, Writing - Reviewing and Editing, Funding acquisition.

Declaration of competing interest

The authors declare that there are no conflicts of interest.

Acknowledgments

This research was funded by the National Natural Science Foundation of China (Grant Nos.: 81891012 and U19A2010), the National Interdisciplinary Innovation Team Program of Traditional Chinese Medicine (Grant No.: ZYYCXTD-D-202209), Chinese Medicine Science and Technology Industry Innovation Team Program of Sichuan Province (Grant No.: 2022C001), and Chengdu University of Traditional Chinese Medicine “Xinglin Scholars” Discipline Talent Research Promotion Program (Grant No.: XCZX2022010). We would like to thank Adobe Illustrator for their valuable contribution to this review. The software's powerful graphic design and editing capabilities allow us to create visually appealing numbers and illustrations. We acknowledge the important role Adobe Illustrator played in the success of this study, and I am grateful for its contributions.

References

[1] S. Surma, M. Banach, Fibrinogen and atherosclerotic cardiovascular diseases-review of the literature and clinical studies, Int. J. Mol. Sci. 23 (2021), 193.
[2] P. Libby, J.E. Buring, L. Badimon, et al., Atherosclerosis, Nat. Rev. Dis. Primers 5 (2019), 56.
[3] M. Sanz, A.M. del Castillo, S. Jepsen, et al., Periodontitis and cardiovascular diseases. consensus report, Glob. Heart 15 (2020), 1.
[4] G.A. Roth, G.A. Mensah, C.O. Johnson, et al., Global burden of cardiovascular diseases and risk factors, 1990-2019: Update from the GBD 2019 study, J. Am. Coll. Cardiol. 76 (2020) 2982–3021.
[5] N.D. Wong, M.J. Budoff, K. Ferdinand, et al., Atherosclerotic cardiovascular disease risk assessment: An American Society for Preventive Cardiology clinical practice statement, Am. J. Prev. Cardiol. 10 (2022), 100335.
[6] M. Cainzos-Achirica, K. Glassner, H.S. Zawahir, et al., Inflammatory bowel disease and atherosclerotic cardiovascular disease: JACC review topic of the week, J. Am. Coll. Cardiol. 76 (2020) 2895–2905.
[7] A. Lazaro, G. Alvarez-Llamas, J. Gallego-Delgado, et al., Pharmacoproteomics in cardiac hypertrophy and atherosclerosis, Cardiovasc. Hematol. Disord. Drug Targets 9 (2009) 141–148.
[8] B. Rauff, A. Malik, Y.A. Bhatti, et al., Association of viruses in the development of cardiovascular diseases, Curr. Pharm. Des. 27 (2021) 3913–3923.
[9] Y. Geng, Molecular mechanisms for cardiovascular stem cell apoptosis and growth in the hearts with atherosclerotic coronary disease and ischemic heart failure, Ann. N. Y. Acad. Sci. 1010 (2003) 687–697.
[10] G.D. Flora, M.K. Nayak, A brief review of cardiovascular diseases, associated risk factors and current treatment regimes, Curr. Pharm. Des. 25 (2019) 4063–4084.
[11] A.N. Hasso, W.A. Stringer, K.D. Brown, Cerebral ischemia and infarction, Neuroimaging, Clin. N. Am. 4 (1994) 733–752.
[12] Y. Wan, J. Xia, J. Xu, et al., Nuciferine, an active ingredient derived from lotus leaf, lights up the way for the potential treatment of obesity and obesity-related diseases, Pharmacol. Res. 175 (2022), 106002.
[13] X. Dong, Y. Zeng, Y. Liu, et al., *Aloe*-emodin: A review of its pharmacology, toxicity, and pharmacokinetics, Phytother. Res. 34 (2020) 270–281.
[14] A. Zia, T. Farkhondeh, A.M. Pourbagher-Shahri, et al., The role of curcumin in aging and senescence: Molecular mechanisms, Biomed. Pharmacother. 134 (2021), 111119.
[15] B. Kulczyński, A. Gramza-Michałowska, J. Sulibursk, et al., Puerarin-an isoflavone with beneficial effects on bone health, Front. Biosci. Landmark Ed. 26 (2021) 1653–1667.
[16] J. Wu, Y. Yang, Y. Wan, et al., New insights into the role and mechanisms of ginsenoside Rg1 in the management of Alzheimer's disease, Biomed. Pharmacother. 152 (2022), 113207.
[17] Y. Wan, J. Wang, J. Xu, et al., *Panax ginseng* and its ginsenosides: Potential candidates for the prevention and treatment of chemotherapy-induced side effects, J. Ginseng Res. 45 (2021) 617–630.
[18] J. Xu, Y. Wan, F. Tang, et al., Emerging significance of ginsenosides as potentially reversal agents of chemoresistance in cancer therapy, Front. Pharmacol. 12 (2021), 720474.
[19] Y. Wan, D. Liu, J. Xia, et al., Ginsenoside CK, rather than Rb1, possesses potential chemopreventive activities in human gastric cancer via regulating PI3K/AKT/NF-κB signal pathway, Front. Pharmacol. 13 (2022), 977539.
[20] A.B. Smith, B.H. Toder, P.J. Carroll, et al., Andrographolide: An X-ray crystallographic analysis, J. Crystallogr. Spectrosc. Res. 12 (1982) 309–319.
[21] D. Dalawai, C. Aware, J.P. Jadhav, et al., RP-HPLC analysis of diterpene lactones in leaves and stem of different species of *Andrographis*, Nat. Prod. Res. 35 (2021) 2239–2242.
[22] J. Chang, R. Zhang, Y. Zhang, et al., Andrographolide drop-pill in treatment of acute upper respiratory tract infection with external wind-heat syndrome: A multicenter and randomized controlled trial, J. Chin. Integr. Med. 6 (2008) 1238–1245.
[23] E.S. Gabrielian, A.K. Shukarian, G.I. Goukasova, et al., A double blind, placebo-controlled study of *Andrographis paniculata* fixed combination Kan Jang in the treatment of acute upper respiratory tract infections including sinusitis, Phytomed. 9 (2002) 589–597.
[24] Y. Zhao, P. Huang, Z. Chen, et al., Clinical application analysis of andrographolide total ester sulfonate injection, a traditional Chinese medicine licensed in China, Huazhong Keji Daxue Xuebao Yixue Yingdewen Ban 37 (2017) 293–299.
[25] J. Melchior, S. Palm, G. Wikman, Controlled clinical study of standardized *Andrographis paniculata* extract in common cold - a pilot trial, Phytomed. 3 (1997) 315–318.
[26] S.K. Wong, K.Y. Chin, S. Ima-Nirwana, A review on the molecular basis underlying the protective effects of *Andrographis paniculata* and andrographolide against myocardial injury, Drug Des. Devel. Ther. 15 (2021) 4615–4632.
[27] V. Arya, V.K. Gupta, Chemistry and pharmacology of plant cardioprotectives: A review, International Journal of Pharmaceutical Sciences and Research 2 (2011) 1156–1167.
[28] S.K. Ojha, M. Nandave, S. Kumari, et al., Antioxidant activity of *Andrographis paniculata* in ischemic myocardium of rats, Global Journal of pharmacology 3 (2009) 154–157.
[29] Y. Dai, S. Chen, L. Chai, et al., Overview of pharmacological activities of *Andrographis paniculata* and its major compound andrographolide, Crit. Rev. Food Sci. Nutr. 59 (2019) S17–S29.
[30] M.T. Islam, Andrographolide, a new hope in the prevention and treatment of metabolic syndrome, Front. Pharmacol. 8 (2017) 571.
[31] K. Driscoll, A.D. Cruz, J.T. Butcher, Inflammatory and biomechanical drivers of endothelial-interstitial interactions in calcific aortic valve disease, Circ. Res. 128 (2021) 1344–1370.
[32] Y. Li, K.C. Ueng, J.S. Jeng, et al., Taiwan lipid guidelines for high risk patients, J. Formos. Med. Assoc. 116 (2017) 217–248.
[33] A.M. Shafter, K. Shaikh, A. Johanis, et al., De-risking primary prevention: Role of imaging, Ther, Adv. Cardiovasc. Dis. 15 (2021), 17539447211051248.
[34] J.T. Wilkins, S.S. Gidding, J.G. Robinson, Can atherosclerosis be cured? Curr. Opin. Lipidol. 30 (2019) 477–484.
[35] T. Quillard, G. Franck, T. Mawson, et al., Mechanisms of erosion of atherosclerotic plaques, Curr. Opin. Lipidol. 28 (2017) 434–441.
[36] A.E. Neele, L. Willemsen, H.J. Chen, et al., Targeting epigenetics as atherosclerosis treatment: An updated view, Curr. Opin. Lipidol. 31 (2020) 324–330.
[37] R. Ross, Atherosclerosis: An inflammatory disease, N. Engl. J. Med. 340 (1999) 115–126.
[38] S.N. Bhupathiraju, F.B. Hu, Epidemiology of obesity and diabetes and their cardiovascular complications, Circ. Res. 118 (2016) 1723–1735.
[39] S. Mitra, T. Goyal, J.L. Mehta, Oxidized LDL, LOX-1 and atherosclerosis, Cardiovasc, Drugs Ther 25 (2011) 419–429.
[40] F. Lovren, H. Teoh, S. Verma, Obesity and atherosclerosis: Mechanistic insights, Can. J. Cardiol. 31 (2015) 177–183.
[41] J. Tian, Y. Liu, Y. Liu, et al., Cellular and molecular mechanisms of diabetic atherosclerosis: Herbal medicines as a potential therapeutic approach, Oxid. Med. Cell. Longev. 2017 (2017) 1–16.
[42] R.P. Mason, Optimal therapeutic strategy for treating patients with hypertension and atherosclerosis: Focus on olmesartan medoxomil, Vasc. Health Risk Manag. 7 (2011) 405–416.
[43] K. Iglay, H. Hannachi, P.J. Howie, et al., Prevalence and co-prevalence of comorbidities among patients with type 2 diabetes mellitus, Curr. Med. Res. Opin. 32 (2016) 1243–1252.
[44] S. Tabaei, S.S. Tabaee, DNA methylation abnormalities in atherosclerosis, Artif. Cells Nanomed. Biotechnol. 47 (2019) 2031–2041.
[45] D. Mauricio, E. Castelblanco, N. Alonso, Cholesterol and inflammation in atherosclerosis: An immune-metabolic hypothesis, Nutrients 12 (2020), 2444.
[46] L.M. Buja, Nikolai N. anitschkow and the lipid hypothesis of atherosclerosis, Cardiovasc. Pathol. 23 (2014) 183–184.
[47] M. Naito, Amide-adducts in atherosclerosis, Sub Cell, Biochem 77 (2014) 95–102.
[48] P. Sun, K.M. Dwyer, C.N. Merz, et al., Blood pressure, LDL cholesterol, and intima-media thickness: A test of the "response to injury" hypothesis of atherosclerosis, Arterioscler. Thromb. Vasc. Biol. 20 (2000) 2005–2010.
[49] Z. Liu, R.A. Khalil, Evolving mechanisms of vascular smooth muscle contraction highlight key targets in vascular disease, Biochem. Pharmacol. 153 (2018) 91–122.
[50] R. Wang, M. Wang, J. Ye, et al., Mechanism overview and target mining of atherosclerosis: Endothelial cell injury in atherosclerosis is regulated by glycolysis (Review), Int. J. Mol. Med. 47 (2021) 65–76.
[51] R. Kaur, M. Kaur, J. Singh, Endothelial dysfunction and platelet hyperactivity in type 2 diabetes mellitus: Molecular insights and therapeutic strategies, Cardiovasc. Diabetol. 17 (2018), 121.
[52] S. Paone, A.A. Baxter, M.D. Hulett, et al., Endothelial cell apoptosis and the role of endothelial cell-derived extracellular vesicles in the progression of atherosclerosis, Cell, Mol. Life Sci. 76 (2019) 1093–1106.
[53] A. Gaiz, S. Mosawy, N. Colson, et al., Thrombotic and cardiovascular risks in type two diabetes; Role of platelet hyperactivity, Biomed, Pharmacother 94 (2017) 679–686.
[54] J. Hurtubise, K. McLellan, K. Durr, et al., The different facets of dyslipidemia and hypertension in atherosclerosis, Curr. Atheroscler. Rep. 18 (2016) 82.
[55] A.J. van Boven, J.W. Jukema, R. Paoletti, Endothelial dysfunction and dyslipidemia: Possible effects of lipid lowering and lipid modifying therapy, Pharmacol. Res. 29 (1994), 261–272.
[56] J.M. van Gils, J.J. Zwaginga, P.L. Hordijk, Molecular and functional interactions among monocytes, platelets, and endothelial cells and their relevance for cardiovascular diseases, J. Leukoc. Biol. 85 (2009) 195–204.
[57] P. Libby, P.M. Ridker, G.K. Hansson, et al., Inflammation in atherosclerosis: From pathophysiology to practice, J. Am. Coll. Cardiol. 54 (2009) 2129–2138.
[58] A. Tedgui, Z. Mallat, Cytokines in atherosclerosis: Pathogenic and regulatory pathways, Physiol. Rev. 86 (2006) 515–581.
[59] L. Groh, S.T. Keating, L.A.B. Joosten, et al., Monocyte and macrophage immunometabolism in atherosclerosis, Semin. Immunopathol. 40 (2018) 203–214.
[60] G.L. Basatemur, H.F. Jørgensen, M.C.H. Clarke, et al., Vascular smooth muscle cells inatherosclerosis, Nat. Rev. Cardiol 16 (2019) 727–744.
[61] S. Taleb, Inflammation in atherosclerosis, Arch. Cardiovasc. Dis. 109 (2016) 708–715.

[62] A.C. Newby, Metalloproteinases and vulnerable atherosclerotic plaques, Trends Cardiovasc. Med. 17 (2007) 253–258.
[63] Z.A. Massy, W.F. Keane, Pathogenesis of atherosclerosis, Semin. Nephrol. 16 (1996) 12–20.
[64] M. Sponder, M. Fritzer-Szekeres, R. Marculescu, et al., A new coronary artery disease grading system correlates with numerous routine parameters that were associated with atherosclerosis: A grading system for coronary artery disease severity, Vasc. Heath, Risk Manag 10 (2014) 641–647.
[65] M. Sekulic, M. Zacharias, B. Medalion, Ischemic cardiomyopathy and heart failure, Circ. Heart Fail. 12 (2019), e006006.
[66] N. Narula, J.W. Olin, N. Narula, Pathologic disparities between peripheral artery disease and coronary artery disease, Arterioscler, Thromb. Vasc. Biol. 40 (2020) 1982–1989.
[67] F. Malakootikhah, H. Naghavi, N. Firouzabadi, et al., Association of human platelet alloantigens encoding gene polymorphisms with the risk of Coronary artery disease in Iranian patients, BMC Cardiovasc. Disord. 21 (2021), 68.
[68] R. Arasu, A. Arasu, J. Muller, Carotid artery stenosis: An approach to its diagnosis and management, Aust. J. Gen. Pract. 50 (2021) 821–825.
[69] J. Pappachan, F.J. Kirkham, Cerebrovascular disease and stroke, Arch. Dis. Child. 93 (2008) 890–898.
[70] Y. Wang, R. Meng, G. Liu, et al., Intracranial atherosclerotic disease, Neurobiol. Dis. 124 (2019) 118–132.
[71] N. Nirala, R. Periyasamy, A. Kumar, Noninvasive diagnostic methods for better screening of peripheral arterial disease, Ann. Vasc. Surg. 52 (2018) 263–272.
[72] M. Luczak, D. Formanowicz, Ł. Marczak, et al., Deeper insight into chronic kidney disease-related atherosclerosis: Comparative proteomic studies of blood plasma using 2DE and mass spectrometry, J. Transl. Med. 13 (2015), 20.
[73] C. Heiss, Chronic mesenteric ischemia, Dtsch. Med. Wochenschr. 1946 143 (2018) 1426–1429.
[74] Y. Zhu, X. Xian, Z. Wang, et al., Research progress on the relationship between atherosclerosis and inflammation, Biomolecules 8 (2018), 80.
[75] Q. Zhang, J. Liu, H. Duan, et al., Activation of Nrf2/HO-1 signaling: An important molecular mechanism of herbal medicine in the treatment of atherosclerosis *via* the protection of vascular endothelial cells from oxidative stress, J. Adv. Res. 34 (2021) 43–63.
[76] W. Dröge, Free radicals in the physiological control of cell function, Physiol. Rev. 82 (2002) 47–95.
[77] X. Yu, X. Zheng, C. Tang, Nuclear factor-κB activation as a pathological mechanism of lipid metabolism and atherosclerosis, Adv. Clin. Chem. 70 (2015) 1–30.
[78] X. Yang, T. He, S. Han, et al., The role of traditional Chinese medicine in the regulation of oxidative stress in treating coronary heart disease, Oxid. Med. Cell. Longev. 2019 (2019), 3231424.
[79] T.V. Arumugam, S.H. Baik, P. Balaganapathy, et al., Notch signaling and neuronal death in stroke, Prog. Neurobiol. 165-167 (2018) 103–116.
[80] J. Zeng, Y. Chen, R. Ding, et al., Isoliquiritigenin alleviates early brain injury after experimental intracerebral hemorrhage via suppressing ROS- and/or NF-κB-mediated NLRP3 inflammasome activation by promoting Nrf2 antioxidant pathway, J. Neuroinflammation 14 (2017), 119.
[81] A. Gisterå, G.K. Hansson, The immunology of atherosclerosis, Nat. Rev. Nephrol. 13 (2017) 368–380.
[82] J. Pedro-Botet, E. Climent, D. Benaiges, Atherosclerosis and inflammation. New therapeutic approaches, Med. Clin. 155 (2020) 256–262.
[83] G. Kyriakos, L.V. Quiles-SÁnchez, E. Diamantis, et al., Lipid-lowering drugs and neurocognitive function: A systematic review, Vivo Athens Greece 34 (2020) 3109–3114.
[84] G.A. Fitzgerald, E.A. Meagher, Antiplatelet drugs, Eur. J. Clin. Investig. 24 (1994) 46–49.
[85] M.N. McComb, J.Y. Chao, T.M.H. Ng, Direct vasodilators and sympatholytic agents, J. Cardiovasc. Pharmacol. Ther. 21 (2016) 3–19.
[86] J. Yee, C.G. Kaide, Emergency reversal of anticoagulation, West, J. Emerg. Med. 20 (2019) 770–783.
[87] A. Tiwari, V. Bansal, A. Chugh, et al., Statins and myotoxicity: A therapeutic limitation, Expert Opin. Drug Saf. 5 (2006) 651–666.
[88] D.N. Kiortsis, T.D. Filippatos, D.P. Mikhailidis, et al., Statin-associated adverse effects beyond muscle and liver toxicity, Atherosclerosis 195 (2007) 7–16.
[89] H.L. Figge, J. Figge, P.F. Souney, et al., Nicotinic acid: A review of its clinical use in the treatment of lipid disorders, Pharmacotherapy 8 (1988) 287–294.
[90] T. Yang, H. Shi, Z. Wang, et al., Hypolipidemic effects of andrographolide and neoandrographolide in mice and rats, Phytother. Res. 27 (2013) 618–623.
[91] R. Al Batran, F. Al-Bayaty, M.M. Al-Obaidi, et al., Acute toxicity and the effect of andrographolide on *Porphyromonas gingivalis*-induced hyperlipidemia in rats, BioMed Res. Int. 2013 (2013), 594012.
[92] L. Ding, J. Li, B. Song, et al., Andrographolide prevents high-fat diet-induced obesity in C57BL/6 mice by suppressing the sterol regulatory element-binding protein pathway, J. Pharmacol. Exp. Ther. 351 (2014) 474–483.
[93] L.J. Engelking, M.J. Cantoria, Y. Xu, et al., Developmental and extrahepatic physiological functions of SREBP pathway genes in mice, Semin. Cell Dev. Biol. 81 (2018) 98–109.
[94] S. Muraoka, Y. Nitta, T. Yamada, et al., Increase of anti-oxidative capacity during differentiation of 3T3-L1 preadipocytes into adipocytes, YAKUGAKU ZASSHI 137 (2017) 1137–1145.
[95] W. Chen, H. Su, L. Feng, et al., Andrographolide suppresses preadipocytes proliferation through glutathione antioxidant systems abrogation, Life Sci 156 (2016) 21–29.
[96] N. Umek, S. Horvat, E. Cvetko, Skeletal muscle and fiber type-specific intramyocellular lipid accumulation in obese mice, Bosn. J. Basic Med. Sci. 21 (2021) 730–738.
[97] A. Engin, Fat cell and fatty acid turnover in obesity, Adv. Exp. Med. Biol. 960 (2017) 135–160.
[98] C.C. Chen, W. Chuang, A.H. Lin, et al., Andrographolide inhibits adipogenesis of 3T3-L1 cells by suppressing C/EBPβ expression and activation, Toxicol, Appl. Pharmacol. 307 (2016) 115–122.
[99] L. Jin, W. Fang, B. Li, et al., Inhibitory effect of andrographolide in 3T3-L1 adipocytes differentiation through the PPARγ pathway, Mol. Cell. Endocrinol. 358 (2012) 81–87.
[100] M. Kaewkittikhun, N. Boonmuen, P. Kheolamai, et al., Andrographolide reduces lipid droplet accumulation in adipocytes derived from human bone marrow mesenchymal stem cells by suppressing regulators of adipogenesis, J. Agric. Food Chem. 69 (2021) 9259–9269.
[101] M.A. Kalwat, M.H. Cobb, Mechanisms of the amplifying pathway of insulin secretion in the β cell, Pharmacol. Ther. 179 (2017) 17–30.
[102] S.L. Shumak, M. Gulan, B. Zinman, et al., Determination and kinetic analysis of non-insulin mediated glucose uptake in type 1 (insulin-dependent) diabetes mellitus, Diabetologia 32 (1989) 28–33.
[103] K. Cheng, A. Asakawa, Y. Li, et al., Opioid μ-receptors as new target for insulin resistance, Pharmacol. Ther. 139 (2013) 334–340.
[104] S.A. Wohaieb, D.V. Godin, Alterations in free radical tissue-defense mechanisms in streptozocin-induced diabetes in rat. Effects of insulin treatment, Diabetes 36 (1987) 1014–1018.
[105] A.E. Nugroho, I.R. Rais, I. Setiawan, et al., Pancreatic effect of andrographolide isolated from *Andrographis paniculata* (Burm. f.) Nees, Pak, J. Biol. Sci. 17 (2014) 22–31.
[106] B. Ahmed, R. Sultana, M.W. Greene, Adipose tissue and insulin resistance in obese, Biomed, Pharmacother 137 (2021), 111315.
[107] L. Jin, G. Shi, G. Ning, et al., Andrographolide attenuates tumor necrosis factor-alpha-induced insulin resistance in 3T3-L1 adipocytes, Mol. Cell. Endocrinol. 332 (2011) 134–139.
[108] R. Ballotti, Y. Le Marchand-Brustel, S. Gammeltoft, et al., Insulin receptor: Tyrosine kinase activity and insulin action, Reprod. Nutr. Dev. 29 (1989) 653–661.
[109] S. Khan, A.A.L. Evans, S. Hughes, et al., Beta-endorphin decreases fatigue and increases glucose uptake independently in normal and dystrophic mice, Muscle Nerve 31 (2005) 481–486.
[110] A.A.L. Evans, M.E. Smith, Opioid receptors in fast and slow skeletal muscles of normal and dystrophic mice, Neurosci. Lett. 366 (2004) 339–341.
[111] A.A. Evans, S. Khan, M.E. Smith, Evidence for a hormonal action of beta-endorphin to increase glucose uptake in resting and contracting skeletal muscle, J. Endocrinol. 155 (1997) 387–392.
[112] B.C. Yu, C.K. Chang, C.F. Su, et al., Mediation of beta-endorphin in andrographolide-induced plasma glucose-lowering action in type I diabetes-like animals, Naunyn. Schmiedebergs. Arch. Pharmacol. 377 (2008) 529–540.
[113] J. Berger, C. Biswas, P.P. Vicario, et al., Decreased expression of the insulin-responsive glucose transporter in diabetes and fasting, Nature 340 (1989) 70–72.
[114] A. Consoli, N. Nurjhan, F. Capani, et al., Predominant role of gluconeogenesis in increased hepatic glucose production in NIDDM, Diabetes 38 (1989) 550–557.
[115] B.C. Yu, C.R. Hung, W. Chen, et al., Antihyperglycemic effect of andrographolide in streptozotocin-induced diabetic rats, Planta Med 69 (2003) 1075–1079.
[116] S.J. Custodio-Chablé, R.A. Lezama, E. Reyes-Maldonado, Platelet activation as a trigger factor for inflammation and atherosclerosis, Cir, Cir 88 (2020) 233–243.
[117] D.A. Chistiakov, Y.V. Bobryshev, A.N. Orekhov, Macrophage-mediated cholesterol handling in atherosclerosis, J. Cell. Mol. Med. 20 (2016) 17–28.
[118] E. Butoi, A.M. Gan, I. Manduteanu, Molecular and functional interactions among monocytes/macrophages and smooth muscle cells and their relevance for atherosclerosis, Crit. Rev. Eukaryot. Gene Expr. 24 (2014) 341–355.
[119] J. Liu, S. Dong, Y. Ru, A review: Pathological and molecular biological study on atherosclerosis, Clin. Chim. Acta 531 (2022) 217–222.
[120] R. Al Batran, F. Al-Bayaty, M.M. Al-Obaidi, et al., Evaluation of the effect of andrographolide on atherosclerotic rabbits induced by *Porphyromonas gingivalis*, BioMed Res. Int. 2014 (2014), 724718.
[121] R. Batran, F. Al-Bayaty, M.M.J. Al-Obaidi, et al., Insights into the anti-atherogenic molecular mechanisms of andrographolide against *Porphyromonas gingivalis*-induced atherosclerosis in rabbits, Naunyn Schmiedeberg's Arch. Pharmacol. 387 (2014) 1141–1152.
[122] T. Wu, Y. Peng, S. Yan, et al., Andrographolide ameliorates atherosclerosis by suppressing pro-inflammation and ROS generation-mediated foam cell formation, Inflammation 41 (2018) 1681–1689.
[123] M.Y. Hamidy, F. Oenzil, Yanwirasti, et al., Effect of andrographolide on foam cell formation at the initiation stage of atherosclerosis, Kne Eng 1 (2019) 329.
[124] M. Yulis Hamidy, F. Oenzil, Y. Yanwirasti, et al., Effect of andrographolide on monocyte chemoattractant protein-1 expression at the initiation stage of atherosclerosis in atherogenic diet-fed rats, Biomed. Pharmacol. J. 12 (2019) 1167–1173.

[125] M.M. Kavurma, M.R. Bennett, Expression, regulation and function of trail in atherosclerosis, Biochem. Pharmacol. 75 (2008) 1441–1450.
[126] X. Lin, S. Ouyang, C. Zhi, et al., Focus on ferroptosis, pyroptosis, apoptosis and autophagy of vascular endothelial cells to the strategic targets for the treatment of atherosclerosis, Arch. Biochem. Biophys. 715 (2022), 109098.
[127] N. Song, L. Jia, H. Cao, et al., Gypenoside inhibits endothelial cell apoptosis in atherosclerosis by modulating mitochondria through PI3K/Akt/bad pathway, BioMed Res. Int. 2020 (2020), 2819658.
[128] M. Duan, H. Zhou, Q. Wu, et al., Andrographolide protects against HG-induced inflammation, apoptosis, migration, and impairment of angiogenesis via PI3K/AKT-eNOS signalling in HUVECs, Mediators Inflamm 2019 (2019), 6168340.
[129] J.H. Chen, G. Hsiao, A. Lee, et al., Andrographolide suppresses endothelial cell apoptosis via activation of phosphatidyl inositol-3-kinase/Akt pathway, Biochem. Pharmacol. 67 (2004) 1337–1345.
[130] S. Sitia, L. Tomasoni, F. Atzeni, et al., From endothelial dysfunction to atherosclerosis, Autoimmun. Rev. 9 (2010) 830–834.
[131] M. Mudau, A. Genis, A. Lochner, et al., Endothelial dysfunction: The early predictor of atherosclerosis, Cardiovasc, J. Afr. 23 (2012) 222–231.
[132] G. Du, Y. Song, T. Zhang, et al., Simvastatin attenuates TNF-α-induced apoptosis in endothelial progenitor cells via the upregulation of SIRT1, Int. J. Mol. Med. 34 (2014) 177–182.
[133] M.A. Incalza, R. D'Oria, A. Natalicchio, et al., Oxidative stress and reactive oxygen species in endothelial dysfunction associated with cardiovascular and metabolic diseases, Vasc. Pharmacol. 100 (2018) 1–19.
[134] A.J. Valente, A.M. Irimpen, U. Siebenlist, et al., OxLDL induces endothelial dysfunction and death via $TRAF_3IP_2$: Inhibition by HDL3 and AMPK activators, Free. Radic. Biol. Med. 70 (2014) 117–128.
[135] T. Jain, E.A. Nikolopoulou, Q. Xu, et al., Hypoxia inducible factor as a therapeutic target for atherosclerosis, Pharmacol. Ther. 183 (2018) 22–33.
[136] T.F. Lüscher, R.R. Wenzel, Endothelin and endothelin antagonists: Pharmacology and clinical implications, Agents Actions Suppl 45 (1995) 237–253.
[137] H.C. Lin, S.L. Su, C.Y. Lu, et al., Andrographolide inhibits hypoxia-induced HIF-1α-driven endothelin 1 secretion by activating Nrf2/HO-1 and promoting the expression of prolyl hydroxylases 2/3 in human endothelial cells, Environ, Toxicol 32 (2017) 918–930.
[138] H.C. Lin, S.L. Su, W. Lin, et al., Andrographolide inhibits hypoxia-induced hypoxia-inducible factor 1α and endothelin 1 expression through the heme oxygenase 1/CO/cGMP/MKP-5 pathways in EA.hy926 cells, Environ. Toxicol. 33 (2018) 269–279.
[139] I.M. Fenyo, A.V. Gafencu, The involvement of the monocytes/macrophages in chronic inflammation associated with atherosclerosis, Immunobiology 218 (2013) 1376–1384.
[140] A. Yu, C.Y. Lu, T.S. Wang, et al., Induction of heme oxygenase 1 and inhibition of tumor necrosis factor alpha-induced intercellular adhesion molecule expression by andrographolide in EA.hy926 cells, J. Agric. Food Chem. 58 (2010) 7641–7648.
[141] C. Chao, C.K. Lii, I.T. Tsai, et al., Andrographolide inhibits ICAM-1 expression and NF-κB activation in TNF-α-treated EA.hy926 cells, J. Agric. Food Chem. 59 (2011) 5263–5271.
[142] C.Y. Lu, Y. Yang, C.C. Li, et al., Andrographolide inhibits TNFα-induced ICAM-1 expression via suppression of NADPH oxidase activation and induction of HO-1 and GCLM expression through the PI3K/Akt/Nrf2 and PI3K/Akt/AP-1 pathways in human endothelial cells, Biochem. Pharmacol. 91 (2014) 40–50.
[143 H.C. Lin, C.C. Li, Y. Yang, et al., *Andrographis paniculata* diterpenoids and ethanolic extract inhibit TNFα-induced ICAM-1 expression in EA.hy926 cells, Phytomedicine 52 (2019) 157–167.
[144] K.D. Mason, M.R. Carpinelli, J.I. Fletcher, et al., Programmed anuclear cell death delimits platelet life span, Cell 128 (2007) 1173–1186.
[145] G.L. Dale, P. Friese, Bax activators potentiate coated-platelet formation, J. Thromb. Haemost. 4 (2006) 2664–2669.
[146] M.K.S. Lee, M.J. Kraakman, D. Dragoljevic, et al., Apoptotic ablation of platelets reduces atherosclerosis in mice with diabetes, Arterioscler. Thromb. Vasc. Biol. 41 (2021) 1167–1178.
[147] L. Lien, C. Su, W.H. Hsu, et al., Mechanisms of andrographolide-induced platelet apoptosis in human platelets: Regulatory roles of the extrinsic apoptotic pathway, Phytother. Res. 27 (2013) 1671–1677.
[148] E. Khodadi, Platelet function in cardiovascular disease: Activation of molecules and activation by molecules, Cardiovasc. Toxicol. 20 (2020) 1–10.
[149] R. Lordan, A. Tsoupras, I. Zabetakis, Investigation of platelet aggregation in atherosclerosis, Meth. Mol. Biol. Clifton N J 2419 (2022) 333–347.
[150] W.J. Lu, J.J. Lee, D.S. Chou, et al., A novel role of andrographolide, an NF-kappa B inhibitor, on inhibition of platelet activation: The pivotal mechanisms of endothelial nitric oxide synthase/cyclic GMP, J. Mol. Med. Berlin Ger. 89 (2011) 1261–1273.
[151] P. Thisoda, N. Rangkadilok, N. Pholphana, et al., Inhibitory effect of *Andrographis paniculata* extract and its active diterpenoids on platelet aggregation, Eur. J. Pharmacol. 553 (2006) 39–45.
[152] E. Amroyan, E. Gabrielian, A. Panossian, et al., Inhibitory effect of andrographolide from *Andrographis paniculata* on PAF-induced platelet aggregation, Phytomed 6 (1999) 27–31.
[153] W.J. Lu, K.H. Lin, M.J. Hsu, et al., Suppression of NF-κB signaling by andrographolide with a novel mechanism in human platelets: Regulatory roles of the p38 MAPK-hydroxyl radical-ERK2 cascade, Biochem. Pharmacol. 84 (2012) 914–924.
[154] T. Wu, M. Tan, H. Gong, et al., Co-delivery of andrographolide and Notch1-targeted siRNA to macrophages with polymer-based nanocarrier for enhanced anti-inflammation, Chin. J. Polym. Sci. 36 (2018) 1312–1320.
[155] H.C. Lin, C.K. Lii, H. Chen, et al., Andrographolide inhibits oxidized LDL-induced cholesterol accumulation and foam cell formation in macrophages, Am. J. Chin. Med. 46 (2018) 87–106.
[156] A. Roy, S. Banerjee, U. Saqib, et al., NOS_1-derived nitric oxide facilitates macrophage uptake of low-density lipoprotein, J. Cell. Biochem. 120 (2019) 11593–11603.
[157] W.F. Chiou, J.J. Lin, C.F. Chen, Andrographolide suppresses the expression of inducible nitric oxide synthase in macrophage and restores the vasoconstriction in rat aorta treated with lipopolysaccharide, Br. J. Pharmacol. 125 (1998) 327–334.
[158] W.F. Chiou, C.F. Chen, J.J. Lin, Mechanisms of suppression of inducible nitric oxide synthase (iNOS) expression in RAW 264.7 cells by andrographolide, Br. J. Pharmacol. 129 (2000) 1553–1560.
[159] F. Li, S. Li, Effects of andrographolide on the activation of mitogen activated protein kinases and nuclear factor-κB in mouse peritoneal macrophage-derived foam cells, Chin, J. Integr. Med. 18 (2012) 391–394.
[160] Y. Chen, M.J. Hsu, J.R. Sheu, et al., Andrographolide, a novel NF- κ B inhibitor, induces vascular smooth muscle cell apoptosis via a ceramide-p47phox-ROS signaling cascade, Evid. Based Complement. Alternat. Med. 2013 (2013), 821813.
[161] Y. Chen, C.Y. Hsieh, T. Jayakumar, et al., Andrographolide induces vascular smooth muscle cell apoptosis through a SHP-1-PP2A-p38MAPK-p53 cascade, Sci. Rep. 4 (2014), 5651.
[162] Y. Wang, J. Wang, Q. Fan, et al., Andrographolide inhibits NF-kappaBeta activation and attenuates neointimal hyperplasia in arterial restenosis, Cell Res 17 (2007) 933–941.
[163] Z. Zhu, X. Jiang, B. Wang, et al., Andrographolide inhibits intimal hyperplasia in a rat model of autogenous vein grafts, Cell Biochem. Biophys. 60 (2011) 231–239.
[164] Y. Chen, M.J. Hsu, C.Y. Hsieh, et al., Andrographolide inhibits nuclear factor-κB activation through JNK-Akt-p65 signaling cascade in tumor necrosis factor-α-stimulated vascular smooth muscle cells, Sci. World J. 2014 (2014), 130381.
[165] C.Y. Hsieh, M.J. Hsu, G. Hsiao, et al., Andrographolide enhances nuclear factor-kappaB subunit p65 Ser536 dephosphorylation through activation of protein phosphatase 2A in vascular smooth muscle cells, J. Biol. Chem. 286 (2011) 5942–5955.
[166] A.C. Doran, N. Meller, C.A. McNamara, Role of smooth muscle cells in the initiation and early progression of atherosclerosis, Arterioscler, Thromb. Vasc. Biol. 28 (2008) 812–819.
[167] C.C. Chang, Y.F. Duann, T.L. Yen, et al., Andrographolide, a novel NF-κB inhibitor, inhibits vascular smooth muscle cell proliferation and cerebral endothelial cell inflammation, Acta Cardiol. Sin. 30 (2014) 308–315.
[168] D.J. Medina-Leyte, O. Zepeda-García, M. Domínguez-Pérez, et al., Endothelial dysfunction, inflammation and coronary artery disease: Potential biomarkers and promising therapeutical approaches, Int. J. Mol. Sci. 22 (2021), 3850.
[169] T. Lawrence, D.W. Gilroy, P.R. Colville-Nash, et al., Possible new role for NF-kappaB in the resolution of inflammation, Nat. Med. 7 (2001) 1291–1297.
[170] L. Yang, H. Guo, Y. Li, et al., Oleoylethanolamide exerts anti-inflammatory effects on LPS-induced THP-1 cells by enhancing PPARα signaling and inhibiting the NF-κB and ERK1/2/AP-1/STAT3 pathways, Sci. Rep. 6 (2016), 34611.
[171] Z. Khuchua, A.I. Glukhov, A.W. Strauss, et al., Elucidating the beneficial role of PPAR agonists in cardiac diseases, Int. J. Mol. Sci. 19 (2018) 3464.
[172] J. Shu, R. Huang, Y. Tian, et al., Andrographolide protects against endothelial dysfunction and inflammatory response in rats with coronary heart disease by regulating PPAR and NF-κB signaling pathways, Ann. Palliat. Med. 9 (2020) 1965–1975.
[173] A. Lejay, F. Fang, R. John, et al., Ischemia reperfusion injury, ischemic conditioning and diabetes mellitus, J. Mol. Cell. Cardiol. 91 (2016) 11–22.
[174] S.N. Goyal, S. Bharti, S. Arora, et al., Endothelin receptor antagonist BQ-123 ameliorates myocardial ischemic-reperfusion injury in rats: A hemodynamic, biochemical, histopathological and electron microscopic evidence, Biomed. Pharmacother. 64 (2010) 639–646.
[175] A.Y. Woo, M.M. Waye, S.K. Tsui, et al., Andrographolide up-regulates cellular-reduced glutathione level and protects cardiomyocytes against hypoxia/reoxygenation injury, J. Pharmacol. Exp. Ther. 325 (2008) 226–235.
[176] K. Thygesen, J.S. Alpert, H.D. White, et al., Universal definition of myocardial infarction, J. Am. Coll. Cardiol. 50 (2007) 2173–2195.
[177] S.E. Elasoru, P. Rhana, T. de Oliveira Barreto, et al., Andrographolide protects against isoproterenol-induced myocardial infarction in rats through inhibition of L-type Ca^{2+} and increase of cardiac transient outward K^+ currents, Eur. J. Pharmacol. 906 (2021), 174194.
[178] S.E. Elasoru, Biophysical and pharmacological evaluation of protective potentials of *andrographolide* against isoproterenol-induced myocardial infarction in rats [dissertation], Universidade Federal de Minas Gerais 906 (2021), 174194.

[179] S. Xie, W. Deng, J. Chen, et al., Andrographolide protects against adverse cardiac remodeling after myocardial infarction through enhancing Nrf2 signaling pathway, Int. J. Biol. Sci. 16 (2020) 12–26.
[180] Y. Li, L. Xiang, J. Miao, et al., Protective effects of andrographolide against cerebral ischemia-reperfusion injury in mice, Int. J. Mol. Med. 48 (2021), 186.
[181] S. Chan, W.S. Fred Wong, P.T. Wong, et al., Neuroprotective effects of andrographolide in a rat model of permanent cerebral ischaemia, Br. J. Pharmacol. 161 (2010) 668–679.
[182] T.L. Yen, R.J. Chen, T. Jayakumar, et al., Andrographolide stimulates p38 mitogen-activated protein kinase-nuclear factor erythroid-2-related factor 2-heme oxygenase 1 signaling in primary cerebral endothelial cells for definite protection against ischemic stroke in rats, Transl. Res. 170 (2016) 57–72.
[183] C.M. Chern, Liou, Y.H. Wang, et al., Andrographolide inhibits PI3K/AKT-dependent NOX2 and iNOS expression protecting mice against hypoxia/ischemia-induced oxidative brain injury, Planta Med 77 (2011) 1669–1679.
[184] D. Wang, K. Kang, J. Sun, et al., URB597 and andrographolide improve brain microvascular endothelial cell permeability and apoptosis by reducing oxidative stress and inflammation associated with activation of Nrf2 signaling in oxygen-glucose deprivation, Oxid. Med. Cell. Longev. 2022 (2022), 4139330.
[185] X. Li, T. Wang, D. Zhang, et al., Andrographolide ameliorates intracerebral hemorrhage induced secondary brain injury by inhibiting neuro-inflammation induction, Neuropharmacology 141 (2018) 305–315.
[186] W. Zhang, Z. Zhang, Z. Zhang, et al., Andrographolide induced acute kidney injury: Analysis of 26 cases reported in Chinese Literature, Nephrology 19 (2014) 21–26.
[187] C. Calabrese, S.H. Berman, J.G. Babish, et al., A phase I trial of andrographolide in HIV positive patients and normal volunteers, Phytother. Res. 14 (2000) 333–338.
[188] E. Ciampi, R. Uribe-San-Martin, C. Cárcamo, et al., Efficacy of andrographolide in not active progressive multiple sclerosis: A prospective exploratory double-blind, parallel-group, randomized, placebo-controlled trial, BMC Neurol 20 (2020), 173.
[189] M.A. Akbarsha, P. Murugaian, Aspects of the male reproductive toxicity/male antifertility property of andrographolide in albino rats: Effect on the testis and the cauda epididymidal spermatozoa, Phytother. Res. 14 (2000) 432–435.
[190] H. Liang, S. Lu, Z. Yan, et al., Andrographolide disrupts meiotic maturation by blocking cytoskeletal reorganisation and decreases the fertilisation potential of mouse oocytes, Reprod. Fertil. Dev. 29 (2017) 2336–2344.
[191] H. Huang, H. Cao, C. Xing, et al., Andrographolide induce human embryonic stem cell apoptosis by oxidative stress response, Mol. Cell. Toxicol. 15 (2019) 209–219.
[192] L. Gu, X. Zhang, W. Xing, et al., Andrographolide-induced apoptosis in human renal tubular epithelial cells: Roles of endoplasmic reticulum stress and inflammatory response, Environ. Toxicol. Pharmacol. 45 (2016) 257–264.
[193] T.L. Yen, W.H. Hsu, S.K. Huang, et al., A novel bioactivity of andrographolide from Andrographis paniculata on cerebral ischemia/reperfusion-induced brain injury through induction of cerebral endothelial cell apoptosis, Pharm. Biol. 51 (2013) 1150–1157.
[194] M. Rajani, N. Shrivastava, M.N. Ravishankara, A rapid method for isolation of andrographolide from Andrographis paniculata nees (kalmegh), Pharm. Biol. 38 (2000) 204–209.
[195] R. Wongkittipong, L. Prat, S. Damronglerd, et al., Solid-liquid extraction of andrographolide from plants—Experimental study, kinetic reaction and model, Sep. Purif. Technol. 40 (2004) 147–154.
[196] S. Sharma, Y.P. Sharma, Comparison of different extraction methods and HPLC method development for the quantification of andrographolide from Andrographis paniculata (Burm.f.) Wall. ex Nees, Ann. Phytomed. 7 (2018) 119–130.
[197] A.C. Kumoro, M. Hasan, Proceedings of the 1st International Conference on Natural Resources Engineering & Technology July 24-25, Putrajaya, Malaysia, 2006, pp. 664–670.
[198] A. Kumoro, Singh Hasan, Effects of solvent properties on the soxhlet extraction of diterpenoid lactones from Andrographis paniculata leaves, ScienceAsia 35 (2009) 306–309.
[199] K. Chen, W. Yin, W. Zhang, et al., Technical optimization of the extraction of andrographolide by supercritical CO_2, Food Bioprod. Process. 89 (2011) 92–97.
[200] A.C. Kumoro, M. Hasan, H. Singh, Extraction of andrographolide from Andrographis paniculata dried leaves using supercritical CO_2 and ethanol mixture, Ind. Eng. Chem. Res. 58 (2019) 742–751.
[201] M. Karpakavalli, K.R. Sini, I. Arthi, Microwave assisted extraction and estimation of *piperine, andrographolide* using HPLC techniques, Pharmacie Globale 3 (2012), 1.
[202] S. Vasu, V. Palaniyappan, S. Badami, A novel microwave-assisted extraction for the isolation of andrographolide from *Andrographis paniculata* and its *in vitro* antioxidant activity, Nat. Prod. Res. 24 (2010) 1560–1567.
[203] M. Mohan, S. Khanam, B. Shivananda, Optimization of microwave assisted extraction of *andrographolide* from *Andrographis paniculata* and its comparison with refluxation extraction method, Journal of Pharmacognosy and Phytochemistry 2 (2013) 342–348.
[204] M. Bhan, S. Satija, C. Garg, et al., Optimization of ionic liquid-based microwave assisted extraction of a diterpenoid lactone-andrographolide from *Andrographis paniculata* by response surface methodology, J. Mol. Liq. 229 (2017) 161–166.
[205] R.V. Rubi, A. University, J. Olay, et al., Ultrasound-microwave assisted extraction (UMAE) of andrographolide from sinta (*Andrographis paniculata*) with its bioactivity assessment, J. Environ. Sci. Manag. (2020) 1–7.
[206] L. Chen, H. Jin, L. Ding, et al., On-line coupling of dynamic microwave-assisted extraction with high-performance liquid chromatography for determination of andrographolide and dehydroandrographolide in *Andrographis paniculata* Nees, J. Chromatogr. A 1140 (2007) 71–77.
[207] P.R. Rao, V.K. Rathod, Rapid extraction of andrographolide from *Andrographis paniculata* Nees by three phase partitioning and determination of its antioxidant activity, Biocatal. Agric. Biotechnol. 4 (2015) 586–593.
[208] P.R. Rao, V.K. Rathod, Microwave assisted three phase extraction of andrographolide from *Andrographis paniculata*, J. Biol. Act. Prod. Nat. 9 (2019) 215–226.
[209] H. Gao, B. Wang, W.D.Z. Li, Synthetic applications of homoiodo allylsilane II. total syntheses of (-)-andrographolide and (+)-rostratone, Tetrahedron 70 (2014) 9436–9448.
[210] L. Yang, T. Wurm, B.S. Poudel, et al., Enantioselective total synthesis of andrographolide and 14-hydroxy-colladonin: Carbonyl reductive coupling and trans-decalin formation by hydrogen transfer, Angew. Chem. Int. Ed. 59 (2020) 23169–23173.
[211] L. Ye, T. Wang, L. Tang, et al., Poor oral bioavailability of a promising anti-cancer agent andrographolide is due to extensive metabolism and efflux by P-glycoprotein, J. Pharm. Sci. 100 (2011) 5007–5017.
[212] H.W. Chen, C.S. Huang, C.C. Li, et al., Bioavailability of andrographolide and protection against carbon tetrachloride-induced oxidative damage in rats, Toxicol. Appl. Pharmacol. 280 (2014) 1–9.
[213] A. Panossian, A. Hovhannisyan, G. Mamikonyan, et al., Pharmacokinetic and oral bioavailability of andrographolide from Andrographis paniculata fixed combination Kan Jang in rats and human, Phytomed 7 (2000) 351–364.
[214] R. Bera, S.K. Milan Ahmed, L. Sarkar, et al., Pharmacokinetic analysis and tissue distribution of andrographolide in rat by a validated LC-MS/MS method, Pharm. Biol. 52 (2014) 321–329.
[215] F. Xu, S. Fu, S. Gu, et al., Simultaneous determination of andrographolide, dehydroandrographolide and neoandrographolide in dog plasma by LC-MS/MS and its application to a dog pharmacokinetic study of Andrographis paniculata tablet, J. Chromatogr. B Analyt. Technol. Biomed. Life Sci. 990 (2015) 125–131.
[216] K. Liu, L. He, H. Gao, et al., Simultaneous determination of andrographolide and dehydroandrographolide in chicken plasma for application to pharmacokinetic studies, Chromatographia 70 (2009) 1441–1445.
[217] L. Xu, D. Xiao, S. Lou, et al., A simple and sensitive HPLC-ESI-MS/MS method for the determination of andrographolide in human plasma, J. Chromatogr. B Analyt. Technol. Biomed. Life Sci. 877 (2009) 502–506.
[218] N. Pholphana, D. Panomvana, N. Rangkadilok, et al., *Andrographis paniculata*: Dissolution investigation and pharmacokinetic studies of four major active diterpenoids after multiple oral dose administration in healthy Thai volunteers, J. Ethnopharmacol. 194 (2016) 513–521.
[219] J. Wangboonskul, S. Daodee, K. Jarukamjorn, et al., Pharmacokinetic study of *Andrographis paniculata tablets* in healthy Thai male volunteers, Thai Pharm Health Sci J 1 (2006) 209–218.
[220] X. He, J. Li, H. Gao, et al., Identification of a rare sulfonic acid metabolite of andrographolide in rats, Drug Metab. Dispos. 31 (2003) 983–985.
[221] D.P. Yeggoni, C. Kuehne, A. Rachamallu, et al., Elucidating the binding interaction of andrographolide with the plasma proteins: Biophysical and computational approach, RSC Adv 7 (2017) 5002–5012.
[222] H. Zhao, H. Hu, Y. Wang, Comparative metabolism and stability of andrographolide in liver microsomes from humans, dogs and rats using ultra-performance liquid chromatography coupled with triple-quadrupole and Fourier transform ion cyclotron resonance mass spectrometry, Rapid Commun. Mass Spectrom. 27 (2013) 1385–1392.
[223] T. Yang, C. Xu, Z. Wang, et al., Comparative pharmacokinetic studies of andrographolide and its metabolite of 14-deoxy-12-hydroxy-andrographolide in rat by ultra-performance liquid chromatography-mass spectrometry, Biomed. Chromatogr. 27 (2013) 931–937.
[224] X. He, J. Li, H. Gao, et al., Six new andrographolide metabolites in rats, Chem. Pharm. Bull. 51 (2003) 586–589.
[225] L. Cui, F. Qiu, X. Yao, Isolation and identification of seven glucuronide conjugates of andrographolide in human urine, Drug Metab. Dispos. 33 (2005) 555–562.
[226] L. Cui, W. Chan, F. Qiu, et al., Identification of four urea adducts of andrographolide in humans, Drug Metab. Lett. 2 (2008) 261–268.
[227] L. Xu, D. Xiao, S. Lou, et al., A simple and sensitive HPLC-ESI-MS/MS method for the determination of andrographolide in human plasma, J. Chromatogr. B Anal. Technol. Biomed. Life Sci. 877 (2009) 502–506.
[228] L.G. Vaishali, J.H. Patel, R.D. Varia, et al., Pharmacokinetics and anti-inflammatory activity of andrographolide in rats, Int.J.Curr.Microbiol.App.Sci 6 (2017) 1458–1463.
[229] M. Casamonti, L. Risaliti, G. Vanti, et al., Andrographolide loaded in micro- and nano-formulations: Improved bioavailability, target-tissue distribution, and efficacy of the “king of bitters”, Engineering 5 (2019) 69–75.
[230] J.P. Loureiro Damasceno, H.S. da Rosa, L.S. de Araújo, et al., Andrographis paniculata formulations: Impact on diterpene lactone oral bioavailability, Eur. J. Drug Metab. Pharmacokinet. 47 (2022) 19–30.

[231] S. Dokania, A.K. Joshi, Self-microemulsifying drug delivery system (SMEDDS): challenges and road ahead, Drug Deliv 22 (2015) 675–690.
[232] M.J. Lawrence, G.D. Rees, Microemulsion-based media as novel drug delivery systems, Adv. Drug Deliv. Rev. 45 (2000) 89–121.
[233] H. Du, X. Yang, H. Li, et al., Preparation and evaluation of andrographolide-loaded microemulsion, J. Microencapsul. 29 (2012) 657–665.
[234] Y. Zhu, J. Ye, Q. Zhang, Self-emulsifying drug delivery system improve oral bioavailability: Role of excipients and physico-chemical characterization, Pharm. Nanotechnol. 8 (2020) 290–301.
[235] N. Sermkaew, W. Ketjinda, P. Boonme, et al., Liquid and solid self-microemulsifying drug delivery systems for improving the oral bioavailability of andrographolide from a crude extract of *Andrographis paniculata*, Eur. J. Pharm. Sci. 50 (2013) 459–466.
[236] J. Wen, E.B. Moloney, A. Canning, et al., Synthesized nanoparticles, biomimetic nanoparticles and extracellular vesicles for treatment of autoimmune disease: Comparison and prospect, Pharmacol. Res. 172 (2021), 105833.
[237] K. Rajpoot, Solid lipid nanoparticles: A promising nanomaterial in drug delivery, Curr. Pharm. Des. 25 (2019) 3943–3959.
[238] R. Shankar, M. Joshi, K. Pathak, Lipid nanoparticles: A novel approach for brain targeting, Pharm. Nanotechnol. 6 (2018) 81–93.
[239] G. Graverini, V. Piazzini, E. Landucci, et al., Solid lipid nanoparticles for delivery of andrographolide across the blood-brain barrier: *in vitro* and *in vivo* evaluation, Colloids Surf. B Biointerfaces 161 (2018) 302–313.
[240] T. Kulsirirat, K. Sathirakul, N. Kamei, et al., The *in vitro* and *in vivo* study of novel formulation of andrographolide PLGA nanoparticle embedded into gelatin-based hydrogel to prolong delivery and extend residence time in joint, Int. J. Pharm. 602 (2021), 120618.
[241] L. Hao, Y. Jiang, R. Zhang, et al., Preparation and in vivo/in vitro characterization of Ticagrelor PLGA sustained-release microspheres for injection, Des. Monomers Polym. 24 (2021) 305–319.
[242] Y. Jiang, F. Wang, H. Xu, et al., Development of andrographolide loaded PLGA microspheres: Optimization, characterization and in vitro-in vivo correlation, Int. J. Pharm. 475 (2014) 475–484.
[243] Y. Zhang, X. Hu, X. Liu, et al., Dry state microcrystals stabilized by an HPMC film to improve the bioavailability of andrographolide, Int. J. Pharm. 493 (2015) 214–223.
[244] D. Zhang, J. Lin, F. Zhang, et al., Preparation and evaluation of andrographolide solid dispersion vectored by silicon dioxide, Pharmacogn. Mag. 12 (2016) S245–S252.
[245] G. Zhao, Q. Zeng, S. Zhang, et al., Effect of carrier lipophilicity and preparation method on the properties of Andrographolide-Solid dispersion, Pharmaceutics 11 (2019), 74.
[246] S. Hu, Z. Zhang, X. Jia, Study on andrographolide solid dispersion vectored by hydroxyapatite, Zhongguo Zhong Yao Za Zhi 38 (2013) 341–345.
[247] C.C. Yen, Y. Liang, C. Cheng, et al., Oral bioavailability enhancement and antifatigue assessment of the andrographolide loaded solid dispersion, Int. J. Mol. Sci. 21 (2020), 2506.
[248] Y. Ma, Y. Yang, J. Xie, et al., Novel nanocrystal-based solid dispersion with high drug loading, enhanced dissolution, and bioavailability of andrographolide, Int. J. Nanomed. 13 (2018) 3763–3779.
[249] O. Indrati, R. Martien, A. Rohman, et al., Development of nanoemulsion-based hydrogel containing andrographolide: Physical properties and stability evaluation, J. Pharm. Bioallied Sci. 12 (2020) S816–S820.
[250] Z.A. Awan, U.A. Fahmy, S.M. Badr-Eldin, et al., The enhanced cytotoxic and pro-apoptotic effects of optimized simvastatin-loaded emulsomes on MCF-7 breast cancer cells, Pharmaceutics 12 (2020), 597.
[251] M.A. Elsheikh, S.A. Rizk, Y.S.R. Elnaggar, et al., Nanoemulsomes for enhanced oral bioavailability of the anticancer phytochemical andrographolide: Characterization and pharmacokinetics, AAPS PharmSciTech 22 (2021), 246.
[252] R. Sari, A. Widyawaruyanti, F.B.T. Anindita, et al., Development of andrographolide-carboxymethyl chitosan nanoparticles: Characterization, *in vitro* release and *in vivo* antimalarial activity study, Turk. J. Pharm. Sci. 15 (2018) 136–141.
[253] E. Feng, K. Shen, F. Lin, et al., Improved osteogenic activity and inhibited bacterial biofilm formation on andrographolide-loaded titania nanotubes, Ann. Transl. Med. 8 (2020) 987.
[254] F. De Jaeghere, E. Allémann, R. Cerny, et al., pH-Dependent dissolving nano- and microparticles for improved peroral delivery of a highly lipophilic compound in dogs, AAPS PharmSci 3 (2001), E8.
[255] B. Chellampillai, A.P. Pawar, Improved bioavailability of orally administered andrographolide from pH-sensitive nanoparticles, Eur. J. Drug Metab. Pharmacokinet. 35 (2011) 123–129.
[256] H.N. Ginsberg, C.J. Packard, M.J. Chapman, et al., Triglyceride-rich lipoproteins and their remnants: Metabolic insights, role in atherosclerotic cardiovascular disease, and emerging therapeutic strategies-a consensus statement from the European Atherosclerosis Society, Eur. Heart J. 42 (2021) 4791–4806.
[257] O. Taskin, K. Rikhraj, J. Tan, et al., Link between endometriosis, atherosclerotic cardiovascular disease, and the health of women midlife, J. Minim. Invasive Gynecol. 26 (2019) 781–784.
[258] L. Monnier, A. Avignon, C. Colette, et al., Primary nutritional and drug prevention of atherosclerosis, Rev. Med. Interne 20 (1999) 360s–370s.
[259] M.D. Huffman, S. Yusuf, Polypills: Essential medicines for cardiovascular disease secondary prevention? J. Am. Coll. Cardiol. 63 (2014) 1368–1370.
[260] G.R. Prozzi, M. Cañás, M.A. Urtasun, et al., Cardiovascular risk of non-steroidal anti-inflammatory drugs, Medicina 78 (2018) 349–355.
[261] X. Li, Y. Liu, H. Zhang, et al., Animal models for the atherosclerosis research: A review, Protein Cell 2 (2011) 189–201.
[262] Y. Zhao, H. Qu, Y. Wang, et al., Small rodent models of atherosclerosis, Biomed, Pharmacother 129 (2020), 110426.
[263] A. Sharma, K. Lal, S.S. Handa, Standardization of the Indian crude drug Kalmegh by high pressure liquid chromatographic determination of andrographolide, Phytochem. Anal. 3 (1992) 129–131.
[264] N.A. Yusof, A. Isha, I.S. Ismail, et al., Infrared-metabolomics approach in detecting changes in Andrographis paniculata metabolites due to different harvesting ages and times, J. Sci. Food Agric. 95 (2015) 2533–2543.
[265] X. Zhang, L. Lv, Y. Zhou, et al., Efficacy and safety of Xiyanping injection in the treatment of COVID-19: A multicenter, prospective, open-label and randomized controlled trial, Phytother. Res. 35 (2021) 4401–4410.
[266] Y.S. Tu, D.M. Sun, J.J. Zhang, et al., Preparation and characterisation of andrographolide niosomes and its anti-hepatocellular carcinoma activity, J. Microencapsul. 31 (2014) 307–316.
[267] S. Shrivastava, C.D. Kaur, Development of andrographolide-loaded solid lipid nanoparticles for lymphatic targeting: Formulation, optimization, characterization, in vitro, and in vivo evaluation, Drug Deliv. Transl. Res. 13 (2023) 658–674.
[268] K. Wu, B. Yu, D. Li, et al., Recent advances in nanoplatforms for the treatment of osteosarcoma, Front. Oncol. 12 (2022), 805978.
[269] N.T. Huynh, C. Passirani, P. Saulnier, et al., Lipid nanocapsules: A new platform for nanomedicine, Int. J. Pharm. 379 (2009) 201–209.
[270] L. Zhao, G. Shen, G. Ma, et al., Engineering and delivery of nanocolloids of hydrophobic drugs, Adv. Colloid Interface Sci. 249 (2017) 308–320.
[271] B. Begines, T. Ortiz, M. Pérez-Aranda, et al., Polymeric nanoparticles for drug delivery: Recent developments and future prospects, Nanomaterials 10 (2020), 1403.
[272] H. Daraee, A. Etemadi, M. Kouhi, et al., Application of liposomes in medicine and drug delivery, Artif. Cells Nanomed, Biotechnol 44 (2016) 381–391.
[273] R.J. Ahiwale, B. Chellampillai, A.P. Pawar, Investigation of 1, 2-dimyristoyl-sn-glycero-3-phosphoglycerol-sodium (DMPG-Na) lipid with various metal cations in nanocochleate preformulation: Application for andrographolide oral delivery in cancer therapy, AAPS PharmSciTech 21 (2020), 279.
[274] V. Piazzini, E. Landucci, G. Graverini, et al., Stealth and cationic nanoliposomes as drug delivery systems to increase andrographolide BBB permeability, Pharmaceutics 10 (2018), 128.
[275] V.K. Verma, M.K. Zaman, S. Verma, et al., Role of semi-purified andrographolide from Andrographis paniculata extract as nano-phytovesicular carrier for enhancing oral absorption and hypoglycemic activity, Chin. Herb. Med. 12 (2020) 142–155.
[276] B.A. Oseni, C.P. Azubuike, O.O. Okubanjo, et al., Encapsulation of andrographolide in poly(lactide-co-glycolide) nanoparticles: Formulation optimization and *in vitro* efficacy studies, Front. Bioeng. Biotechnol. 9 (2021), 639409.